Ionisation in Flames,
with Special Regard to Aluminium

by

Roger Neil Newman, B.Sc.

A Thesis submitted for
the Degree of Doctor
of Philosophy in
the University
of Aston in
Birmingham.

September, 1971.

PREFACE

This dissertation, which is being submitted for the Degree of Doctor of Philosophy in the University of Aston in Birmingham, is an account of the work done under the supervision of Professor F. M. Page, B.A., Ph.D., Sc.D., in the Department of Chemistry of the University of Aston in Birmingham from November, 1967 to April, 1971. Except where references are given in the text the work described herein is original and has not been submitted for a degree at any other University.

SUMMARY

The gas phase equilibria between aluminium metal, oxygen, and hydrogen, existing in a laminar, premixed hydrogen-oxygen flame, have been investigated by a quantitative study of the emission spectra from the metal and its monoxide. The stability of the monoxide was estimated by second and third law methods, and a thermochemical analysis was made to determine the nature of possible aluminium compounds containing both hydrogen and oxygen, which were believed to be the major species present. The measurements were carried out at flame temperatures above 2300 K, below which it was found that alumina particles were formed in the flame, when aluminium was added in the form of vapours of its isopropoxide.

Also as a parallel topic, a study was made using a rotating electrostatic probe, of inhomogeneous distributions of charged species in the flame. The ionisation was produced by seeding the flame with both stable inert particles, and small evaporating crystals. The observations gave information on the relative particle gas velocities in the flames used, and the chemical origin of the ionisation detected in the region of the particles.

CONTENTS

CHAPTER 1

INTRODUCTION

Research work into combustion processes has been generated by the importance of the phenomena to modern technology. Simple examples would be the generation of heat and eventual conversion to electricity from the burning of coal, and the use of rocket, turbojet, and internal combustion engines. A further impetus to the quest for knowledge in this field is the need to analyse and control the products of such systems, where these may be harmful to the environment.

Investigations falling to the chemist, physicist or engineer may be divided into two broad classes. Firstly, to ascertain the bulk properties of shape, mass and heat transport, and total enthalpy of flames or explosions, and secondly, to gain an understanding of the atomic and molecular processes taking place. The latter category may involve the separation and transfer of electrical charge. In spite of this type of classification it is frequently found in combustion problems that a solution requires an approach derived from many scientific disciplines, and the subject as a whole is not the preserve of one particlar class of scientist.

A further mode of research is the use of carefully controlled flames as high temperature reaction solvents to study atomic and molecular processes of more general scientific interest, and the work to be described here would, in part, fall within this description. Furthermore, the results from this type of flame study, can often be correlated with those from other high temperature systems such as furnances, plasmas, and arcs or discharges.

It has been remarked by Gaydon and Wolfhard[1] that an exact definition of what is meant by the word flame is difficult to compose, and they suggest that certain properties such as the emission of light, the rapid attainment of high temperatures, and the occurrence of rapid reactions such as oxidation processes, while being common to many flames, are not universally present and do not form a complete definition. In the present context however, the flame used, in which mixtures of hydrogen oxygen and nitrogen were burnt at atmospheric pressure, are properly described as such, and would appear so even to the casual observer.

This dissertation contains the accounts of two studies in flames which although complementary to each other appear separately in the text for the sake of clarity. They are an investigation of the gaseous reactions of aluminium, and a development of the Langmuir electrostatic probe technique to ascertain whether it can be used in flames to measure ionisation of both particulate and gaseous origin.

The use of aluminium metal as an additive to solid and hybrid fuel propulsion systems has led to a need for an understanding of the processes and equilibria involved in its combustion, and more accurate data concerning the enthalpy changes of these processes. In particular, the stabilities of the monoxide AlO, its dimer Al_2O_2 and the suboxide Al_2O are of importance in this respect. Also it has often been found that an undesired result of this use of the metal was to increase the interference to radiofrequency guidance signals, caused by the generation of free electrons in the secondary burning of a rocket motor.

The emitted light from an aluminium bearing flame has been examined by many investigators. The most common features are the first Al resonance doublet, the blue-green[2] and sometimes the U.V. systems of AlO[3], and, with the correct conditions of temperature and concentration, continuum radiation originating from alumina in the condensed phase[4]. The metal was introduced to the premixed laminar hydrogen flames as vapours of its chloride or isopropoxide, and as a spray of the chloride, with methanol as the solvent, and found to give strong emissions of the atomic lines and the blue-green molecular bands. From the measured emission intensities from Al and AlO, as functions of flame temperature, together with the measured concentrations of the flame radical species, the dissociation energy of the monoxide was found by second law methods. The values thus obtained was somewhat higher than that of the preferred value in the J.A.N.A.F.[5] tables, but found to be close to that from a previous flame study by Gurvich and Veits[6].

Overall equilibrium calculations, however, showed that the monoxide was not the major species present, but rather that the metal was present in other forms still monatomic in aluminium, and tentative proposals are made concerning the nature of these species based mainly on the established behaviour of boron in flames, to which aluminium should show a strong similarity. Measurement of the AlO band intensity allowed a direct estimate of the AlO concentration, using a known value of the oscillator strength of the $A^2\Sigma^+ \rightarrow X^2\Sigma^+$ band, which was used to calculate the bond dissociation energy of the molecule by third law means.

The three principle direct methods of measuring ionisation in flame gases, are mass spectrometry, microwave attenuation, and the use of electrostatic probes, all of which have been widely and successfully used. Of the three the electrostatic probe technique is the simplest to use from a practical point of view, the most

complicated to interpret theoretically, and possibly the most versatile.

While using a probe for the measurement of positive ions in a seeded flame, both Miller[7] and Kelly and Padley[8], noticed time dependent components or "spikes" in the current flowing from the probe, when shown as a voltage profile on a C.R.O. display. In both cases the flames contained material in the condensed phase, and the effect was assigned by Miller[7] to be due to the thermal emission of electrons from incandescent particles while in contact with the probe, and evaluated the work functions of the particle materials from the "spike pulses". It was apparent that if Miller's idea was correct then an important new technique would be available to the flame chemist, to study systems where the added material could exist in gaseous and condensed phases, by relating the concentration and size of the particles to the frequency and amplitude of the spikes. Also as pointed out by Miller, the measurement of work functions of materials under flame conditions was of importance in its own right.

It was found by the author that under high resolution the probe profile showed fluctuations even for flames seeded with potassium and caesium chlorides as sprays, materials which should be completely volatalized at flame temperatures. With a much diluted delivery of spray to that produced by a normal atomiser, individual spikes were resolved and measured, the results showing striking similarities to those from the work on the solid particles. An analysis of these results was attempted in terms of the normal diffusion of ion clouds produced from evaporating crystallites with some success, which pointed to the possibility of an alternative explanation to that given by Miller to account for his solid particle spikes.

CHAPTER 2

CONSIDERATIONS OF FLAME EQUILIBRIA

2.i. Introduction

The emission and adsorption of radiation in flames are well recognised phenomena which have found widespread applications particularly in the field of chemical analysis. A flame or medium of hot gases provides thermal energy to atomiser materials such that they are in a suitable state to interact with radiation, hence the use of flame sources in atomic absorption spectroscopy, and also to excite molecules or atoms to higher quantum levels, thereby giving rise to emission spectra. As a consequence of the energy available in the flame the majority of molecules existing at such temperatures are di or triatomic and many will be free radicals.

For a system of particles of mass m in thermal equilibrium, their distribution of velocities will be in accord with the law of Maxwell. If a number of the particles dn, having a resultant velocity in the range c, $c + dc$ with N as the total number of the particles, then

$$\frac{dn}{N} = 4\pi \left(\frac{m}{2\pi kT} \right)^{3/2} \left\{ \exp\left(\frac{-mc^2}{2kT} \right) \right\} c^2 \, dc \qquad 2.1$$

This may be used to estimate the resultant distribution of kinetic energies of the particles, through the relationship

$$E_{KINETIC} = \frac{1}{2} m c^2$$

It can easily be proved that the mean translational kinetic energy $\bar{E}$ is given by

$$\bar{E} = \frac{3}{2} kT$$

and the root mean square velocity by

$$\bar{C} = \sqrt{\frac{3kT}{m}}$$

The rate of collisions taking place in any system of particles will be an important parameter when considering the transfer of energy in the system. This may be given to a first approximation by simple kinetic theory by

$$v = 2N_1N_2 \left(\frac{\sigma_1 + \sigma_2}{2} \right)^2 \sqrt{\frac{2\pi (m_1 + m_2) kT}{m_1 m_2}} \qquad 2.2$$

for the number of collisions between species 1 and 2.

The collision rate per second per unit volume is v, N_1 and N_2 are the number densities of the two species, and m_1m_2, and $\sigma_1\sigma_2$, are the respective masses and diameters. For a fuel rich flame at 2500 K at one atmosphere pressure containing the species H_2O, N_2 and H_2, from the combustion of a mixture of N_2, O_2 and H_2 with aluminium added such that its partial pressure was of the order of 1×10^{-6} atmos., the number of collisions between aluminium and all other species per unit time per unit volume is given by equation 2.2 to be approximately 1×10^{20}. The energy needed to excite the atoms and molecular species in the flame gases to their electronic vibrational and rotational degrees of freedom may be drawn from various sources including that produced by a chemical reaction, the absorption of radiation and from inelastic

collisions. When these excitations are thermally equilibrated, then the transfer by collision becomes the dominant mechanism, and the populations of the various available levels may be ascertained from the Boltzmann distribution law.

2.ii. The Emission of Radiation[9, 10, 11].

For the emission of radiation in the simple case from an atom or molecule, during a transition from an upper electronic state n to a lower state m, the intensity of the emission of wave number w is given by:-

$$I_{em} = N_n h c w A_{nm} \qquad 2.3.$$

Where, N_n is the number of species in state n, and A_{nm} is the Einstein coefficient of spontaneous emission for this transition and is given by:-

$$A_{nm} = \frac{64\pi^4 w^3}{3h} \sum_{x,y,z} |R^{nm}|^2 \qquad 2.4$$

R^{nm} being the component of the matrix element of the electric dipole moment. The quantum mechanical oscillator strength f_{nm} is defined by

$$f_{nm} = \frac{8\pi^2 w m c}{3h^2 e^2} \sum_{x,y,z} |R^{nm}|^2 \qquad 2.5$$

and may be substituted into equation 2.3 to yield

$$I_{em} = \frac{N_n 8\pi^2 e^2 h w^3}{m} f_{nm} \qquad 2.6$$

m being the electronic mass.

If the system is in thermal equilibrium, then Nn may be derived from the Boltzmann distribution law via

$$\left.\begin{aligned} \frac{N_n}{N_{TOTAL}} &= \frac{g_n e^{\frac{-E_n}{kT}}}{Q_{TOTAL}} \\ \text{and} \\ \frac{N_m}{N_{TOTAL}} &= \frac{g_m e^{\frac{-E_n}{kT}}}{Q_{TOTAL}} \end{aligned}\right\} \qquad 2.7$$

Where, E is the energy of a level, g the degeneracy, and Q the partition function.

It is possible to write

$$\frac{N_n}{N_m} = \frac{g_n e^{\frac{-(E_n - E_m)}{kT}}}{g_m} \qquad 2.8$$

Therefore, from equations 2.6 and 2.8

$$I_{em} = \frac{8\pi^2 e^2 h^2 w^3 f_{nm} N_m g_n e^{\frac{-hcw}{kT}}}{m \qquad g_m} \qquad 2.9$$

Since $E_n - E_m = hcw$

For transitions involving a change of electronic quantum number at flame temperatures <3000 K, m is frequently the ground state, and within the accuracies of most determinations, Nm may be approximated to N_{TOTAL}.

Equation 2.9 therefore allows the intensity of an emission to be related to the number of a particular species present in the flame, and could be applied, for example, to the resonance radiation of an atom, or a strong band of a molecular emission, if this were treated as a broad atomic line.

A more rigorous application of the distribution law to a spectral band system originated from a molecular transition is more complicated, but as in this study much of the data was obtained from the measurement of the $A^2\Sigma^+ \rightarrow X^2\Sigma^+$ emission from the molecule AlO, a simplified account is presented below.

The intensity of a particular molecular emission may, as in the case of an atomic emission, be related to the number density of the emitting species via

$$I_{nmv'v''} = N_{nv'} hcw A_{nmv'v''} \qquad 2.10$$

Where, Nnv' is the number density of the molecules in all rotational states of the upper state defined by quantum numbers n and v', w is the wave number of the emitted radiation (cm^{-1}), and $A_{nmv'v''}$ is the Einstein coefficient of spontaneous emission for the transition. $A_{nmv'v''}$ may be related to the matrix element $R^{nmv'v''}$ of the transition by re-expressing equation 2.4 in the form

$$A_{nmv'v''} = \frac{64\pi^4 w^3}{3h} \sum_{x,y,z} |R^{nmv'v''}|^2 \qquad 2.11$$

The matrix element $R^{nmv'v''}$ may be related to the variable electric dipole moment M, and the eigenfunctions $\psi nv'$, $\psi mv''$, of the states involved in the transition

$$R^{nmv'v''} = \int \psi^*_{nv'} M \psi_{mv''} \, d\tau \qquad 2.12$$

Assuming that ψ may be factorised into two functions, one dependant on the electrons ψ_e, and one on the nucleus ψ_v, and neglecting the rotation of the molecule, then

$$\psi = \psi_e \psi_r \qquad 2.13$$

The dipole moment may be separated in a similar manner thus,

$$M = Me + Mv \qquad 2.14$$

and substitution into equation 2.12 gives

$$R^{nmv'v''} = \int \psi_{v'}\psi_{v''} d\tau n \int Me\psi_e^{*n}\psi_e^{m} d\tau e + \int Mm\psi_{v'}\psi_{v''} d\tau n \int \psi_e^{*n}\psi_e^{m} d\tau e \qquad 2.15$$

Where the volume element $d\tau$ has also been separated into its components $d\tau e$ and $d\tau n$. Replacing $d\tau n$ by dr, and using the fact that $\psi_e^{*n}\psi_e^{m} d\tau e = o$, due to the mutual orthogonality of the two states then

$$R^{nmv'v''} = \int \psi_{v'}\psi_{v''} dr \int Me\psi_e^{*n}\psi_e^{m} d\tau e \qquad 2.16$$

The electronic part of 2.16 is called the electronic transition moment R_e, and for most purposes can be replaced by a mean value $\bar{R}e$ since ψe only varies slightly with r. This may be expressed more formally in terms of the r-centroid, with $\bar{r}_{v'v''}$ being the effective value of r over the band and $\bar{R}e$ can be written as $Re(\bar{r}_{v'v''})$ following Fraser[12], and Wallace and Nicholls[13]. Therefore $R^{nmv'v''}$ is given by:

$$R^{nmv'v''} = \bar{R}e \int \psi_{v'}\psi_{v''} dr \qquad 2.17$$

and $$\sum_{x,y,z} |R^{nmv'v''}|^2 = q_{v'v''} \sum_{x,y,z} |\bar{R}e|^2$$ 2.18

where $q_{v'v''}$ is the Franck Condon factor and represents the vibrational part of the transition probability.

The oscillator strength for the transition can now be written as

$$f_{nmv'v''} = \frac{8\pi^2 c w m}{3he^2} \sum_{x,y,z} |\bar{R}e|^2 \quad q_{v'v''}$$ 2.19

and the intensity of emission given by

$$I_{nmv'v''} = \frac{8\pi^2 e^2 h w^3}{m} f_{nm} \; q_{v'v''} \; N_{nv'}$$ 2.20

where f_{nm} is the purely electronic oscillator strength.

The estimation of Nnv' over a band by the distribution law is more complex for the molecular case, but if one particular band is considered, then the electronic excitation energy required will pertain to the origin of that band, or, for a whole system, the band origin of the $\Delta v = o$ band. The full expression for the population of any state n, vibrational state v' can be expressed in the following way if there is no interaction between the electronic, vibrational and rotational states.

$$\frac{\sum_{v=o}^{v'=k} N_{nv'}}{N_{TOTAL}} = \frac{g_n e^{\frac{-En}{kT}} \sum_{v=o}^{v=k} e^{-\frac{\left[(v'+\frac{1}{2})hcw_e - (v'+\frac{1}{2})^2 hcw_e x_e\right]}{kT}} Q_{rot}}{Q_{elec.} Q_{vib.} Q_{rot.}}$$ 2.21

For most purposes, the vibrational term may be estimated with the inclusion of only the first anharmonicity correction and En the electronic energy is taken as $h\omega_{o,o}$, using the wave number of the origin of the o,o band. The distribution of rotational states is assumed to be unchanged by the change in n and v.

The establishment of whether a particular emission is thermally excited can be of great importance in flame photometric studies and may be ascertained from a plot of the natural logarithm of a measured intensity versus, the reciprocal temperature of the species, the slope of which should give the excitation energy of the transition over kT.

2.iii The Absorption of Radiation[10]

The absorption of radiation by molecular or atomic species may be expressed by

$$dN_{m \to n} = B_{m \to n}\, p(\nu)\, Nm \qquad 2.22$$

where dNm is the number of particles absorbing radiation of frequency ν and density p, going from state m to state n, the levels being $h\nu$ energy units apart. Nm is the total number of particles in the lower state m, and B_{mn} is the Einstein coefficient of absorption for that transition.

For an incident beam of monochromatic radiation, intensity I_o, sent through an absorbing medium of thickness l, the resultant transmitted intensity I_ν at frequency ν, is defined by

$$I_\nu = I_o \exp(-k(\nu)l) \qquad 2.23$$

$k(\nu)$ being the spectral absorption coefficient of the medium. The

integrated absorption coefficient K over a frequency range, is defined by

$$\int k(\nu)d\nu = K\,Nm \qquad 2.24$$

Relative values of Nm, may be obtained from measurements of I_o and I_ν, using a constant source of incident radiation, or absolute values by using K. This is the simple basis of absorption spectroscopy, and by comparison with the equations for emission, it can be seen that the intensity of absorption is proportional to the number of species in the lower state whereas, emission intensities are proportional to the number in the excited or upper state.

Since absorption of radiation may take place in flames some account must be taken of the absorption by species in the flame of emitted radiation. The most important case is the one where both the emitting species are identical, and the transitions involve the ground electronic state, known as self absorption.

According to Mitchell and Zemansky[14] the intensity of emission I from a column of hot gases, thickness l, at temperature T is

$$I = \frac{\propto 8\pi h\nu^3}{C^2}\left\{\exp\left(\frac{-h\nu}{kT}\right)\right\}\int_o^\infty \left[1 - \exp\left(k\nu l\right)\right] d\nu \qquad 2.25$$

where $\propto$ is a constant of measurement.

At low concentrations of the emitting species this simplifies to

$$I = \frac{\alpha 8\pi h\nu^3}{c^2} \left\{ \exp\left(\frac{-h\nu}{kT}\right) \right\} \frac{\pi e^2}{mc} \; N \; fl \qquad 2.26$$

which is of the same form as equation 2.9. At higher concentrations

$$\int_0^\infty \left[1 - \{\exp(-k\lambda l)\}\right] d\nu = \left[\frac{2\pi e^2 \Delta\nu_D a'}{mc\sqrt{\pi}}\right]^{\frac{1}{2}} (Nfl)^{\frac{1}{2}} \qquad 2.27$$

where $\Delta\nu_D$ is the Doppler half width of the line, and a' the ratio of Lorentz collision broadening to Doppler broadening. I now becomes proportional to $\sqrt{N}$. This change of order has been discussed by van der Held[15], and the so called curve of growth of emission line intensity against increasing concentration as shown in Figure 1 for sodium, is sometimes referred to as a van der Held plot. Such plots have been used by James and Sugden[16] to relate the number of free atoms of sodium in a flame to the molarity of the solution sprayed.

From the above discussion it can be seen that in quantitative flame photometry the simplest interpretation of results may be achieved when the emitting species is at such a dilution that self-absorption effects are negligible. As a consequence of this, and the fact that intensity is a more sought after criterion than resolution, resulting in the measurements being made on integrated smoothed spectra, the various modes of line broadening may be ignored for the purposes of such studies. Errors in intensity measurements due to self reversal of resonance radiation may be eliminated by the use of flames shielded by a flame of similar temperature and rise velocity, the species under examination being introduced to the inner flame only.

Figure 1 dilution plot for sodium

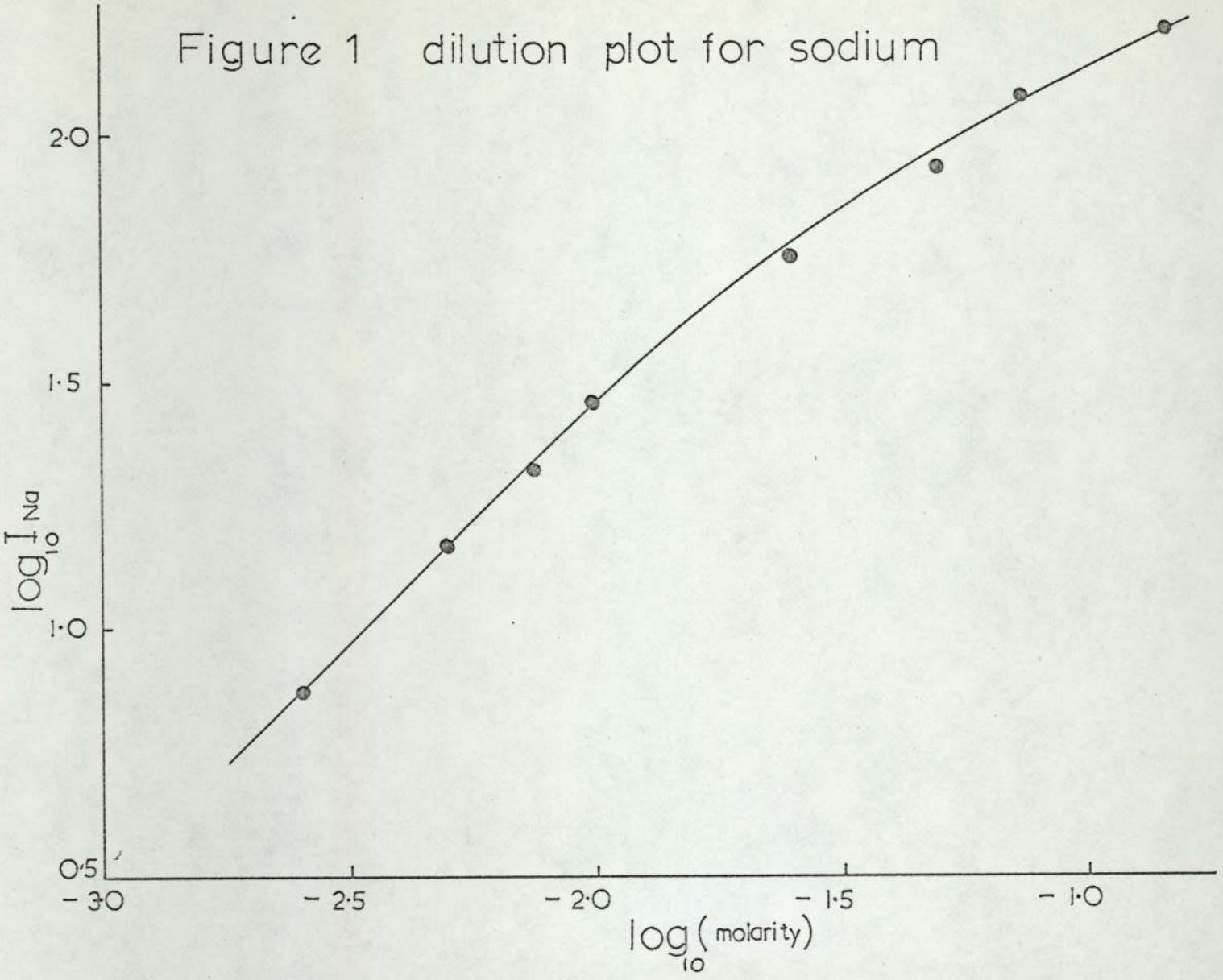

The temperature referred to in the above discussion is the electronic excitation temperature, which pertains to the flame burnt gases rather than the reaction zone, where the principle of equipartition of energy may not be applied. Further discussion of the particular flame temperatures and their measurement is deferred to Chapter 3.

2.iv. The Determination of Dissociation Energies from Studies of Flame Equilibria

The characterisation of a chemical reaction in any system will depend primarily on whether the system is in true equilibrium or under kinetic control. Assuming that the former case is so, then measurement of the concentrations of the reacting species will allow a determination of the equilibrium constant at the temperature of the system. Enthalpies of reaction and dissociation energies may then be derived from the equilibrium constant, by two approaches often referred to as second and third law methods (e.g. Sugden[17]). The second law method utilises the fact that plots of ln. Kp, against $^1/T$, Kp being the equilibrium constant for the gas phase reaction, gives a straight line of slope equal to $-\Delta H^\circ_T/R$, assuming that ΔH°_T varies little over the temperature range used. Since the method is graphical, relative values of the reactant concentrations are sufficient, which in many cases is a supreme advantage. Caution is needed however in the application of this method, since the use of too small a temperature range may cause large errors in the measured slope, and also other factors may contribute to a straight line plot to produce an apparent rather than real Kp.

The third law procedure involves the measurement of Kp in absolute terms at one temperature, allowing ΔG°_T to be calculated from $\Delta G^\circ_T = -RT \ln Kp$. ΔH°_T may then be found from, $\Delta G^\circ_T = \Delta H^\circ_T - T\Delta S^\circ_T$,

providing that ΔS_T^o for the process can be calculated, the name for the approach coming from the third law of thermodynamics upon which the calculation of ΔS_T^o is based. Whenever possible it is desirable to employ both methods, the agreement between the values obtained for ΔH_T^o from both methods being in some ways a measure of the correctness of choice of the reaction.

In a flame system where the concentration of possible reactants are being followed by their emission spectra, the chief difficulty encountered is in relating intensity measurements to absolute concentrations, via the equations previously described. Firstly, the intensity measurements are not absolute due to geometric factors and the response of the recording system. Secondly, the oscillator strengths of the emitters, especially if they are molecular rather than atomic, may not be known.

The first difficulty may be overcome by comparing the measured relative intensity of a species to that from a known amount of sodium introduced to the flame, which is known to form no significant proportion of compounds in the flame gases. Given the oscillator strength of the emitter, then its absolute concentration may be calculated. If such an emitter were an element whose total delivery to the system was known, and which formed one major compound in excess of the free element at equilibrium, then the amount of the compound may be found by the difference, and second and third law procedures may be used to estimate the enthalpy of its formation. If however it is found necessary to follow the concentration of a compound formed by its emission intensity due to it being one of several present, or a minor species, then absolute measurements and third law procedures may not be possible due to a lack of knowledge of the oscillator strength, and a second law approach must be employed.

The flames generally used for this type of study have convective velocities of the order of 10 ms^{-1}, and may only maintain their temperature constant for some 1×10^{-1} m, allowing only a few milliseconds for reactions to achieve equilibrium under steady conditions. The kinetic aspects of compound formation must therefore be taken into account.

Sugden[17] has considered this problem in detail for the case of the formation of a compound MZ in a hydrogen-oxygen flame, by the two mechanisms:-

$$\text{I} \quad M + HZ \underset{k_{-1}}{\overset{k_1}{\rightleftharpoons}} MZ + H \qquad K_1 = k_1/k_{-1}$$

$$\text{II} \quad M + Z + X \underset{k_{-2}}{\overset{k_2}{\rightleftharpoons}} MZ + X \qquad K = k_2/k_{-2}$$

X being a third body, and Z in this particular instance being either H or OH. The ratio ϕ is defined by $\phi = \frac{[MZ]}{[M]}$ and under flame conditions $\phi > 1$ when the energy of dissociation of MZ is $> \sim 418$ kJ mol^{-1}, and $\phi << 1$ when < 355 kJ mol^{-1}. A careful analysis of the rate equations involved and estimates of the activation energies reveals, that at around 2000 K ternary recombination (reaction I) becomes dominant for E_{-2} (activation energy) < 302 kJ mol^{-1}, and at greater values of E_{-2}, the bimolecular exchange will dominate (reaction II). For these cases E_{-2} is taken as the heat of dissociation of the compound. Further, it was shown that the time taken for [MZ] to reach 90% of its equilibrium level was $\sim 2 \times 10^{-4}$ secs, for biomolecular exchange predominating, and $\sim 5 \times 10^{-5}$ for ternary recombination, taking E_{-2} as 293 kJ mol^{-1}. For values of the bond dissociation energy greater than 293 kJ mol^{-1}, the times to reach equilibrium were further reduced.

In the calculations of the rate constants it was assumed that water was the third body. Therefore in times of 1 millisecond or greater effective equilibration of these types of processes is to be expected.

The same general arguments may be extended to the formation of oxides in the flame gases, and gives a rule of thumb, as to whether bimolecular exchange or ternary recombination reactions will predominate in the formation of a compound according to its bond dissocation energy. While the reactions above have been shown to equilibrate in most flame conditions, many involving the flame radical species, especially at low temperatures, i.e. below 2000 K do not. In particular, the work of Bulewicz, James and Sugden[18] has shown that for H_2, O_2, N_2 flames, the principle radicals H, OH, and O are many times above their equilibrium value with respect to their recombinations:-

$$H + H + X \rightleftarrows H_2 + X$$
$$OH + H + X \rightleftarrows H_2O + X$$
$$O + O + X \rightleftarrows O_2 + X$$

The recombinations proceed to reduce the disequilibrium downstream from the reaction zone, and the level of disequilibrium increases with decreasing flame temperature. It has been shown however that the radicals are maintained in equilibrium proportions to one another by the more rapid bimolecular exchange process:-

$$H_2O + H \rightleftarrows H_2 + OH$$
$$H_2 + O \rightleftarrows OH + H$$

At temperatures in excess of 2000 K and one millisecond downstream from the reaction zone, the radical concentrations are effectively equilibrated, and may be calculated with some surety. In the lower temperature region this disequilibrium and change of radical level

with height in the flame has been used to diagnose the particular species reacting with metal additives, e.g. Bulewicz and Sugden[19], but at higher temperatures this is not possible. This point was particularly relevant to the study of the formation of aluminium compounds in these flames, as will be discussed later. For the moment it is sufficient to consider the three mechanisms

$$M + O + X \rightleftarrows MO + X$$

$$M + H_2O \rightleftarrows MO + H_2$$

$$M + OH \rightleftarrows MO + H$$

for the formation of a metal monoxide. At higher temperatures all three become thermodynamically indistinguishable due to the parallel equilibrated reactions of the radical species. Therefore a study of the values of $[MO]/[M]$ may be based on any one of such a set of reactions without implying a specific mechanism.

2.v. Ionisation in Flames

The existence of ionisation in hydrocarbon flames and those containing metal additives has been well established, and because of the relevance to rocket vehicle guidance and M.H.D. power generation, has received much addition in recent years. The majority of investigations have been concerned with the formation of positive species and electrons rather than the generally less abundant negative ions[20, 21, 22].

For equilibrium ionisation of a metal M through the process

$$M \rightleftarrows M^+ + e^-$$

the equilibrium constant Kp may be expressed by the well known Saha

equation in the form[10]

$$Kp = \frac{Qm^+ \; Qe^- \; kT}{Qm} \exp -(X/kT) \qquad 2.28$$

where X is the ionisation potential of the species M.

Equation 2.28 may be re-expressed as

$$\log_{10}Kp = \frac{-5050X}{T} + \frac{5}{2} \log_{10}T - 6.5 + \log_{10} \frac{g_m^+ \; g_e^-}{g_m} \qquad 2.29$$

X having units of electron volts and the g being the statistical weight.

In considering ionisation levels in flame situations it is often found that equilibrium conditions are not achieved and the Saha equation not applicable, except at high temperatures or where the species M has a low ionisation potential, such as in the case of cesium.

The principle ions found in hydrocarbon flames are H_3O^+, CHO^+ and $C_3H_3^+$[23, 24], H_3O^+ being the most long lived, and produced by a charge exchange process from the ion CHO^+ in the following way[25].

$$CH + O \rightarrow CHO^+ + e^-$$
$$CHO^+ + H_2O \rightarrow H_3O^+ + CO$$
$$H_3O^+ + e^- \rightarrow H_2O + H$$

These ions tend to be produced in levels far in excess of the equilibrium situation in the reaction zone, which decay progressively in the downstream gases through recombination. When metal additives are introduced into a hydrocarbon flame, or one containing H_3O^+ ions from a trace of acetylene, a charge exchange reaction

$$H_3O^+ + M \rightarrow M^+ + H_2O + H \text{ (or products)}$$

is found to take place[26]. This has the effect of either speeding the

attainment of the Saha equilibrium level of the metal ion as for sodium and potassium, or in the case of metals with high ionisation potentials such as lead, the production of initially large excess ion concentrations, the ionisation downstream from the reaction zone being dominated by the recombination of ions and electrons.

The ionisation of the alkali metals in "clean" flames has been shown to be in accord with the mechanism[27]

$$M + X \rightarrow M^+ + e^- + X$$

and may be described as a thermal ionisation process. This is probably applicable to many metals, and has been shown to account for the ionisation of the lower group III metals, gallium, indium and thallium by Kelly and Padley[28]. Owing to the high activation energy involved in the forward step however, the process may not be equilibrated at moderate temperatures as has been shown for the upper Group I metals by Schofield and Sugden[29]. These workers have also studied the production of ions of the type MOH^+ in flames containing alkaline earth metals and have proposed the schemes

$$M + OH \rightleftarrows MOH^+ + e^-$$
$$MO + H \rightleftarrows MOH^+ + e^-$$
$$MOH^+ + H \rightleftarrows M^+ + H_2O$$

which may be termed chemi-ionisation processes. The metal hydroxy ion was found to be the major species and equilibrium according to the above reactions achieved due to the more rapid forward step involved than in thermal ionisation.

The possibility of charge residing on solid phases contained in a flame plasma has also be examined in detail, due in many ways to the use of solid propellants in rocketry. The chief interest in this

field has been the surface emission of electrons from materials of low work function, and elegant equations describing this process have been set up by a number of workers including Sugden and Thrush[30], Einbinder[31], and Smith[32]. The general method of approach has been to modify the Richardson equation for saturated thermionic emission, to account for the image forces produced on the particle by the departing electron. Other studies notably by Weinberg[33, 34], have shown that collection of negative charge, due to the greater random thermal velocity of electrons over that of positive ions, is also viable. Furthermore the attainment of a large number of charges per particle at least in the case of carbon particles in sooting flames is unlikely. Kelly and Padley[8] on the other hand have attributed the ionisation found in flames containing transition metals, many of which formed oxide particles in situ, to that from gas phase material evaporated from the condensed phase.

The subject of ionisation from condensed phases in flames is somewhat less well understood than that of the gas phase phenomenon, but for many cases such as levels in rocket exhausts it can be said to be of less importance.

CHAPTER 3

THE APPARATUS

3.i. Burner Design

The burner used in the studies is shown in Figure 2 approximately to scale. The upper chamber allows cooling water to circulate around the hypodermic tubes, a necessary feature as the parts were soldered together. The central chamber supplies the gas for the outer shield flame, and the lower chamber, the gases and additives for the inner flame. The stainless steel hypodermic tubes were of internal diameter 8.125×10^{-4} m and the bundle arranged to give a flame hexagonal in cross-section. The flow rate to the outer flame was the greater, 51 tubes being used to supply the gases, as opposed to 37 to the inner flame. Such water cooled Heker type burners have been used for a number of years in this type of study, the chief virtue of this design however, was the development of Miller's[7] in spacing the tubes to account for the lateral expansion of the burnt gases, approximately by a factor $7^{2/3}$. The tubes were held in place by being soldered into three predrilled circular brass plates, themselves held in position inside the outer barrel by rubber 'O' rings. The bottom plate was also supported on 'O' rings rather than a more rigid attachment to allow a safety blow off facility. The effect of the multitube double flame burner is to produce a flame baving a flat, short reaction zone $< 1 \times 10^{-3}$ m, in height. The burnt gas region moves with laminar, piston flow effectively steady in temperature and composition for up to 8×10^{-2} m above the burner surface. Above this distance the effect of entrained air becomes noticeable. The burner assembly was mounted on an adjustable jack, so that the flame could be moved easily in the vertical plan relative to the probe and slit of the spectrophotometer.

Figure 2 burner design

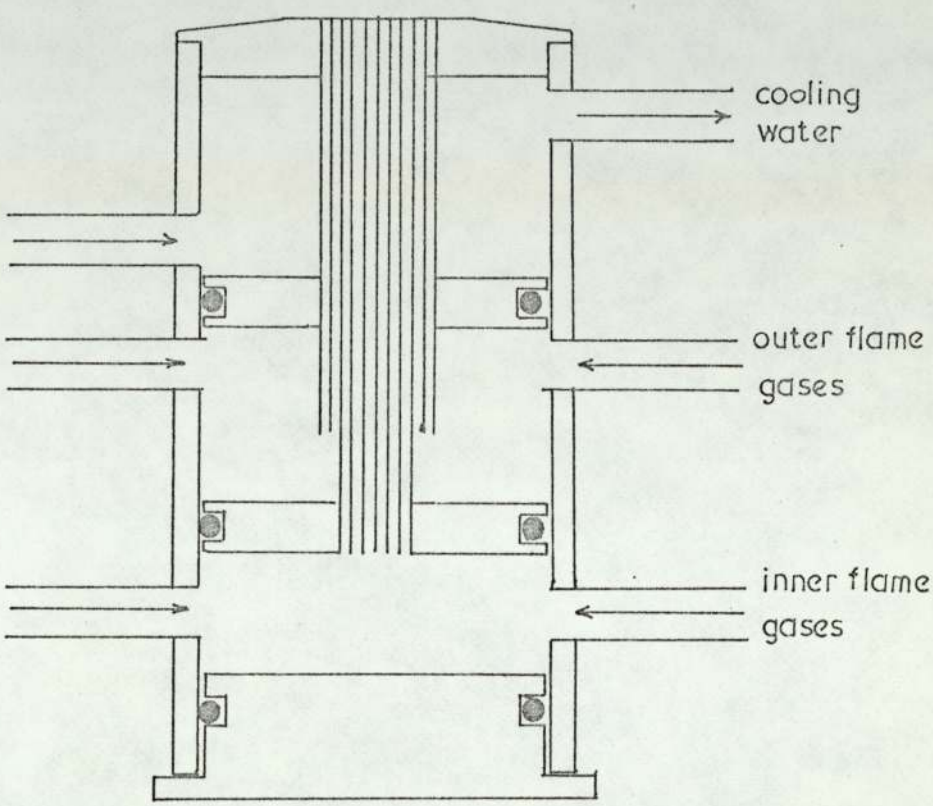

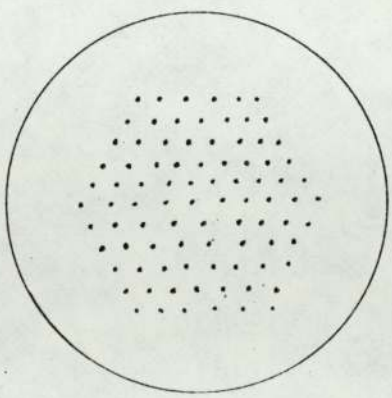

plan view

3.ii. The Gas Delivery System

Unburnt mixtures of commercial hydrogen oxygen and "white spot" nitrogen fed to the flame, were monitored by means of calibrated "Rotameters" and controlled by "Clockhouse" needle valves in the fuel lines. As a minimum safety measure contact between the oxygen and hydrogen only took place in the two mixing chambers of the burner. Flow rates to the outer and inner flames were arranged to be such that both had the same convective velocity. Additives in solution form were added as fine sprays generated in a conventional scent spray atomiser, driven by nitrogen diverted from the inner flame supply. Large unwanted droplets were removed by passing the suspended spray upward through a settling chamber, and through a baffle chamber at the junction with the main inner flame supply. The pressure drop across the atomiser was monitored by means of a mercury manometer, and the unit was operated at a constant volume throughout found from a calibration of pressure drop and flow rate. Delivery of material to the flame was found to be linear with flow rate for most solutions up to 0.25 molar concentration, above this, blocking of the atomiser nozzle occurred due to salt deposition. Figure 3 shows the general scheme of the gas delivery system.

The aluminium isopropoxide vapour and was generated in the thermostated oven shown in Figure 4. The oven consisted of a cylindrical duralamin block, 1.0×10^{-1} m in diameter and 22.0×10^{-1} m in length with a cylindrical section, 2.54×10^{-2} m in diameter drilled from the axis wherein the material was placed. Suitable threads were cut at each end of the hollow section and Enots gas connectors fitted to 6×10^{-3} m. O.D. copper tubing to carry nitrogen gas through the system. The whole arrangement was suspended in a thermostated oil bath. The nitrogen carrier gas diverted from the inner flame supply was preheated by passing through 2.54×10^{-1} m of coiled copper tubing

Figure 3 gas delivery system

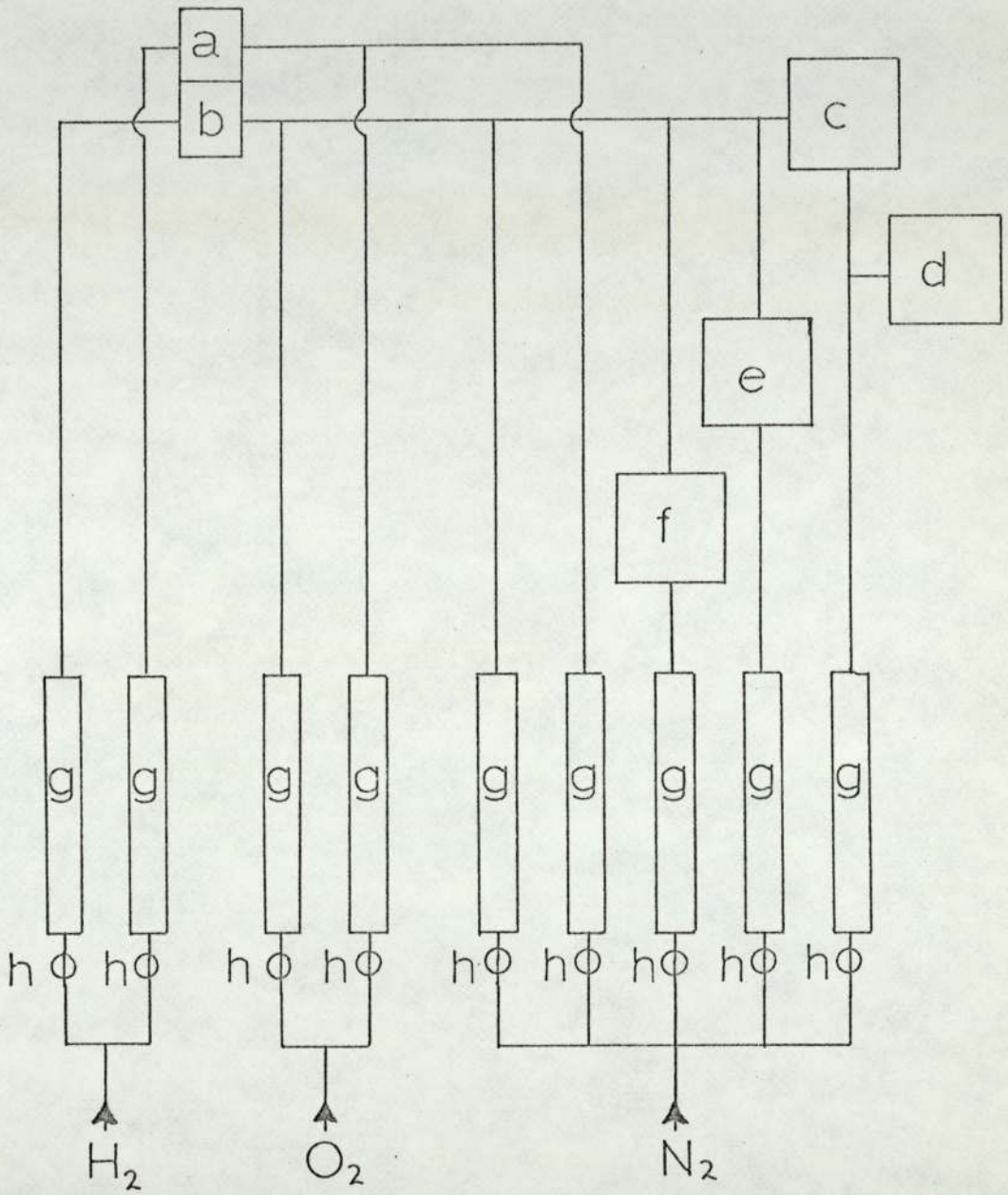

a, outer flame b, inner flame c, atomiser

d, mercury manometer e, breaking bubble atomiser

f, furnace g, 'rotameters' h, needle valves

Figure 4 spectrograph and furnace

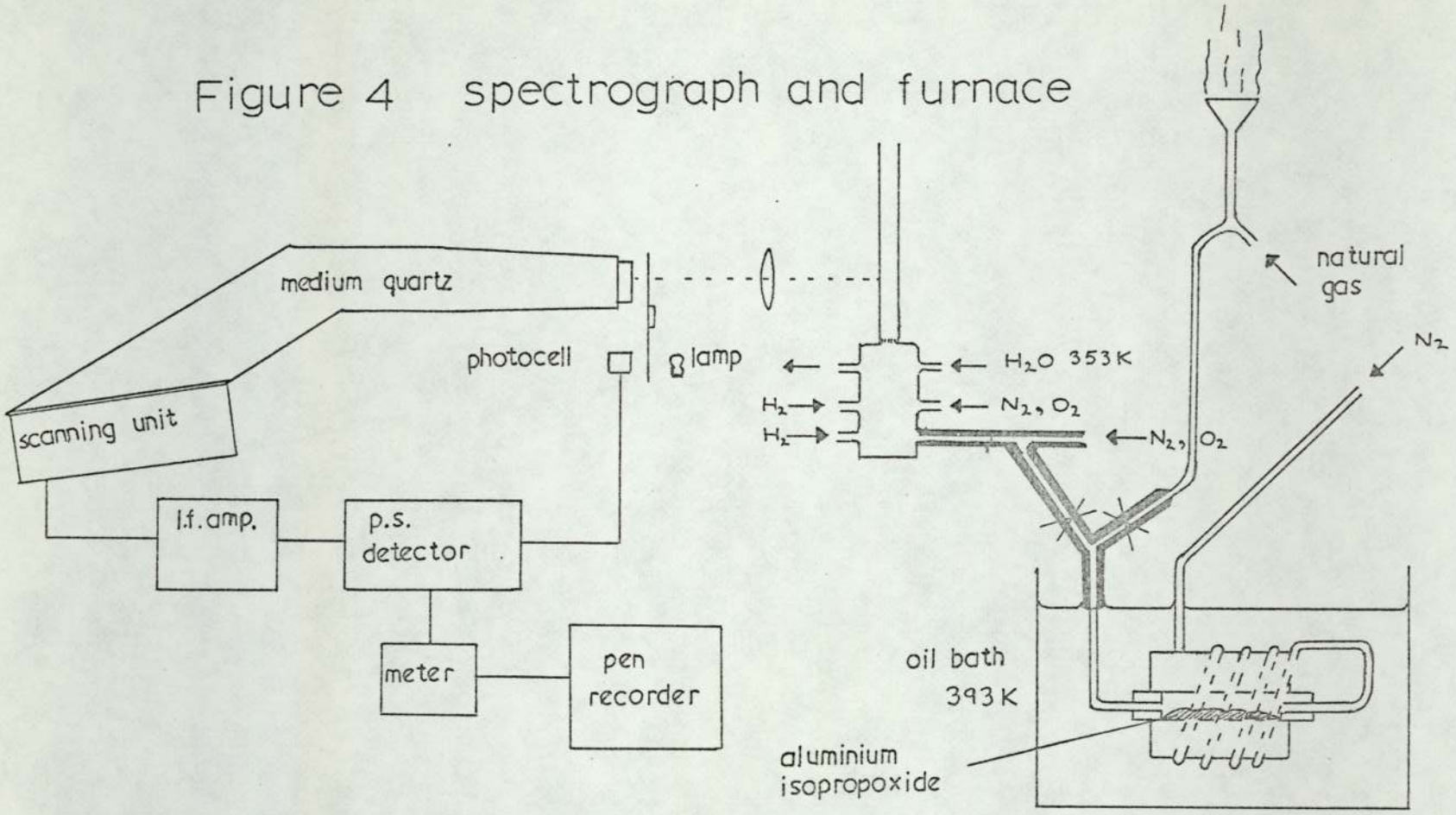

also immersed in the oil bath. The nitrogen carrier gas was found to saturate with the isopropoxide vapour for flow rates of up to 3 litres/min. After passage through the furnance, provision was made for diversion of the saturated gas to a natural gas diffusion flame, by means of a Y piece and double tap switching device as shown. This arrangement allowed rapid recording of background conditions in the flame during the course of the spectroscopic investigations. All fuel lines carrying the isopropoxide vapour were heated by electrical heating tapes to reduce deposition on the walls. Also, heating by the same method was applied to the mixing chamber of the inner flame, and the cooling water in the upper chamber was raised to 80°C, to prevent blocking of the hypodermic burner tubes. It was found by trial and error that raising the burner above this temperature caused leaking from the cooling chamber into the upper mixing chamber, due presumably to spurious expansion forces, thus rendering measurements impossible above this point. The oil bath was operated for the most part at 119°C, the melting point of the aluminium isopropoxide, and periods of about two hours were allowed for the apparatus to attain thermal equilibrium. A certain amount of deposition however did occur, mainly at the junction of the saturated nitrogen stream with the remaining nitrogen and oxygen gases to the inner flame, and complete cleaning of the burner and fuel lines after every 20 minutes of operation was found necessary to ensure a constant delivery to the flame. The temperature of the lines and that of the unburnt gases at the burner exist were measured by means of thermocouples. The use of annealed copper tubing allowed the burner to be moved relative to the furnance, and the operation of the delivery system was found to be effective, but time consuming. The only hazard found during its use occurred when the molten salt in the furnance was forced by the nitrogen flow enmasse through the system to appear as a very spectacular flare at the burner face, but the fault was rectified by the careful positioning of some glass wool at the furnance exit.

3.iii. Flame Temperatures

The flame temperatures were measured by the sodium 'D' line reversal technique, which is widely used and accepted for these types of flames, and described in many texts, e.g. Gaydon and Wolfhard[1]. The method depends on the line reversal of the emitted resonance radiation of sodium atoms, thermally equilibrated with the bulk flame gases, and gives the electronic excitation temperature, which may be assumed to be equal to the general thermodynamic temperature of such a system.

Light from a tungsten strip filament lamp was focused by a lens onto the flame and by means of a slit and second lens onto the aperture slit of a Hilger constant deviation spectrograph. A spray of sodium chloride was introduced to the flame and, with a small current passing through the lamp, the 'D' lines at around 5890 Å were viewed in emission through the spectrograph over the continuum from the lamp. The current was then increased until the lines could not be distinguished from the background and the value of the current recorded. The brightness temperature of the lamp for various current values were found from the calibration of the lamp at 6550 Å, against a Leeds and Northrop disappearing filament pyrometer, itself standardised against a blackbody.

From the brightness temperature the radiant intensity $J(\lambda b)$ at that temperature may be found, but what is required is the radiant temperature at 5890 Å. Knowing the emissivity of the tungsten filament appropriate to this wave length, its radiant intensity can be found at its true temperature, if it were acting as a perfect blackbody. Hence the flame temperature can be found from tabulations of $J(\lambda)$ against T for such a body.

Expressed mathematically the radiant or true temperature may be found from the application of Wiens Law in the form

$$\frac{1}{T} - \frac{1}{T\lambda} = \frac{\lambda \ln \varepsilon(\lambda)}{C_2} \qquad 3.1$$

where C_2 is the second radiation constant, and $\varepsilon\lambda$ the emissivity at wave length λ. The radiation data used was taken from International Critical Tables[35].

The flame temperatures thus measured were found to rise sharply to a constant value at around 1.5×10^{-2} m above the burner face, and to vary only over 20 K or less up to 8×10^{-2} m in the flame. The absolute error is hard to assess, but after consideration of the reproducibility of the measurement, errors of $\pm$ 20 K at 2300 K and below, to $\pm$ 30 K at 2700 K were assigned to the temperatures.

3.iv. Calibration of the Atomiser

The number density of atoms produced in a flame from a known molarity of solution contained in the atomiser, or atomiser calibration, was found using the microwave attenuation procedure described in detail by Woolley[36] and performed using his apparatus. Electromagnetic radiation in the microwave and radiofrequency range is attenuated when passed through a flame or plasma containing free ions, which dissipate their momentum acquired from the electric field in collisions with the bulk gas species. The conductivity of the gas is found to be inversely proportional to the ion mass, so that essentially only electrons rather than positive or negative ions need be considered, and the loss of power of a transmitted signal through a flame may be related to the concentration of free electrons present.

In Woolley's system, the flame was passed through a water cooled cavity resonating at a frequency of 2940 MHz., supplied by an E.M.I. R9559/25204 klystron, and the transmitted signal received by a crystal rectifier and displayed on a Saunders V.S.W.R. amplifier. The measurements were made by adjusting a variable attenuator on the receiver side of the cavity for a clean flame such that a null point was obtained. By further adjustment back to this point when the flame containing the additive was introduced, the attenuation of the signal βdb, caused by the additive, was obtained.

The Q factor of a resonant cavity is defined by

$$Q = \frac{2\pi \text{ energy stored per cycle}}{\text{energy dissipated per cycle}} = \frac{wL}{P} \qquad 3.2$$

where L is the total electromagnetic energy averaged over one cycle, w the angular frequency, and P the loss of energy per cycle. Defining P_1 as the loss due to heating of the walls, external coupling to the cavity, and the presence of electrons in a "clean" flame, then Q_1 is defined by

$$Q_1 = \frac{wL}{P_1} \qquad 3.3$$

If P_F is the extra loss introduced when the flame becomes more conducting, then Q_2 may be written as

$$Q_2 = \frac{wL}{P_1 + P_F} \qquad 3.4$$

P_F can further be related directly to the conductivity of the gas σ, by the relationship:

$$\sigma = \frac{ne^2}{m}\left(\frac{w_1}{w^2 + w_1^2}\right) \qquad 3.5$$

where n is the number density of the electrons, w_1, their collision frequency and m their mass.

From these equations, the relationship between n and Q_1/Q_2 can be derived, i.e.

$$\frac{ne^2}{m}\left(\frac{w_1}{w^2 + w_1^2}\right) \propto \frac{wL}{Q_1}\left(\frac{Q_1}{Q_2} - 1\right) \qquad 3.6$$

from which it can be seen that n is proportional to $(Q_1/Q_2 - 1)$. This term can be related to t, the ratio of the power transmitted at resonance for the clean flame, to that of the conducting flame by

$$ne \propto \frac{1}{Q_1}\left(t^{\frac{1}{2}} - 1\right) \qquad 3.7$$

t being obtained from the measured attenuation β by

$$\beta = 10 \log t \qquad 3.8$$

For the equilibrium ionisation of a metal A according to the scheme

$$A \rightleftharpoons A^+ + e^-$$

K_p the equilibrium constant is given by

$$K_p = \frac{[A^+][e^-]}{[A]} \qquad 3.9$$

If $[A_o]$ is the concentration of total metal present, giving

$[A_o] = [A] + [A^+]$, and the condition of charge balance, $[A^+] = [e^-]$ applies, then

$$[e^-]^2 + K_p[e^-] - K_p[A_o] = 0 \qquad 3.10$$

which gives two solutions, $[e^-] = [A_o]$, at very low values of $[A_o]$ and large values of K_p, and $[e^-] = (K_p[A_o])^{\frac{1}{2}}$, when $[A_o] >> K_p$.

K_p may be found from the Saha Equation for any particular metal and a plot of $\log [e^-]$ vs. $\log [A_o]$, exhibits a slope of 1 at low values of $[A_o]$, changing smoothly to a slope of $\frac{1}{2}$ at higher concentrations. Calibration of the response of the cavity, and the delivery rate of the atomiser, may be achieved simultaneously by fitting a plot of $\log (t^{\frac{1}{2}} - 1)$ vs. log (Molarity of solution), to such a theoretical plot.

Since the theoretical plot requires an equilibrium situation, a metal additive is required which will attain its equilibrium level rapidly in the flame. Cesium is known to ionise rapidly but also forms an appreciable amount of hydroxide at higher concentrations. Potassium on the other hand is involved in little compound formation in the flame, but ionises slowly, especially at low concentrations. The calibration was carried out therefore using the ionisation of cesium for the linear region, and that of potassium for the square root region. The combined theoretical and experimental plots are shown in Figure 5 for a clean flame at 2468 K, and from this and a similar plot, the calibration for the two atomisers used in the work were found to be

A 1 molar solution $\equiv 8 \times 10^{-5}$ atm.

B 1 molar solution $\equiv 1.2 \times 10^{-4}$ atm.

Atomiser A was operated with a flow rate of 3.6 litres min^{-1} and B

Figure 5 atomiser calibration

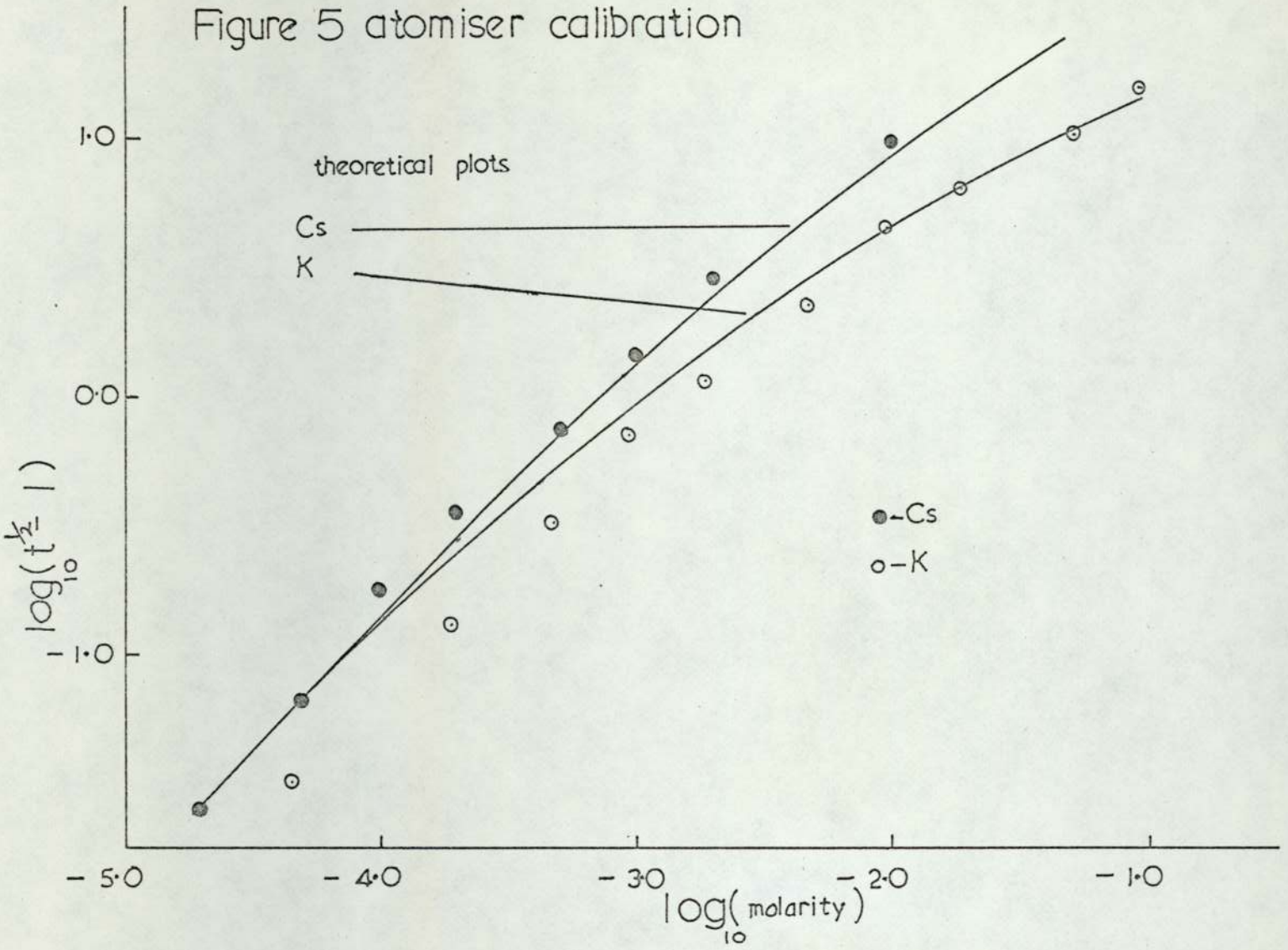

with a flow rate of 3.8 litres min^{-1}. The calibrations were considered to be reasonable when compared to those of atomisers of similar construction, calibrated in this laboratory[37, 38] using the electrostatic probe procedure forwarded by Soundy and Williams[39].

3.v. The Spectrophotometer

The spectra were studied photometrically using a Hilger Medium Quartz spectrograph, with an IP28 photomultiplier scanning unit. The signal level was controlled by a Brookdeal L.A. 635 amplifier and displayed on a Honeywell pen recorder. The radiation from the flame was chopped at 400 Hz by a rotating sectored disc, alternately with that from a pea lamp to a photocell. Both signals were fed into a Brookdeal P.D. 629 phase sensitive detector interposed between the amplifier and pen recorder, this being a standard method in such systems of improving the signal to noise ratio. The spectrograph was laid on its side, and by focusing the radiation from the flame onto the slit, by means of a 1.2×10^{-2} m focal length quartz lens, a vertical resolution of less than 1×10^{-3} m was achieved. The flame speeds were calculated to be 20 ms^{-1} or more, thus giving a resolution in time of about 5×10^{-5} s. The general layout is shown in Figure 4. The electronic scanning unit was easily interchanged with a photographic plate holder.

Using the photographic technique, resolution of the order of a few angstroms was possible but, with the scanning unit, the need for intensity required the resolution to be much less than this. Adjustment of both the spectrograph slit, and that covering the photomultiplier was used to obtain optimum conditions, and these conditions were maintained strictly constant throughout any series of measurements. The principle errors involved in the spectral measurements, were emission from air born impurities drawn into the shield flame, and some variations in flame temperature, caused by

fluctuations in the gas flow rates to the flame. No error was attributed to possible variations in the purity of the gases obtained from the British Oxygen Company. Initially a great deal of interference was detected from a multitude of atomic lines produced by the laboratory discharge lighting, and this was lessened by placing a charcoal covered board immediately behind the flame. For the case of the atomic emissions of aluminium, at the lowest temperatures, however, it was found necessary to carry out the measurements in the absence of all sunlight and room lighting.

The mean error in the intensity measurements was estimated from the results to be 10% or less, a quite acceptable level for the purposes of the second law estimations.

To relate relative intensity measurements to absolute concentrations by comparison with the emission from a known amount of sodium in the flame as an internal standard, it was necessary to calibrate the response of the photomultiplier over the range of wavelength involved. This was achieved by comparing the response of the spectrophotometer to that from a tungsten filament lamp at a known temperature and at various wavelengths. The temperature of the lamp was measured as before using an optical pyrometer, and the final calibration of the response was taken as the mean of the results of three calibrations, corresponding to the three different brightness temperatures of the lamp used; 1800 K, 2100 K, and 2400 K. From the brightness temperatures of the lamp and the emissivity of tungsten at the pyrometer operating wavelength, the radiant temperature of the tungsten filament was found. The true radiant intensity of the lamp over the range 2500 $\mathring{A}$ - 7000 $\mathring{A}$ was then calculated from the product of the emissivity at that temperature and the tabulated radiant intensity of a blackbody at that temperature. The measured response from the spectrophotometer at each wavelength in arbitrary

Figure 6 photomultiplier calibration

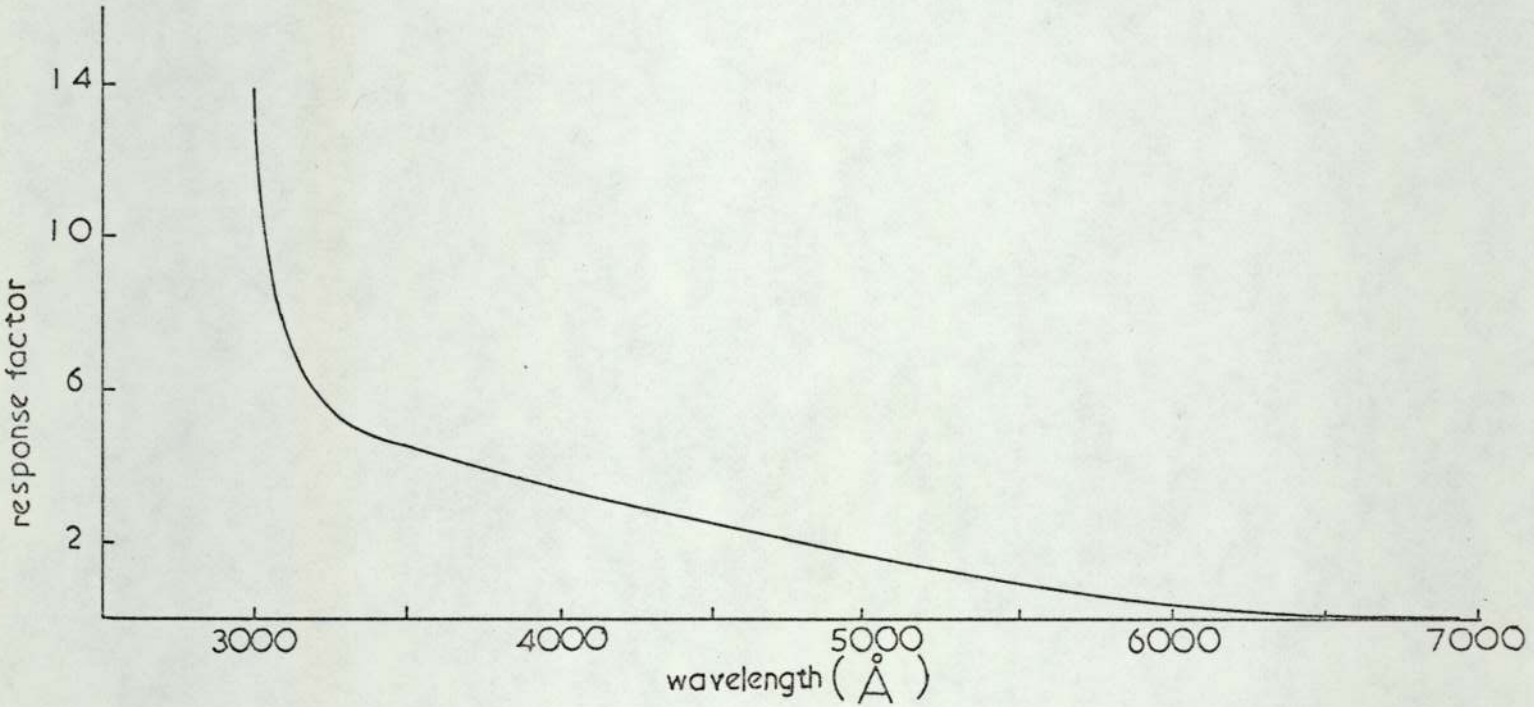

units was divided by the calculated intensity to give a relative scale of response factors at each wavelength. Figure 6 shows part of the calibration.

Wavelengths were indicated on the instrument by a mechanical counter coupled to the drive of the scanning unit. The calibration supplied by the manufacturers was checked against standard atomic line sources and found to be sufficiently accurate for the purposes of the investigation. Using this device any spectral feature could be positioned to better than $\pm$ 20 Å, subject to the limitations of the slit widths used. A more accurate wavelength scale, using the length of travel of the pen recorder paper was constructed, but not used, chiefly due to the inconvenience of referring to a standard emission line each time of usage.

3.vi. Flame Compositions

A series of fuel rich flames were made up to give a range of temperatures between 1800 K and 2700 K, with constant unburnt flow rate. Table 1 (Figure 7) shows the temperatures, unburnt compositions, and equilibrium burnt compositions for the flames used in the quantitative studies on the aluminium reactions. The other principle components of the flame not shown in the table were NH_3, NO and N_2. The preheating of the gases and the use of the aluminium isopropoxide delivery system, caused a 40 K rise in the temperature of the unburnt gas mixture, as measured by a thermocouple at the burner face. Reversal measurements on the preheated flames showed that their temperatures had been raised by some 15 K, and these are shown as the second set of temperatures in Table 1.

Figure 7

TABLE I

FLAME COMPOSITIONS AND TEMPERATURES

Flame	Inner Flame Unburnt Composition			Burnt Composition Partial pressures atm.					Reversal Temp. K.	Reversal Temp. of "preheated" flames K
	Litres/min.									
	H_2	O_2	N_2	H_2O	H_2	OH	H	O		
A	8.2	2.8	9.0	3.2×10^{-1}	1.5×10^{-1}	1.7×10^{-3}	4.5×10^{-3}	3.3×10^{-5}	2336	2351
B	8.56	2.86	8.56	3.3×10^{-1}	1.64×10^{-1}	2.1×10^{-3}	5.6×10^{-3}	4.5×10^{-5}	2370	2385
C	8.2	3.0	8.8	3.5×10^{-1}	1.3×10^{-1}	3.4×10^{-3}	6.4×10^{-3}	1.1×10^{-4}	2427	2442
D	9.24	3.03	7.7	3.6×10^{-1}	1.8×10^{-1}	3.8×10^{-3}	9.2×10^{-3}	1.2×10^{-4}	2468	2483
E	8.?	3.2	8.6	3.7×10^{-1}	1.07×10^{-1}	5.7×10^{-3}	7.7×10^{-3}	2.6×10^{-4}	2487	2503
F	9.6	3.2	7.2	3.7×10^{-1}	1.9×10^{-1}	4.8×10^{-3}	1.1×10^{-2}	1.8×10^{-4}	2507	2522
G	10.2	3.4	6.42	3.9×10^{-1}	2.0×10^{-1}	8.4×10^{-3}	1.8×10^{-2}	4.7×10^{-4}	2607	2622
H	11.0	3.66	5.33	4.3×10^{-1}	2.2×10^{-1}	1.1×10^{-2}	2.2×10^{-2}	7.0×10^{-4}	2655	2670
I	10.9	3.62	5.28	4.8×10^{-1}	1.6×10^{-1}	1.6×10^{-2}	2.1×10^{-2}	1.2×10^{-3}	2675	2690

The calculation of the equilibrium concentrations of the various flames were computed at the R.P.E. Westcott, by kind permission of Mr. H. Williams. The procedure follows the method of Damköhler and Edse[40] described by Gaydon and Wolfhard, in which enthalpy temperature and composition are solved from mass and heat balance equations involving the principle reactions in the flame, by successive approximations. The reactions considered included:-

$$H_2O \rightleftarrows H_2 + \tfrac{1}{2}O_2$$
$$H_2O \rightleftarrows \tfrac{1}{2}H_2 + OH$$
$$\tfrac{1}{2}H_2 \rightleftarrows H$$
$$\tfrac{1}{2}O_2 \rightleftarrows O$$
$$\tfrac{1}{2}N_2 \rightleftarrows \tfrac{1}{2}O_2 + NO.$$

Equilibrium constants were taken from the J.A.N.A.F. tables[5]. The programme produced the equilibrium compositions at the given reversal temperatures of the unpreheated gases shown in table 1 and also at the calculated adiabatic temperatures. Due to heat losses from the flame the adiabatic temperatures were in excess of the measured ones by amounts of 10 K at 2000 K, to 50 K at 2675 K.

The extent of the disequilibrium of the principle radical species, H, OH and O was assessed using the lithium/sodium comparison method of Bulewicz, James and Sugden[18]. This is based on the fact that sodium forms essentially no compounds in the flame, but lithium forms appreciable amounts of LiOH by the equilibrated process

$$Li + H_2O \rightleftarrows LiOH + H$$

Comparison of the intensities of the lithium and sodium doublets at 6707 Å and 5896 and 5890 Å, allows the calculation of the amount of lithium bound as the hydroxide. Knowing the equilibrium constant for the above reaction and a calculated value of $[H_2O]$ at the flame

Figure 8 hydrogen radical concentrations (2268K)

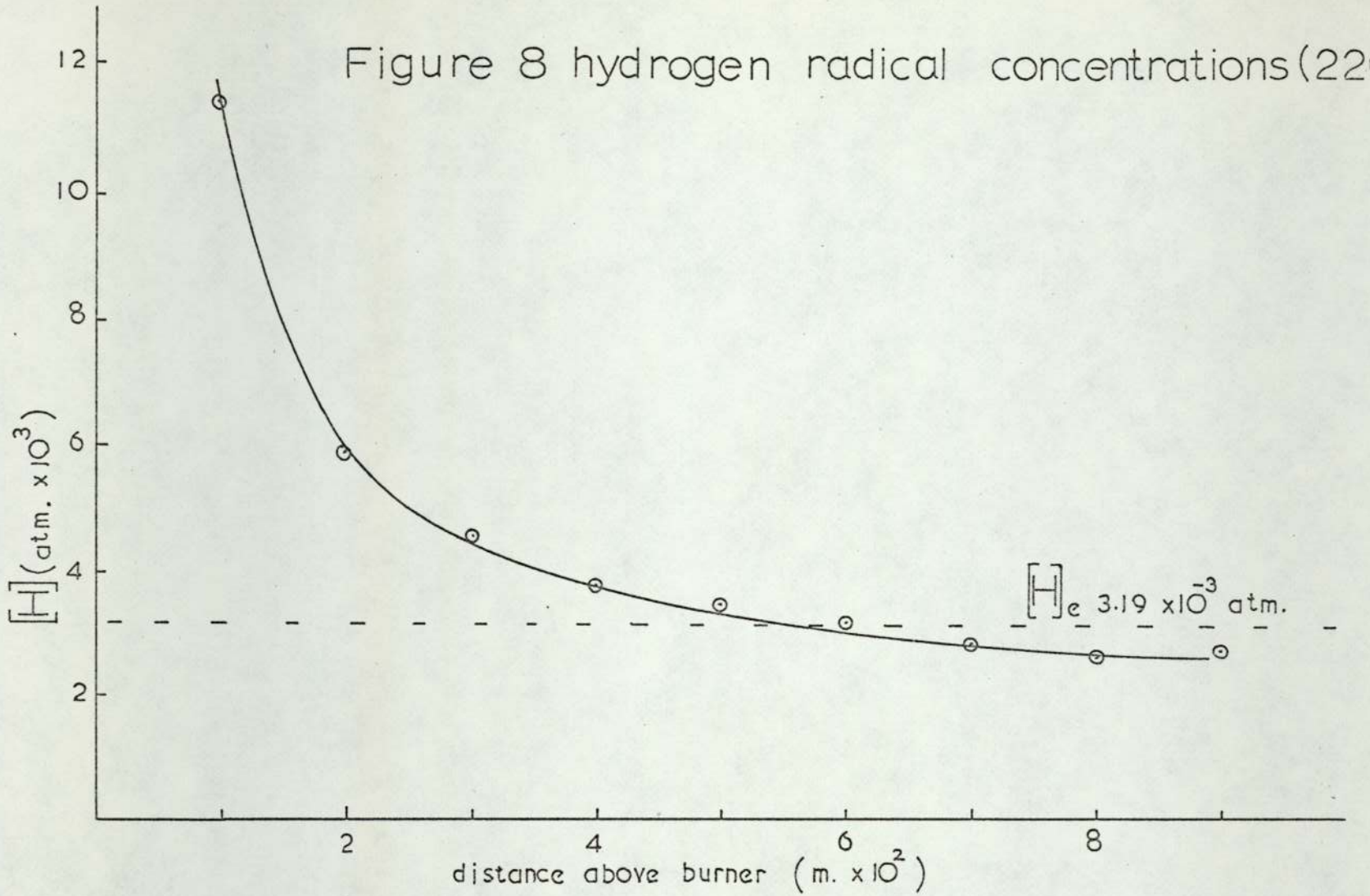

temperature, $[H]$ can be found. The concentrations of the other two radical species are then calculated from consideration of the two balanced reactions

$$H_2O + H \rightleftarrows H_2 + OH$$

$$H + OH \rightleftarrows H_2 + O$$

Dilution plots for the delivery of lithium and sodium to the flame as sprays of their chlorides, were carried out to ensure that the measurements were performed in the absence of self absorption. The oscillator strengths were taken from the tabulations of Corliss and Bozman[41]. The values of $[H_2O]$ and $[H_2]$ used initially were those from Table 1, but the calculation was recycled at least once at each point to ascertain the effect on $[H_2O]$ and $[H_2]$ of excess amounts of the radical species.

A plot of $[H]$ against height in the flame at a temperature of 2268 K, is shown in Figure 8, and it can be seen that the species is only slightly above its equilibrium level, also marked on the graph. This was as expected, and at higher temperatures, and at heights greater than 2×10^{-2} m in the flame the calculated equilibrium concentrations were used in the second and third law estimations.

CHAPTER 4

SPECTROMETRIC STUDY OF ALUMINIUM SEEDED FLAMES

4.i. Introduction

Much of the previous research on the burning of aluminium and aluminium compounds have been studies on the combustion of the materials in particulate or wire form. Notably the studies of Drew, Gordon and Knipe[42], Bruzustowski and Glassman[43, 44, 45] and Mellor and Glassman[46] have shown the importance of the melting point of alumina on the ignition temperature of an aluminium particle, and have attempted to describe the burning of a metal particle in terms of a vapour phase diffusion flame model. Friedman, Macek and Semple[47] in similar studies have observed, but only partially explained, the effect of the water vapour content of the ambient atmosphere on the luminous trail left by burning particle. Other studies have been those of White and Allen[49] on the trails of high speed aluminium pellets and the work of Vanpee on low pressure trimethylaluminium - oxygen flames[50, 3] and trimethylaluminium seeded cyanogen-oxygen flames[51]. The chief conclusions drawn from these studies were that chemiexcitation of the AlO emission was likely in the low pressure flames, and in the latter case the monoxide appeared to be at levels considerably above its calculated equilibrium concentration.

Knudsen cell vapour pressure studies by Brewer and Searcy[52] of the equilibria above an alumina/aluminium melt, and mass spectrometric studies on similar systems by Drowart et al[53] have been the most important thermochemical studies to date, and the principle species present at temperatures around 2000 K were found to be Al_2O and Al_2O_2. No hydroxi or hydro-oxi species were reported supporting the findings of Gatz, Rosser and Smith[54], who found an absence of such species in a mass spectrometric study of alumina bearing flames.

Walter, Efinmenko and Lofgren[55], however, found vapour pressures above an alumina melt in contact with water vapour to be some five times greater than those found by Brewer and Searcy[52] and proposed the formation of AlOH to account for this.

The only quantitative thermochemical study of aluminium in flames known to the author is that of Gurvich and Veits[6], in which aqueous sprays of aluminium chloride were introduced as minor constituents to acetylene-oxygen flames, and the absolute concentration of the free metal found by comparing the intensity of the resonance lines to that from a standard lamp source. The total delivery of the aluminium was known and by making the assumption that the monoxide was the only important species present, its concentration was found by the difference. The stability of the monoxide was then ascertained from a third law calculation. Flame temperatures and compositions used were calculated theoretically. The bond energy produced was in fact slightly higher than other quotes, but the work is criticised on the grounds that no attempt was made to follow or measure directly the concentration of the monoxide.

Some indication of the likely behaviour of aluminium in flames may be gained from the results of flame studies involving elements close to the metal in the periodic table. The Group II metals have been shown to form compounds of the type MO, MOH, and $M(OH)_2$[56, 57, 58] together with appreciable amounts of the ionised species MOH^+ and M^+[29]. The bond energies involved are large and therefore at moderate temperatures the compounds formed are in excess with respect to the freee metal concentration. The lower Group III members have also received attention. Gallium and Indium form monoxi[59] and hydroxi species[19], and thallium undergoes a small amount of compound formation mainly to the hydride[19].

The appropriate bond energies of the compounds formed have been deduced from these photometric studies, but it is possible that in the work of Gurvich[59] the hydroxi, rather than the monoxi, species was involved. A parellel situation to this was the confusion between CaO and CaOH as being the origin of the green and yellow molecular emissions from flames containing calcium. This was finally resolved in favour of CaOH by James and Sugden[60].

Studies of combustion systems involving boron with hydrogen and oxygen reveal a more complicated picture, with the formation of HBO, BO, BO_2 and HBO_2[61, 62]. Under such flame conditions as described in this work HBO_2 would be the most important species, with the free boron present only in very small amounts. Therefore it would not seem unreasonable to expect in the case of aluminium the formation of compounds other than the monoxide, and in hydrogen flames, hydroxi or hydro-oxi species might well be present as the major species.

The principle molecular emissions from flames containing aluminium are those assigned to AlO. The major systems are the $A\,^2\Sigma^+ \rightarrow X\,^2\Sigma^+$ bands 5500 Å - 4300 Å (Pearse and Gaydon[63]), the $B\,^2\Pi \rightarrow X\,^2\Sigma$ bands at 3000 Å (Goodlet and Innes[64]), and the $a\,^2\Sigma \rightarrow X\,^2\Sigma$ system around 2600 Å (Kishnamachari et al[65]). Other systems not involving the assumed ground state of the molecule $X\,^2\Sigma^+$, are the $B\,^2\Pi \rightarrow A\,^2\Sigma$ bands at 8000 Å (Tyte[66]), and the $^2\Delta_i \rightarrow {}^2\Pi_i$ bands at 2500 Å and $^2\Sigma^+ \rightarrow {}^2\Pi_i$ bands at 2800 Å, assigned by Macdonald and Innes[67] involving a new lowlying $^2\Pi_i$ state of the molecule. The two latter systems had been previously reported by Coheur and Rosen[68]. The blue-green system $A\,^2\Sigma^+ \rightarrow X\,^2\Sigma^+$ appears as the major system in atmospheric flames and is easily identified from its series of well spaced sequence of band heads, thereby lending itself readily to quantitative study.

Radiation from the compounds HBO_2, BO_2 and BO has been detected from boron seeded flames by several workers. In such a study by Morrison and Scheller[61], where slurries of aluminium boron and magnesium were burnt in hydrocarbon air flames, the emission from the boron compounds ~~were~~ was detected in the infra red, whereas no emissions in this region were detected or assigned to the corresponding aluminium compounds. The oxide B_2O_3 is known in the gas phase, e.g. Inghram, Porter and Chupka[69], though Al_2O_3 is not, but Vanpee et al[50] have pointed to the spectral intensity maxima, at 2710 Å and 2780 Å shown in a trimethylaluminium-oxygen flame, which exhibit a complicated vibrational structure indicating a polyatomic emitter, to be of interest in this context.

Also found by Vanpee et al[3] in these flames, burning at low pressure, was that two types of continuum were being emitted. That in the red and near infra-red was thought to be the normal greybody emission from alumina particles present but a second continuum, with an observed maximum at 4750 Å in the reaction zone, shifting to 4400 Å in the burnt gases, was also detected. The explanation given for this second continuum was that it appeared through the radiative ~~active~~ combination of AlO with atomic oxygen, by the following sequence of reactions, as suggested by Rosenburg, Golomb and Allen[70] to account for the blue-green continuum observed from the release of trimethylaluminium into the upper atmosphere.

$$AlO + O \rightarrow AlO_2^*$$

$$AlO_2^* \rightarrow AlO_2 + h\nu \quad \text{pseudo-continuum}$$

$$AlO_2 + O \rightarrow AlO + O_2$$

After considering the previous work on aluminium seeded flames it was decided to carry out a flame photometric investigation using the general approach of the Sugden school[17, 71, 72, 19], with a

view to estimating the bond dissociation energy of the AlO molecule, and to examine the possible formation of other aluminium species present. Direct measurement of the monoxide concentration in absolute terms was not possible initially, due to the lack of an experimentally determined oscillator strength of the $A^2\Sigma^+ \rightarrow X^2\Sigma^+$ transition of AlO so that a second law approach was utilised. Recently a value has emerged from the flame studies of Vanpee et al[51], enabling third law calculations of D_o^oAlO to be made.

The principle estimates of the bond dissociation energy of AlO up to 1963 are summarised in the J.A.N.A.F. Tables[5]. They are 480 kJ mol^{-1} from the mass spectrometric inviestigation by Drowart et al[53], 575 kJ mol^{-1} from the flame photometric studies of Gurvich and Veits[6] 532 kJ mol^{-1} derived from the vapour pressure measurements above aluminium and alumina melts by Brewer and Searcy[52] and 486 kJ mol^{-1}, from the Birge extrapolation on the AlO bands, by Becart and Declerck[73] the preferred value being 480 kJ mol^{-1}. More recently Tyte[74] has proposed a figure of 439 kJ mol^{-1} based on a shock tube investigation, but his results have been reinterpreted by Macdonald and Innes[67], in the light of the existence of the new lowlying $^2\Pi_i$ state, to yield a higher value of 506 kJ mol^{-1}. Reports based on the work described here by Newman and Page of 606 kJ mol^{-1} [75], and 594 kJ mol^{-1} [76], tend to support the higher figure proposed by Gurvich and Veits[6].

4.ii. Experimental

The chief difficulty encountered in the work was in finding suitable means of seeding the flame with aluminium in large enough quantities to render the relevant spectral emissions susceptable to quantitative study. The usual method employed in these studies has

been to introduce the material as an atomised spray of a solution of one of its salts, often the chloride or nitrate, and this procedure was followed here.

Using 0.2 molar solutions of the nitrate and sulphate little spectral emission was detected even at the highest temperatures. Neither the UV system of AlO or the metal resonance lines at 3961 and 3944 $\mathring{A}$ were seen, but some diffuse activity was noticed in the region of the blue-green system. It was not possible to identify the features due to the wide slit widths used and the low intensity of the signal but it would seem likely that this was in fact a very weak emission of the $A\,^2\Sigma^+ \rightarrow X\,^2\Sigma^+$ bands. Plate photographs with exposure times of up to 6 hours for the nitrate and sulphate deliveries revealed no more than the photomultiplier recording system had done, and therefore the use of these two salts was abandoned.

Aqueous solutions of the chloride gave better results this time the blue-green system was clearly evident at temperatures above 2400 K. The aluminium lines and the U.V. system were however not detected, and it became apparent that alternative means of seeding would have to be considered.

It was decided that a greater degree of success would be achieved if the aluminium was introduced in the form of the vapour of its chloride or isopropoxide (MP's 453 K and 391.5 K), both of which would have sufficient vapour pressures at temperatures not too far above room temperature. The furnace to effect this delivery was constructed and has been described in its final form. In its original form electrical heating by means of 15 m of nichrome wire wound around the duralamin block was used and the system was then thermostated by way of a mercury contact thermometer immersed in a well, drilled into the block, filled with fine copper powder.

Figure 9 the flame spectra

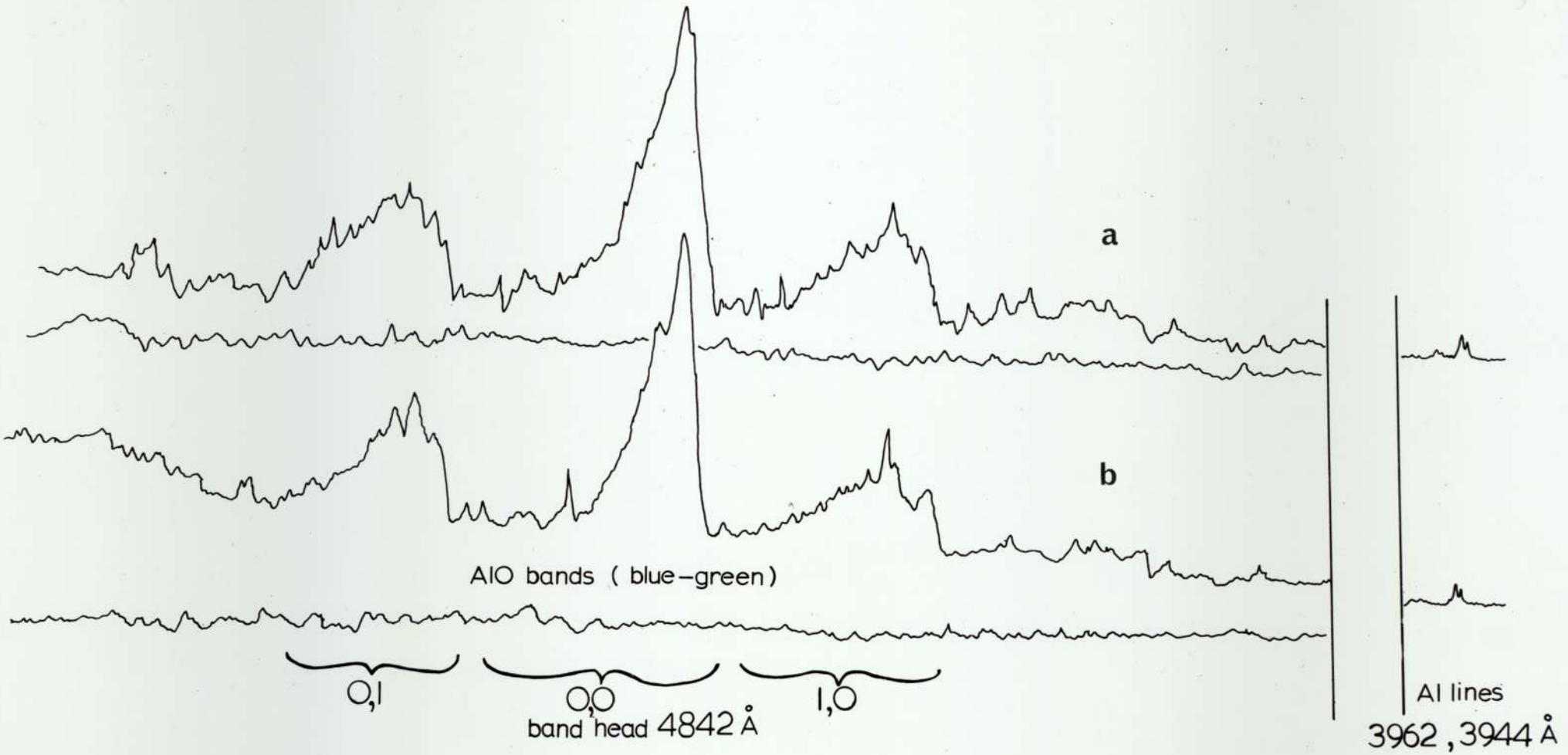

Using aluminium chloride with the furnace at 423 K and a nitrogen flow rate of 1 litre min^{-1} into a flame burning at 2507 K, a pale blue inner flame was produced with the aluminium resonance lines, and blue-green system of AlO easily detected in emission by the scanning unit. No other radiation was detected in the range 2400 Å - 7500 Å which could be attributed to any aluminium containing species. The electrically heated furnace was found to be unsuitable because of the long time it took to attain the operating temperatures and its slow response to the thermostating device, and the oil bath system was adopted and found to be a great improvement in these respects. After the initial studies the use of aluminium chloride was dropped in favour of the aluminium isopropoxide due to the attack on the furnace by hydrogen chloride released from the former when in contact with water vapour.

Sufficient quantities of the isopropoxide vapour could be delivered to the flame with the furnace just below the melting point of the alkoxide, providing that it has first been raised a temperature well above this point. The sample of aluminium isopropoxide obtained from Hopkins and Williams Ltd. was found to be heavily contaminated with alumina, and inert to water, and it was thought that in the preheating process some break up of the oxide coating occurred when the material was molten. The spectra produced with the isopropoxide was almost identical to that produced with the chloride, showing to a first approximation for these two compounds, that their molecular structure had no effect on the eventual equilibria achieved in the flame.

The isopropoxide delivery was used for the majority of the work, but an alternative method, that of atomising solutions of aluminium chloride in methanol was found to give sufficiently intense spectra, and to be suitable for the third law measurements and the estimation of the $A^2\Sigma^+ \rightarrow X^2\Sigma^+$ transition oscillator strength. When making up

these solutions, evolution of hydrogen chloride was detected indicating replacement of the chlorine by methoxi groups. Whilst using this spray the water in the cooling chamber of the burner was maintained at 353 K, but this was found to have no measurable effect on the flame temperatures.

The technique used in the spectral intensity measurements was to scan any particular feature some five to ten times, and take the mean intensity providing that each reading was consistent to the rest with in 10%. Peak height measurements were used on the aluminium resonance lines, except for the determination of the absolute metal concentration by comparison with the sodium D line emission, where peak area measurements were used. The concentration of AlO was followed as the peak height of the unresolved $\Delta v = o$ sequence (o,o band head 4842 $\overset{o}{A}$) of the $A^2\Sigma^+ \rightarrow X^2\Sigma^+$ emission bands. This was found by direct comparison to be a representative measure of the total area under the trace (band intensity) between 4400 $\overset{o}{A}$ and 5400 $\overset{o}{A}$, over the temperature range used in the study.

4.iii. Results

The spectral features of interest from an isopropoxide delivery to a flame at 2385 K, the blue-green system and the metal resonance emission ($3\,^2P_{3/2} - 4\,^2S_{\frac{1}{2}}$, $3\,^2P_{\frac{1}{2}} - 4\,^2S_{\frac{1}{2}}$) are shown in Figure 9(a). Also displayed for comparison 9(b) is the spectrum obtained from a flame at 2507 K seeded with aluminium metal powder, using the delivery devised by Miller[7]. The spectra obtained here shows the blue-green bands superimposed upon a continuum background due to the presence of the condensed metal and droplets of alumina. Some suggestion of a continuous emission exists in (a), but at higher temperatures where the spectra could be examined under greater resolution it was seen to be non-existent. No indication of a continuum exhibiting a

maximum in the blue, assigned by Vanpee[3] to the emission from chemi-excited AlO_2 molecules was observed.

At temperatures below 2300 K a distinct change in the visual appearance of the flame occurred. An intense white emission was observed in the reaction zone giving way to streaks of white-grey light in the burnt gases, due to the presence of condensed particles, presumably of alumina, which are known to give luminescent trails in flames. The proximity of the temperature at which conditions in the flame changed to the melting point of alumina 2288 K, is of obvious significance. As the prime object of the study was to examine the gaseous reactions of aluminium in the flames, this necessitated that the quantitative study be carried out above the temperature of 2300 K, where the recombination of the radical species were equilibrated.

As in the flame study of Morrison and Scheller[61] the U.V. systems of AlO were not detected, though in these flames, the strongest reported feature, the 0,0 band head of the $B^2\Pi_i - X^2\Sigma^+$ system at 3022 Å, would be covered by the bands of the $B^2\Sigma^+ - {}^2\Pi_i$ emissions of OH, which are naturally very intense in flames of this sort.

Figure 10 shows the intensity of the $A^2\Sigma^+ \rightarrow X^2\Sigma^+$ bands of AlO, and the Al resonance doublet as functions of gas flow rate through the isopropoxide furnace. The vapour pressure data of Wilhoit[77] indicates that a flow rate of 1 litre min^{-1} should produce a total partial pressure of aluminium in all forms of 9.41×10^{-4} atm. Figure 11 shows the intensity of the AlO bands as a function of $AlCl_3$ concentration when methanol solutions were sprayed into the flame. Here the maximum partial pressure was estimated to be 2×10^{-4} atm from a comparison of the intensity of the AlO bands shown with that found when an aqueous solution was sprayed in from

Figure 10 delivery of $Al(OC_3H_7)_3$

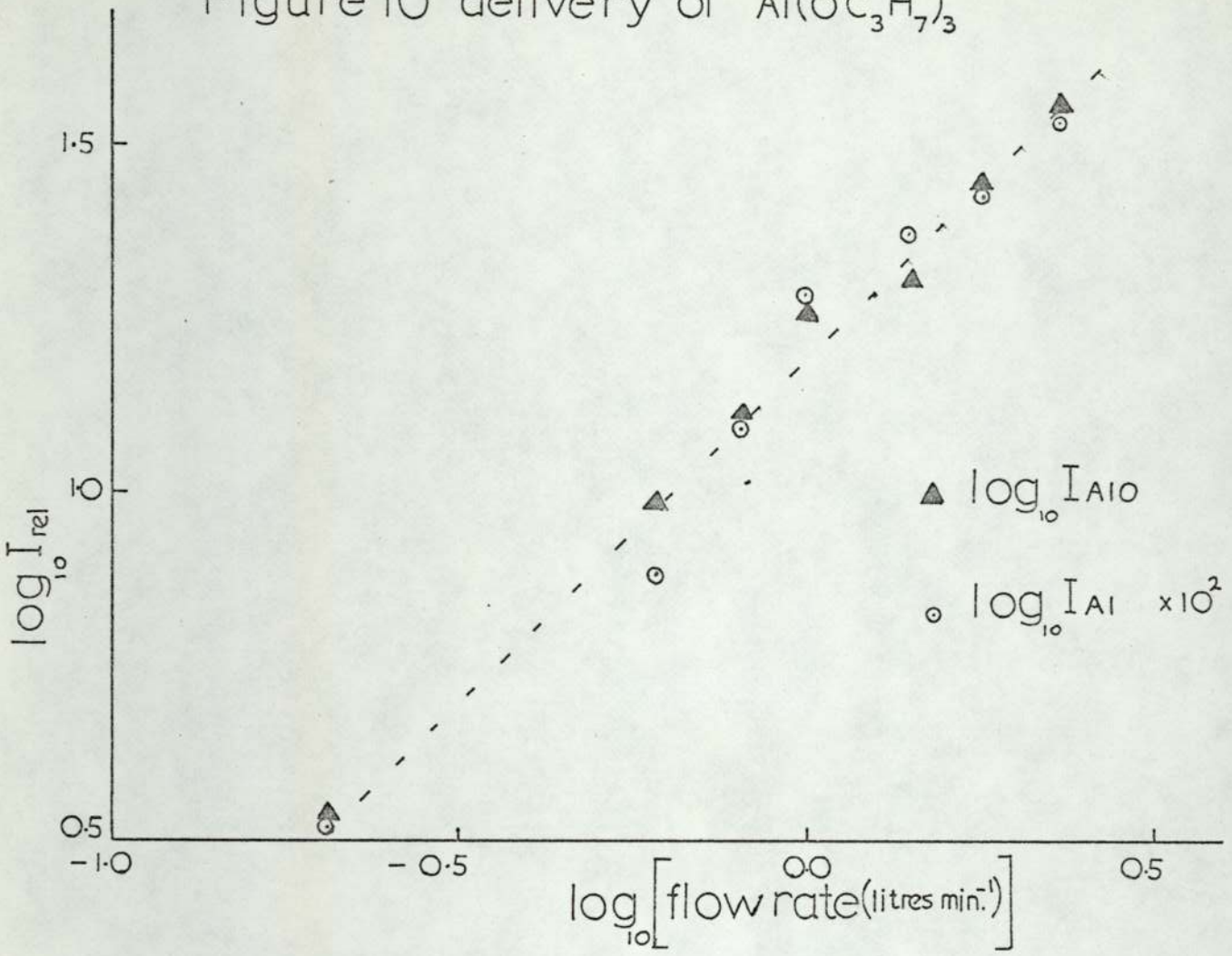

Figure 11 delivery of $AlCl_3$ solution

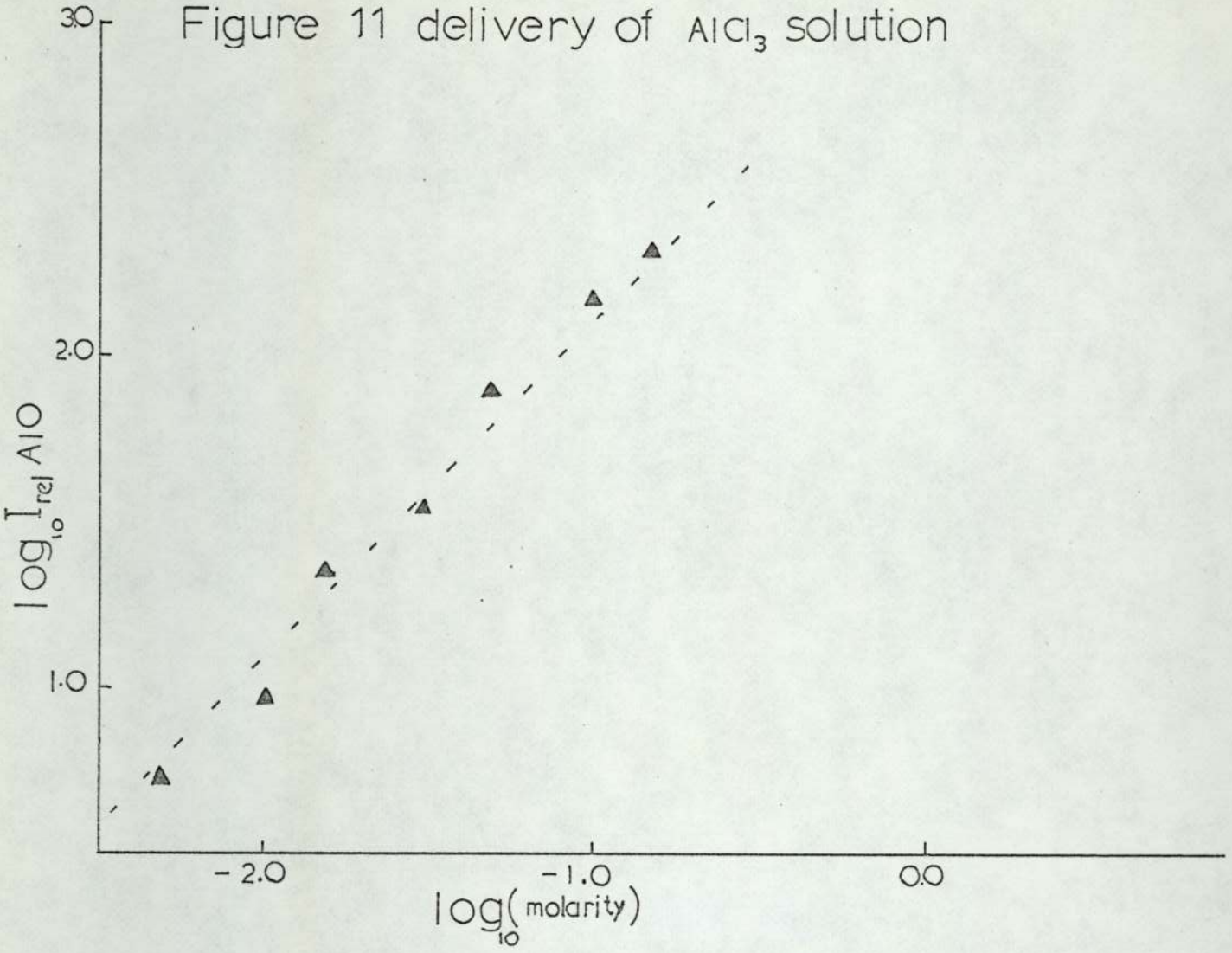

the calibrated atomiser. The increased delivery with the organic solvent was found to be within 20% of that expected on a basis of the volume sprayed in a given time for each solvent. The measured intensities in Figures 10 and 11 were corrected by a factor, vT, after James and Sugden[16], to account for the variation of flame volume with temperature, and unburnt composition.

The linearity shown in both figures between the intensity and total aluminium pressure indicated an absence of appreciable self absorption and of species containing more than one aluminium atom. These measurements were made at 0.045 m above the burner face and repeated at 2351 K and 2690 K and found to give the same results.

The intensity of the metal resonance lines was very much less than that of the AlO emission, which was to be expected since equilibrium considerations using existing data showed that at temperatures in the order of 2×10^3 K - 3×10^3 K, $[AlO] \gg [Al]$. Consequently, if AlO is the major species, and the emission is thermally excited, then plots of log I_{rel} AlO vs $^1/T$ should give a straight line with the slope corresponding to the excitation energy of the transition. A similar plot for the aluminium resonance lines should illustrate the dependence of the free metal concentration on the flame composition. Both plots are shown in Figure 12, the result for the resonance lines being as expected. The plot for the AlO band intensity does not exhibit a uniform slope of 250 kJ appropriate to the excitation energy of the $\Delta v = o$ bands, an approximate fit to the points would give 630 kJ.

Three reasons for this large temperature dependence of the AlO bands were thought possible. Firstly, either or both Al and AlO are chemiexcited at three body collisions, with flame radical species as demonstrated by Padley and Sugden[78]. This was thought to be unlikely as the temperatures are too high, the measurements too far

Figure 12 temperature dependence of I_{AlO} and I_{Al}

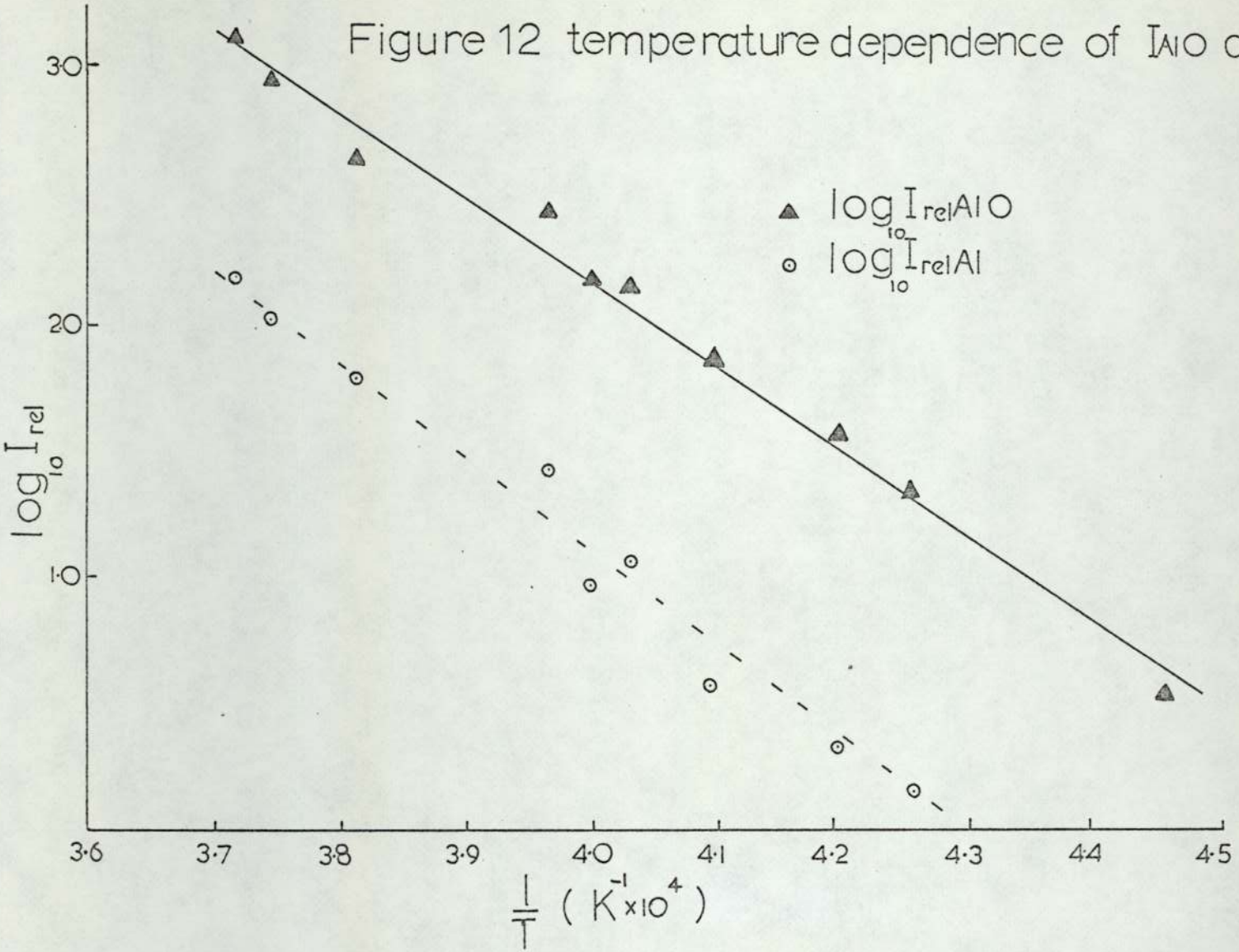

down stream and the departure of the radical species from equilibrium too small for significant contributions from such processes as

$$Al + H + H \rightarrow Al^{*} + H_2$$

and

$$AlO + H + H \rightarrow AlO^{*} + H_2$$

Secondly, such processes as

$$Al + O + M \rightarrow AlO^{*} + M$$

as suggested by Harteck and Reeves[79] to account for the AlO band emission when $AlMe_3$ is released into the upper atmosphere, were likewise not thought to be important. The work of Rautenburg and Johnson[80] on the reaction of Al vapour and O_2 in a flash bulb at 2000 K and that of Zhadanova and Sokolov[81] on a solid aluminium and oxygen system at 5000 K, indicate that under these conditions the excitation of the $A^2\Sigma^+ \rightarrow X^2\Sigma^+$ bands is thermal, and this would be expected to be the case in a flame burning at atmospheric pressure and at temperatures of 2300 K and above.

Thirdly, it seems most likely that the concentration of both AlO and Al are strongly dependent on flame composition and that a third, unidentified compound is present as the major species.

4.iv. The Bond Dissociation Energy of AlO as Estimated by Second Law Methods

Although both Al and AlO may be minor constituents of the system the bond energy of AlO may be estimated from the measured intensities from Al and AlO and the known concentrations of the flame radical species. A number of possible processes for the

production of AlO from free aluminium atoms may be written down among them:-

$$\text{I} \quad Al + H_2O \rightleftarrows AlO + H_2$$

$$\text{II} \quad Al + OH \rightleftarrows AlO + H$$

$$\text{III} \quad Al + O_2 \rightleftarrows AlO + O$$

At temperatures above 2300 K these processes will become indistinguishable from the elementary one.

$$\text{IV} \quad Al + O + M \rightleftarrows AlO + M$$

Figure 13 shows the appropriate second law plot for process IV where $\log I_{rel} [AlO]/I_{rel} [Al] [O]_e$ is plotted against reciprocal temperature. The slope leads to a value for D°_{2500} AlO of 607 ± 34 kJ mol^{-1}, in good agreement with the findings of Gurvich and Veits[6]. Second law plots for processes I and II were found to give equally good straight lines and as expected produced the same result for D°_{2500} AlO.

The partial pressure of free Al atoms produced in flame F (2507 K) from an $AlCl_3$/methanol spray was estimated to be 3.4×10^{-9} atm by comparison of the Al resonance emission intensity, with that from the D lines emitted from a known number of sodium atoms in the flame. Using the value of D°_{2500} AlO, found above and the entropy data from[5], the partial pressure of AlO was calculated to be 1.06×10^{-6} atm from the relationship

$$\Delta H^{\circ}_T = T \Delta S^{\circ}_T - RT \ln K_p$$

The total partial pressure of aluminium in all forms was found to be 1.54×10^{-4} atm from the known delivery of the atomiser with the organic solvent.

Figure 13 second law plot for process IV

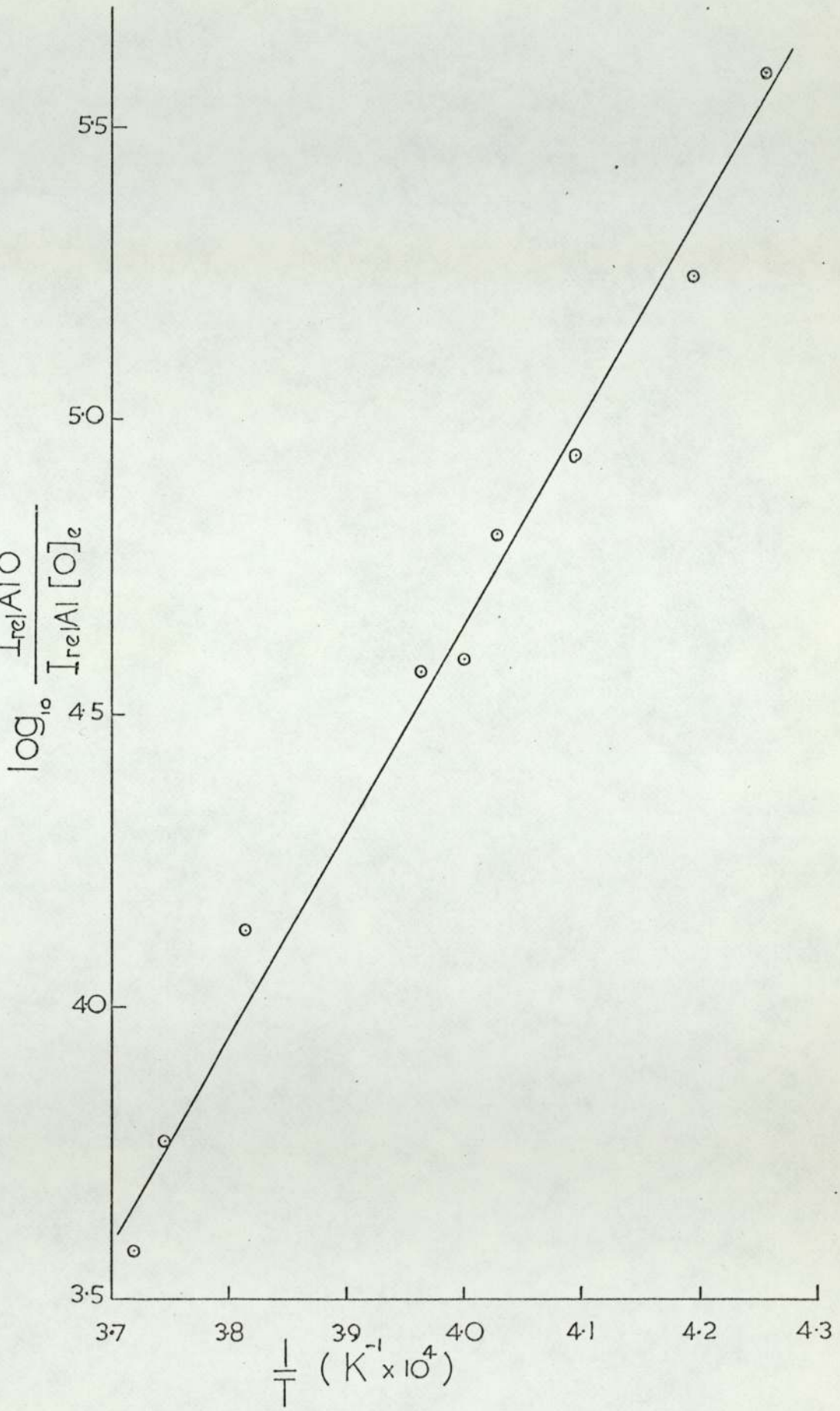

When the isopropoxide was added as the vapour, the total partial pressure of aluminium in all forms was calculated to be 9.41×10^{-4} atm using the vapour pressure data of Wilhoit[77] and the partial pressure of AlO in equilibrium with the free metal was found to be 1.65×10^{-6} atm. Both sets of measurements indicate that the bulk of the metal is present in some form other than the monoxide.

4.v. The Bond Dissociation Energy of AlO as estimated by Third Law Methods and the Oscillator Strength of the AlO $A^2\Sigma^+ \rightarrow X^2\Sigma^+$ Emission

Accepting that the monoxide is only a minor constitutent of the system a third law calculation of the bond energy of AlO requires a direct measurement of its concentration. This was obtained from the emission intensity of the $A^2\Sigma^+ \rightarrow X^2\Sigma^+$ bands, using the oscillator strength f_{elec} for this transition of $3.7 \pm 3 \times 10^{-3}$, quoted by Vanpee, Kineyko and Caruso[51] from their recent work on aluminium containing cyanogen-oxygen flames. The measurements were confined to the $\Delta v = o$ sequence.

The intensity of emission for a molecular transition between states $N_{v'}$ and $M_{v''}$ was given by equation 2.20 and the population of the upper state, $N_{nv'}$, by equation 2.21. If for the sake of convenience the vibrational term is written as $E_{v'}$, $I_{\Delta v=o}$, the intensity of the $\Delta v=o$ sequence can be expressed as

$$I_{\Delta v=o} = C_{(\lambda)} N_{TOTAL} f_{elec} g_A e^{\frac{-hc\omega_{o,o}}{kT}} \frac{\sum_{v',v''=o}^{v',v''=k} q_{(v'v'')} W_{(v'v'')}^3 e^{\frac{-E_{v'}}{kT}}}{Q_{elec} Q_{vib}} \qquad 4.1$$

with the introduction of $C_{(\lambda)}$ a constant of measurement and containing the constant terms in equation 2.20. This constant is written as a function of λ, to indicate that it includes the response factors for the change in sensitivity of the photomultiplier with wavelength, and was found using equation 2.9, and the measured D line intensity from a standard delivery of sodium to the flame.

For the calculation of Q_{elec} only the first $A\,^2\Sigma^+$ state and low-lying $^2\Pi_i$ states were included for the excited states. Q_{vib} was evaluated using the formula for $Q_{vib\text{-}rot}$ developed by Brinkley[82]:-

$$Q_{vib\text{-}rot} = \frac{T\,(1 + YT)}{\left[1 - \exp(-1.4388w_o/T)\right]\ 1.4388B_o} \qquad 4.2$$

and

$$Y = \frac{1}{1.4388}\left(\frac{2w_o w_o}{w_o} + \frac{\alpha_o}{B_o} + \frac{8B_o}{w_o}\right)\frac{1}{w_o} \qquad 4.3$$

where w_o and B_o are the rotational constants of the v=o level, $w_o x_o$ is the first anharmonicity constant for that level and α_o the interaction constant between rotation and vibration.

writing that $$Q_{rot} = \sum_{J=o}^{J=\infty} \frac{2J + 1}{\sigma} e^{\frac{-h^2 J(J+1)}{8\pi^2 IkT}} \rightleftharpoons \frac{kT}{hcBv} \qquad 4.4$$

then $$Q_{vib} = \frac{Q_{vib\text{-}rot}}{kT}\ hcBv \qquad 4.5$$

Values of $q_{v'v''}$ the Franck-Condon factors used in equation 3.1 were taken from the data of Herbert and Tyte[83]. It was found that terms involving v'=5 and greater made no contribution to the summation for the purposes of this investigation. From the intensity of the Δv=o sequence produced from the $AlCl_3$/methanol spray, N_{TOTAL} was found to be 2.2×10^{-6} atm, which gives a value for D°_{2500} from a third law calculation of 595 kJ mol^{-1}, in good agreement with the graphical prediction.

Calculation of the f number by a reversal of the above procedure, using the value for D°_{2500} AlO of 607 kJ mol^{-1} from the second law estimation, produces a figure of 6.45×10^{-3}. The estimable error in f_{elec}, however, becomes greater than 100% unless the bond energy is known to better than ± 12 kJ mol^{-1} by virtue of the log K term in the third law equations.

4.vi. General Compound Formation by Aluminium in the Flame

The evidence presented above suggests strongly that the monoxide was not the major species present in the flame, and that since at the temperatures used in the work equilibrium conditions may be assumed to prevail, it is possible to use thermochemical methods to indicate the nature of the unknown constituent(s).

Professor Gaydon[84] has suggested that alumina (MP 2288 K B.P. 3253 K) might be responsible, but above 2300 K, there was no visible evidence of particle formation, and in the presence of a condensed phase the partial pressure of the gaseous species should be independent of the total material present. The polyatomic oxides of aluminium Al_2O and Al_2O_2 are well known, c.f. Drowart et al[53], but while these may be present they cannot be the dominant species or the slopes of Figures 8 and 9 would be ½ not 1. Ionic species

such as AlO^+ are unlikely to be present as little or no positive ion current was detected by an electrostatic probe passed through the flame, and the third law calculations show that if ionic species were the major constituents then the electron concentrations would be approaching the unusually high value of 10^{20} m^{-3}. Also an examination of the negative ions produced by the surface ionisation of aluminium isopropoxide suggested that AlO^-, AlO_2^- or similar species had low stabilities relative to AlO[85].

The most easily acceptable solution seemed therefore to be in the possible formation of one or all of the compounds, $HAlO_2$, HAlO and AlO_2, by comparison with the known behaviour of boron in flames. Assuming that each in turn is the dominant species whose concentration is effectively constant, the second law plots shown in Figure 14 were constructed for processes V - VII.

V	Al	+	O	+	O	$\rightleftarrows$	AlO_2
VI	Al	+	O	+	H	$\rightleftarrows$	HAlO
VII	Al	+	O	+	OH	$\rightleftarrows$	$HAlO_2$

Absolute values of K_p have been plotted, taking the concentration of the major species from the total delivery of the aluminium isopropoxide to the flame, and the concentration of Al from a comparison of the resonance emission with that from a standard delivery of sodium to the flame at each temperature. The third law enthalpy changes for process V - VII were calculated using entropy data for HAlO and $HAlO_2$ from the J.A.N.A.F. tables[5] and an estimated value of S°_{2500} for AlO_2 from a comparison with its boron analogue, BO_2.

The results of the second and third law estimations are shown in Table II, together with the calculated values of ΔH°_{2500} for the formation of BO_2, HBo and HBO_2 by processes V - VII.

Figure 14 second law plots for processes V —— VII

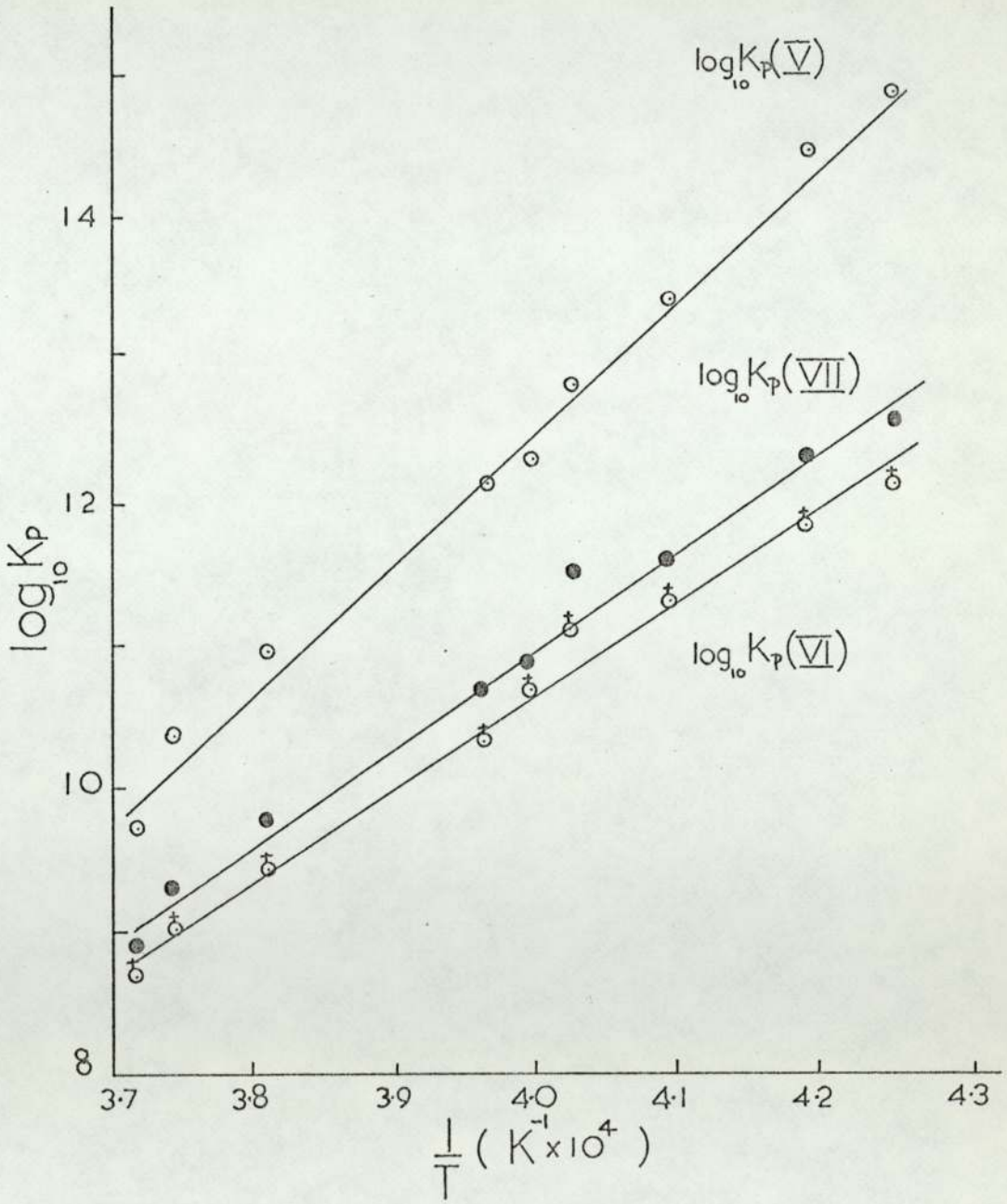

Table II

($kJ\ mol^{-1}$)

	ΔH°_{2500} V (MO_2)	ΔH°_{2500} VI (HMO)	ΔH°_{2500} VII (HMO_2)
M = Al, 2nd Law	-1468 ± 42	-1217 ± 59	-1318 ± 59
M = Al, 3rd Law	-1234 ± 42	-1129 ± 38	-1184 ± 42
M = B, J.A.N.A.F.	-1398	-795	-1418

The mismatch between the second law and third law values for the formation of AlO_2 and $HAlO_2$ appears to be unacceptably large, but consideration of the estimated errors gives a near coincidence for the two sets of figures for the case of HAlO. Here, however, it can be seen that the magnitude of ΔH°_{2500} HAlO is considerably greater than that for the formation of HBO whereas the reverse of this is to be expected.

Further amplification of these points can be gained from the data for the process

VIII $\quad AlO + O \rightleftarrows AlO_2$

IX $\quad AlO + H \rightleftarrows HAlO$

X $\quad AlO + OH \rightleftarrows HAlO_2$

Second law plots for VIII - X (Figure 15) were constructed using the measured AlO band intensity from an $AlCl_3$/methanol delivery, and third law calculations performed with the spectroscopically measured concentration of the monoxide, and the known total delivery to the flame. The results together with the relevant data for the analogous boron compounds are shown in Table III.

Figure 15 second law plots for processes VIII—X

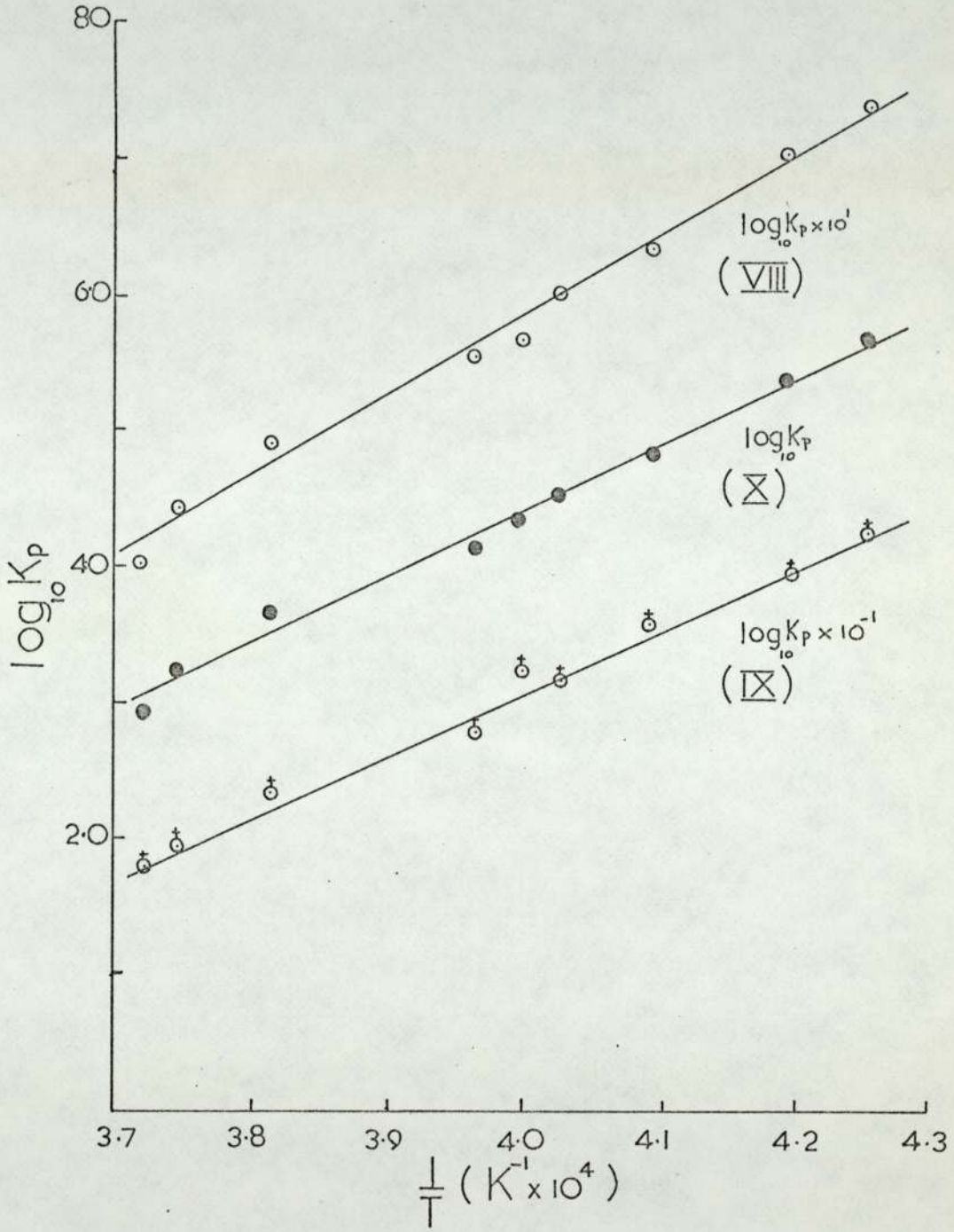

Table III

($kJ\ mol^{-1}$)

	ΔH°_{2500} VIII (MO_2)	ΔH°_{2500} IX (HMO)	ΔH°_{2500} X (HMO_2)
M = Al, 2nd Law	-879 ± 67	-605 ± 50	-723 ± 46
M = Al, 3rd Law	-586 ± 75	-510 ± 75	-556 ± 75
M = B, J.A.N.A.F.	-598	-349	-640

Again the best agreement is obtained between the second and third law estimates for the case of HAlO, but the predicted magnitude of ΔH°_{2500} for process IX is uncomfortably large.

Consider the formation of HAlO or $HAlO_2$, and AlO by reaction with the major constituent of the flame gases:-

$$Al + H_2O \rightleftarrows AlO + H_2$$

$$AlO + H_2O \rightleftarrows HAlO + OH$$

$$AlO + H_2O \rightleftarrows HAlO_2 + H$$

with $[H_2O]$ and either $[HAlO]$ or $[HAlO_2]$ constant at one temperature it can be seen that both $[Al]$ and $[AlO]$ will be proportional to the H or OH concentration. Only in the lowest temperature flames did $[OH]$ and $[H]$ depart even slightly from their equilibrium values, but a small dependence of I_{Al} and I_{AlO}, with height in the flame was observed at a temperature of 2336 K, as shown in Figure 16, which was consistent with this prediction.

Figure 16 variation of I_{AlO} and I_{Al} in the flame

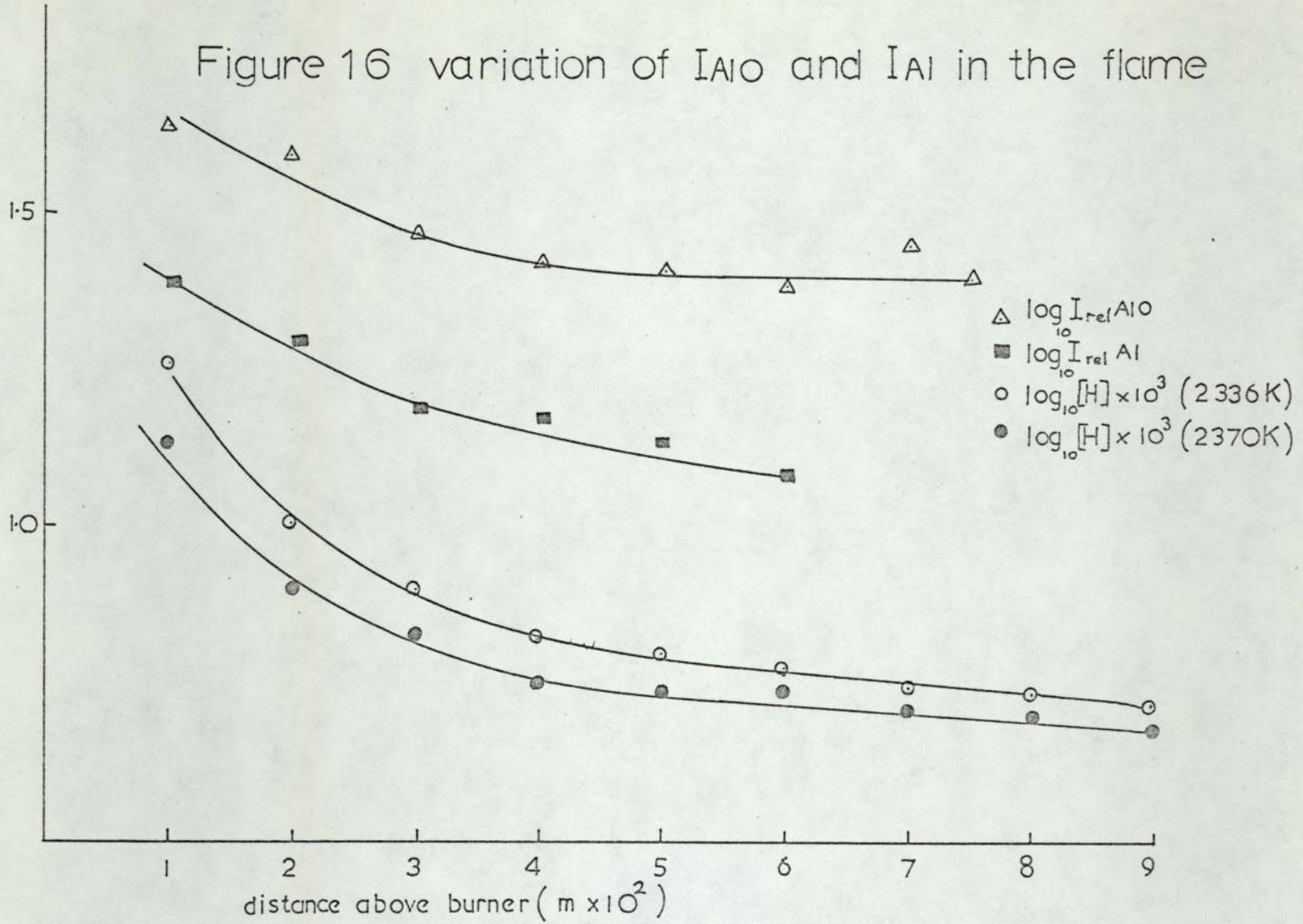

CHAPTER 5

CONCLUDING REMARKS ON THE FLAME PHOTOMETRIC STUDY OF ALUMINIUM

The main points arising from the study are that free aluminium metal and the monoxide species are not the major metal containing species existing in the flame, and that the major species seems to contain only one atom of the metal per molecule. Alternatives to this conclusion would be that either a stable equilibrium situation has not been achieved, or that the excitation of the AlO blue-green bands is not thermal, and previous work on flames of this sort indicates that neither of these suggestions is likely.

It is difficult to assess whether the value for D°_{o} AlO of 594 ± 35 kJ mol^{-1} is more correct than those from other estimations, and no reason can be offered as to why this value is appreciably larger than that from the mass spectrometric study of Drowart et al[53], possibly the most reliable of the estimations. It is close to that from the studies of Gurvich and Veits[6], but here the presence of major species in a flame other than the monoxide, would serve to reduce the figure found for D°_{o} AlO. Brewer and Searcy[52] and Macdonald and Innes[67] have remarked upon the possibility that the lower state of the $A^2\Sigma^+ \rightarrow X^2\Sigma^+$ transition may not be the true ground state of the molecule. If this were the case then a larger excitation correction to the second law plot in Figure 11 would produce an even greater value of D°_{o} AlO from the slope, but give smaller second law values of ΔH°_{2500} for processes VIII - X.

The higher value can be seen to fall well between the bond energies of BO and GaO in Table IV as expected from consideration of its position in the periodic table.

Table IV

(Group IIIb monoxides)

($kJ\ mol^{-1}$)

	D_o^o	
BO	800	(86)
AlO	594	(67)
GaO	484	(59)
InO	430	(59)
TlO	<377	(59)

It is misleading to draw too close a parallel between dissociation energies, force constants, and bond orders except in a semiquantitative way. A comparison of these quantities, however, for the molecules CN, BO, and AlO, which are isoelectronic in their valence shells, shown in Table V, indicates that the bond energy assigned to AlO is of the right order.

Table V

	Force Constant	Bond Order	D_o^o		Ground State
CN	16.29	2.8	700	(87)	$^2\Sigma^+$
BO	13.65	2.5	800	(86)	$^2\Sigma^+$
AlO	5.64	2.0	594		$^2\Sigma^+$

The force constants were calculated from the relationship

$$w_e C = \frac{1}{2\pi}\sqrt{\frac{k}{\mu}}$$

where k is the force constant and μ the reduced mass of the molecule.

The bond order N, was calculated using the empirical relationship of Gordy, suggested by Walker and Straw[11]:-

$$k = 1.67\,N\left(\frac{X_A X_B}{r_e^2}\right)^{3/2} + 0.30$$

Here X_A and X_B are electronegativities on Pauling's scale[88] for a diatomic molecule A-B, and r_e is the equilibrium internuclear separation in angstroms.

The suggestion of either HAlO, $HAlO_2$ or AlO_2 as being possibly the major species present in flame, is at its best only a suggestion, and the main support for the hypothesis lies in the established behaviour of boron in flames of this kind. No direct evidence for their presence has yet been put forward and it would seem to the author that detailed study of the infra-red region of the spectrum from these flames, together with a mass spectrometric investigation should provide the answers to this question. A study of the equilibria existing in a hydrogen free carbon monoxide-oxygen flame seeded with aluminium, would naturally be relevant in this context.

A recent communication from Jensen and Jones[89] has, however, provided what is probably the solution to the question of the unknown aluminium species. From their unpublished evidence on flames seeded with aluminium isopropoxide it appears that the most dominant species is likely to be $Al(OH)_2$, which was not considered above by the author. Using the results obtained here, the heat of atomisation found graphically is 1946 kJ mol^{-1} (2500 K) (Figure 17) which agrees well with a third law estimate of 1958 kJ mol^{-1}. The entropy of $Al(OH)_2$ was estimated from a comparison of the data for $B(OH)_2$, HBO_2, HBO, BF_2, and $HAlO_2$, HAlO, and AlF_2, from the J.A.N.A.F. tables.

Figure 17 second law plot for the atomisation of $Al(OH)_2$

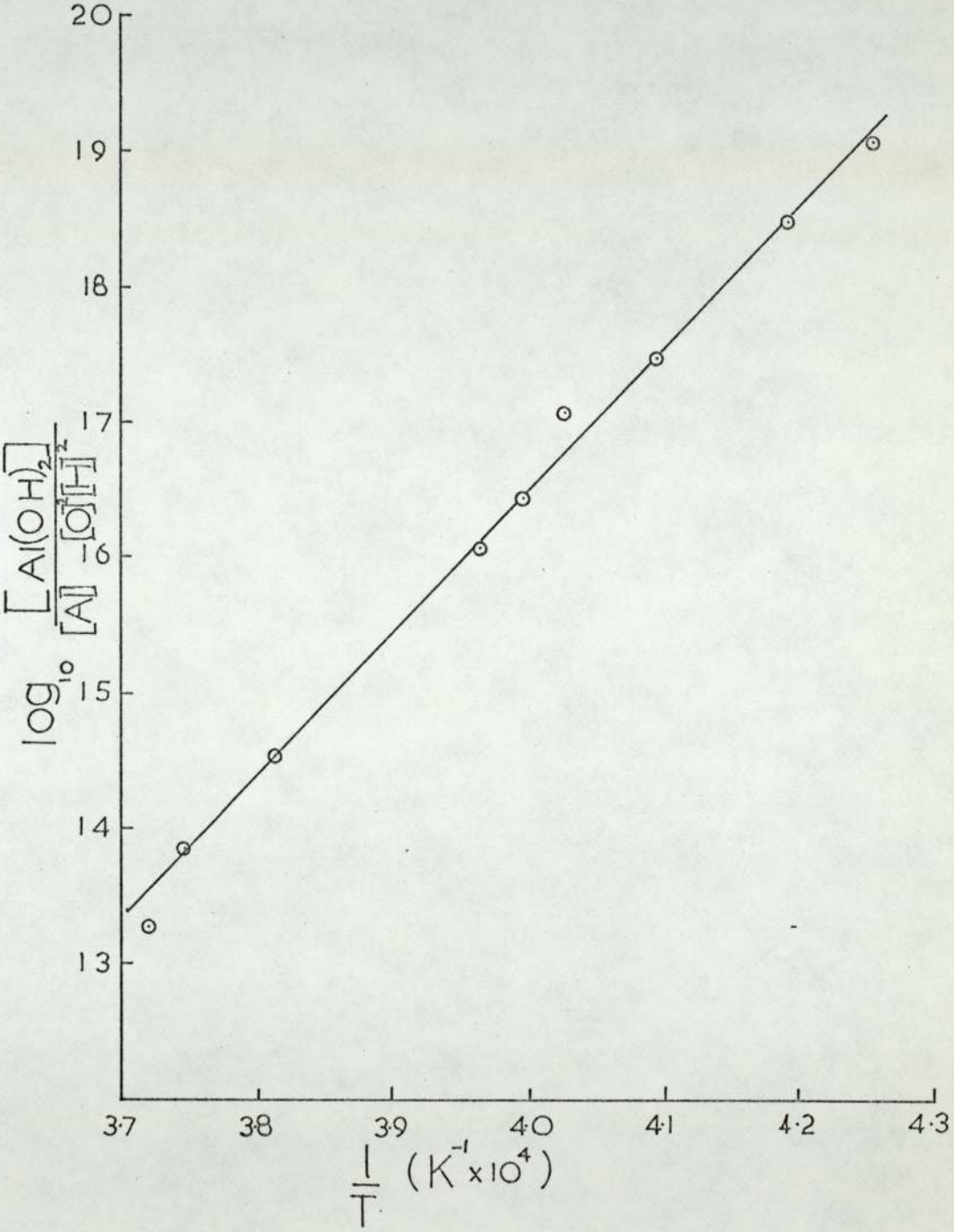

The heat of atomisation of $B(OH)_2$ is 1996 kJ mol^{-1} at 2500 K, showing the expected increase in stability of the boron compound over its aluminium analogue.

The absence of large amounts of the polyatomic oxides Al_2O and Al_2O_2 is somewhat surprising in view of their large heats of formation. Possibly they may be found at lower temperatures below 2300 K where alumina in the solid phase was evident. An aluminium hollow cathode lamp and power supply was assembled with the object of studying the aluminium resonance lines in this region but was never successfully operated.

A continued search for negatively or positively charged ions in aluminium seeded flames would seem worthwhile, and in respect of the latter, the initial observations of a joint study with W. G. Roberts[90] have seemed encouraging. Electrostatic probe measurements in a flame containing a trace of acetylene to which a spray of aluminium chloride in methanol was added have revealed the presence of a large number of positive ions (10^{17} m^{-3}), which exhibit an extremely slow rate of decay with height in the flame, Work is proceeding to investigate this system in more detail.

Finally the study further illustrates the use of the vapours of volatile compounds as superior means of seeding flames with metals to that of atomised sprays. In many cases increased delivery rates may be achieved, and the well recognised effect of the anion attached to the metal in the solution used, on the flame equilibria, may be avoided.

CHAPTER 6

INTRODUCTION TO EXPERIMENTS WITH THE ELECTROSTATIC PROBE

The electrostatic or Langmuir probe has proved a useful tool in the investigation of the levels of ionisation present in a flame plasma, especially in the direct measurement of positive ion densities. It has an advantage of spatial resolution over the measurement of electron densities by microwave attenuation procedures, and the apparatus necessary is simple to assemble and operate, and relatively inexpensive.

The operation of the probe, raised to a certain potential with respect to the plasma with a second probe acting as a second electrode, may usefully be compared to an electrolytic cell, where the current drawn in the external circuit is a function of the charge density in the solution, the applied potential, and local conditions on the electrode surface. Its most frequent use, in flames of the type discussed here, is where the probe consisting of a thin platinum wire, is biased highly negative to the plasma and therefore surrounded by a positive space charge, and the current collected is loosely termed to be the saturated one. The delivery of gases and seeding materials to the plasma is such that the charges are uniformly distributed, and the measurement made is that of a steady state condition.

Miller[7], while using the probe in this manner in a flame containing involatile solid particles, found that above the background current drawn by the probe, there were superimposed pulses of current coinciding with collisions of the probe with the particles. The origin of the pulses presented was the charge transfer involved in the surface emission of electrons from the incandescent particles while in contact with the probe. The variation of this current with the flame

temperature, thought to represent the particle temperature, was related with some success, to the work function of the various materials used.

It was found by the author that an inhomogeneous distribution of charges could be achieved in the flame, by introducing very dilute (low density) sprays of the chlorides of the group I metals, giving again a response from the probe that contained time dependent components. The obvious explanation of this phenomenon was that the highly negative probe was drawing current from charge clouds originating from the isolated evaporated crystals that had entered the flame.

A programme of investigation of these time dependent components was carried out using a variety of volatile seeding materials, together with a re-evaluation of some of the original work of Millers in flames seeded with lanthanum hexaboride powders. Particular attention was paid to the duration of the pulses in view of relating this time to the physical dimensions of the charge clouds, which it was thought might in turn lead to information concerning the evaporation mechanism of the crystals, and also the diffusion rates of the gaseous ions produced.

The work was carried out therefore to find out whether this approach would provide a useful addition to the means of investigating general flame phenomena in seeded flames. The following chapter contains a survey of the principle features of the operation of electrostatic probes with regard to high density plasmas. An attempt was made to characterise the response of the probe to a fluctuating ion flux in a qualitative way, though it was realised that a full description of this situation would involve a proper mathematical analysis, most likely of an extremely complicated nature. It was felt, however, that this analysis was more suited to a theoretical physicist or mathematician, and was not pursued by the author.

CHAPTER 7

THE THEORY OF ELECTROSTATIC PROBES*

7.i. Langmuir Probes in a Collision less Low Density Plasma

The best introduction to the operation of probes is a short discussion of the ideas of Langmuir[92] for a single probe in a low pressure plasma, such as a gas discharge. The current drawn by the probe from the plasma at varying probe bias is shown in Figure 18. In the region AB a saturated electron current is collected due to the formation of a negative space charge over the probe surface. Essentially the current is a space charge-limited one, and further increases in the positive bias will produce no increase in current until the applied bias is sufficient to cause breakdown between the probe and the plasma boundary. A result of this space charge is that the body of the plasma is shielded from the applied voltage. The point Vs marks where the applied voltage is equal to the plasma potential, and both electrons and positive ions may reach the probe. Since the electrons have higher random velocities than the positive ions however, a negative current is collected.

In the transition region BC, the probe becomes less positive than the plasma potential, thus retarding the flow of electrons towards it and attracting a greater number of positive ions. At Vw, known as the wall potential, no net current is drawn. This will be the potential assumed by any isolated body immersed in the plasma. If the probe is biased negative, the number of positive ions collected will exceed that of the electrons and a positive current is registered. As the potential is further increased, a positive space charge is established, and a space charge-limited or saturated positive ion current collected.

* Much of the basic information in this chapter has been taken from the excellent review of the subject by Chen[91].

Figure18 probe characteristic

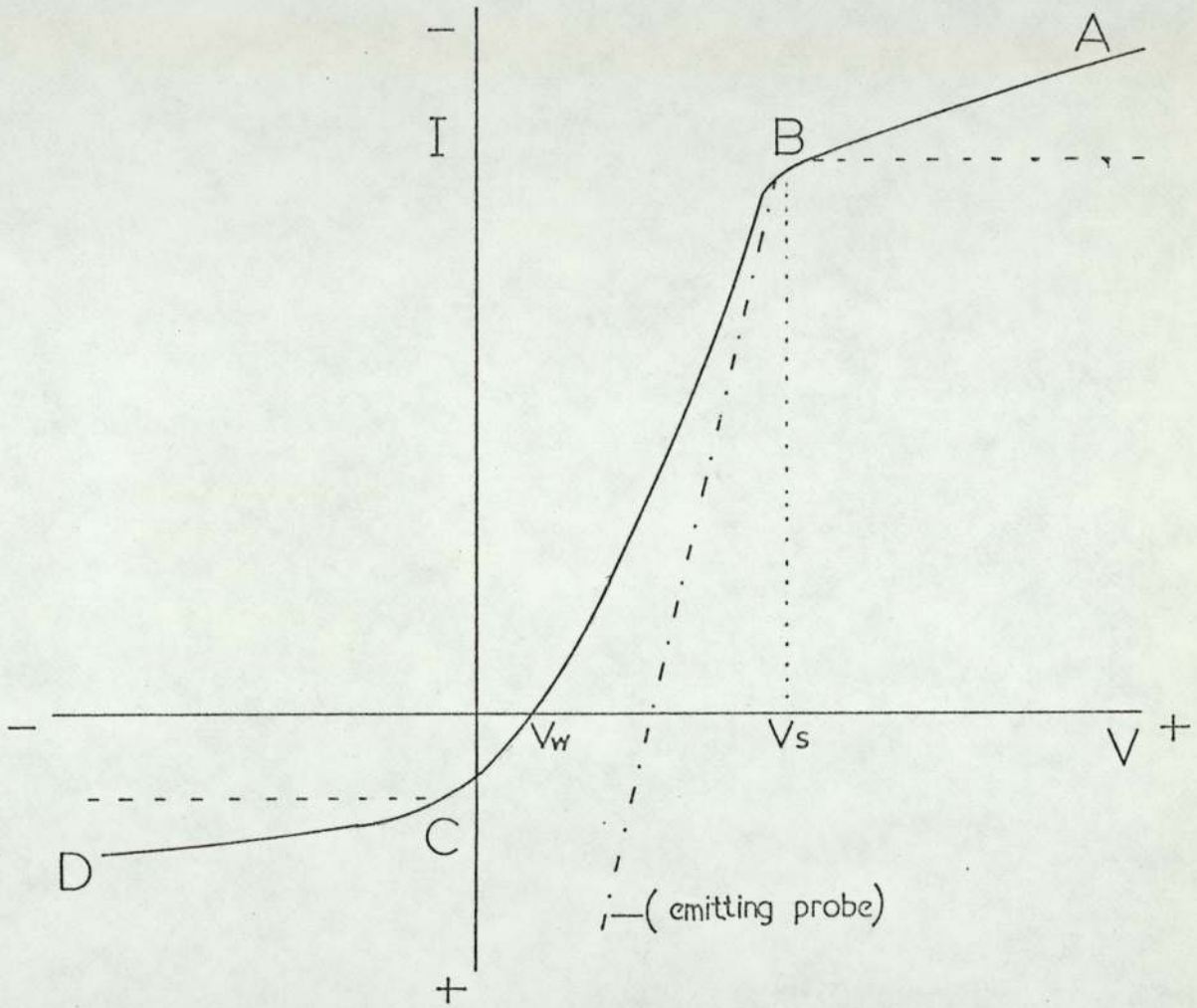

In practice in the regions AB and CD the characteristic will show a slope, as indicated, due to the increase in space charge sheath dimensions with increasing applied voltage, and incomplete shielding of the plasma by the space charge.

The most important characteristic of the bulk plasma is the Debye length λ_D, which represents the maximum charge separation that can be achieved by the plasma, using the available kinetic energy of the electrons, and is given by:

$$\lambda_D = \left(\frac{KTe}{4\pi n_o e^2} \right)^{\frac{1}{2}}, \qquad 7.1$$

where n_o is the charge density and Te the electron temperature. The effective space charge sheath thickness at the plasma boundaries will be in fact of the order of a Debye length, a consequence of which is that the values of n_o and Te must be such that the physical extent of the plasma under study must be many times greater than λ_D. In this simple use of probes in low pressure plasmas the mean free path of the ions and electrons is greater than the Debye length and therefore in calculating the space charge limited currents collected no account need be taken of the collisions of the ions with other neutral or charged species, while crossing the sheath region.

7.ii. Positive Ion and Electron Densities

For the case where the sheath radius S, is small compared to the probe radius a, ie the probe is perfectly absorbing, and orbital motions of the charges within the sheath do not contribute to the calculated current; the probe current, I, is simply:-

$$I = jrAs, \qquad 7.2$$

jr being the random current density, and As the surface area of the sheath. For a Maxwellian distribution of velocities

$$jr = \tfrac{1}{4}n\bar{v} = \tfrac{1}{2}n\left(\frac{2kT}{\pi m}\right)^{\frac{1}{2}} \qquad 7.3$$

where n, $\bar{v}$, T and m refer to the number density, mean velocity, temperature, and mass, of the charged species.

For the thin sheath condition, a >> (S - a), the Langmuir-Childs equation for a space charge-limited current through a sheath region of planar geometry, may be applied:-

$$j = \frac{1}{9\pi}\left(\frac{2}{em}\right)^{\frac{1}{2}} \left|\frac{Vp - Vs}{(S - a)^2}\right|^{3/2} \left(1 + \frac{2.66}{\sqrt{\eta}}\right) \qquad 7.4$$

where $\eta = |e\,(Vp - Vs)/kT|$ and Vp is the probe potential.

Equation 7.4 may be used to compute As from the value obtained for S, and the total current collected by the probe related to the number density of the charged species by equation 7.2 and 7.3. When the condition a >> (S - a) does not hold, i.e. there is a thick sheath, the orbital motions of the charge species within the sheath must be taken into account, and the form of equation 7.4 altered according to whether the probe has cylindrical or spherical geometry. The relationships derived may be used, for either positive ions, or electrons, by using the appropriate values of m and T. Due to the small electronic mass, the electron temperature Te may be very much greater than the neutral gas species in a plasma and must be determined for the particular conditions used. The ions will have a comparable mass to the neutral species and therefore may lose much of their kinetic energy during collisions, thereby equilibrating their temperature with that of the neutral species.

7.iii. Electron Temperatures

In the transition region the electrons arrive at the probe by virtue of their random thermal motion. Assuming the velocity of the electrons to have a Maxwellian distribution then their density will be given by the Boltzmann law:-

$$n = n_o e^{\frac{-eV}{kT_e}} \qquad 7.5$$

n_o being the number density just outside the sheath.

The random current density hitting the probe will then be

$$I = A_a n \left(\frac{kT_e}{2\pi m} \right)^{\frac{1}{2}} \qquad 7.6$$

and therefore

$$I = A_a n_o \left(\frac{kT_e}{2\pi m} \right)^{\frac{1}{2}} e^{\frac{-eV}{kT_e}} \qquad 7.7$$

A plot of ln I against V will be linear of slope $\frac{-e}{kT_e}$, from which Te, the mean electron temperature may be calculated. An important condition here is that the mean free path of the electrons is large compared to the probe diameter such that the distribution of the incoming electrons is not disturbed by collisions near the probe. Strictly this theory may only be applied to a perfectly reflecting probe, where the Maxwellian distribution of electrons coming back from the probe is maintained.

7.iv. Double Probes

An important development in the use of probes was the concept of the double probe by Johnson and Malter[93]. Two probes are introduced into the plasma with a potential applied between them and the system as a whole is made to float so that there is no net flow of current out of the plasma. The sum of the positive and negative currents to both probes must therefore be zero, with the main advantage that the disturbance to the plasma is minimised. Its relevance to flame measurements was pointed out by Travers and Williams[94]. They explained that a single probe biased positive so as to collect electrons was in fact acting as an asymmetrical double probe, since the electron current was limited by the flow of positive ions to the boundary of the plasma, typically the burner top. This may in fact lead to errors in the interpretation of the results with regard to electron temperatures and electron concentrations.

7.v. Emitting Probes

If conditions exist in the plasma such that the probe reaches a temperature where thermionic emission becomes significant, then this will drastically alter the appearance of the probe characteristic. In the electron saturation region the electrons will be drawn back to the probe and the electron current seen will be essentially unaffected. As the bias is made increasingly negative to the space potential, the electrons will be able to leave and the characteristic will diverge as shown in Figure 18. The current received will be an apparent positive ion current, but since the probe cannot now draw a saturated ion current, no measurement of the positive ion density may be made.

Obviously in high density plasmas and especially atmospheric flames, practical steps must be taken to ensure that the probe temperature is kept at a level such that thermionic emission is negligible. The probe will exhibit similar properties when the secondary emission of electrons becomes important due to bombardment by energetic ions.

7.vi. Time Dependent Phenomena

In many applications it is found necessary to vary Vp with time, or to investigate plasmas where Vs, n, and n_e are time dependent. In these situations it is important to know how quickly the probe current will follow changes in Vs, Vp and n_i, n_e, i.e. the response time of the plasma. This question is of particular importance to this study where the probe was used to study changes in n_i generated in the flame.

For a probe in the electron saturation region, when biased further positive, the sheath must expand to include a volume of space charge and momentarily allow a greater flux of electrons to reach the probe. This overshoot in electron current has been observed by Bills et al[95] and is of the order of 1 μs. The effect is not observed at high pressures since collisions within the sheath will prevent any sharp rise in I_e. For the probe in the ion saturation region, the sheath thickness will again increase as Vp increases, the electrons now included in this region are pushed away rapidly. The ion density however in this region must be reduced giving rise to a transient ion current.

In general, if in order to adjust to a new situation, the sheath dimensions change so as to balance the transport of ions to the sheath boundary with the space charge-limited flow to the probe, the time

response is controlled by the time taken for the ions to move to new positions with their random thermal velocities or mobility controlled motions. An additional displacement current may be seen which can be attributed to the capacitance of the sheath for both negative and positive probes. This is considered to be negligible compared to the overshoot for the positive case but Oskam et al[96] found a large overshoot lasting 0.4 μs for the negative case, which he attributed to a displacement current of this kind.

Although no universally applicable theory is available at this time it would appear that, at least for low pressure situations, response times of the order of microseconds are to be expected.

7.vii. The Application of Electrostatic Probes to Collision Dominated High Density Plasmas

Under conditions of relatively high pressure, such as exist in flame conditions, the basic assumptions of Langmuir's original concept, that the mean free paths of the species concerned are very much greater than the Debye length and the probe dimension, are now violated. Therefore descriptions of the current collected by the probe must take account of the diffusive and mobility controlled motions of the species approaching and passing through the space charge region.

The first of the more successful attempts to evaluate probe behaviour under these conditions came from the work of Shultz and Brown[97] for the case of positive ion collection on a cylindrical probe. They determined the probe current by considering the space charge limited flow through the sheath, in which a varying number of collisions would take place corresponding to a range of plasma pressures. Some account was taken of the return to the plasma of ions by collisions within the sheath. Transport to the sheath boundary

was assumed to be via normal diffusive motion. Travers and Williams[94] used the approach of Shultz and Brown for the case of positive ion collection by single and double probes in a flame operating at a few torr pressure.

Calcote[98, 99, 100] has used an approach based on the work of Bohm, Burhop and Massey[101] for a high pressure plasma, with the probe at the plasma potential to study the ionisation in various hydrocarbon flames. The results especially concerning electron temperature measurements have been criticised by Travers and Williams[94], in the context of single probes acting as asymmetric double probes previously mentioned in section 7.iv. A recent development of this approach has been presented by Jensen and Kurzius[102] in which the mass flow effects of a high velocity plasma are dealt with.

Of various full mathematical treatments on the collection of ions in a collision dominated plasma, that of Su and Lam[103] has found the widest application. They make no a priori assumptions of a sheath region and use the continuity equations for ions and electrons and Poisson's equations to determine the potential distribution around a spherical probe, similar in concept to the work of Bernstein and Rabinowitz[104] for a collisionless plasma.

Their analysis leads to the concept of four distinct regions around a negatively biased probe. In the body of the plasma, far removed from the probe, there is a quasi-neutral region, where positive and negative charges are present in equal numbers. On moving nearer to the probe, this gives way to a transition region where some effect of the negative probe bias is seen and the electron concentration decreases. Next there lies a sheath region in which no electrons are present, i.e. there is a positive space charge. Finally a diffusion layer was envisaged to be adjacent to the probe surface.

A further important point in the model is that the field from the probe potential and consequently the space charge region decays asymptotically with distance from the probe.

The equation derived relating the saturated positive ion current I_i to the probe bias by Soundy and Williams[39] from the work of Su and Lam[103] and ion density is

$$N_i = \frac{1}{4\pi kT_i (4 a \mu_i^2)^{2/3}} \left(\frac{I_i^2}{Vp} \right)^{2/3} \qquad 7.8$$

where μ_i is the mobility of the ion species.

The assumptions made in the derivation of this relationship are tabulated below:

(a) Only singly charged species are present.

(b) The current collected is large compared to that when the probe is at the plasma potential.

(c) The probe radius is large compared to the Debye length, i.e. there is a thin sheath condition.

(d) The electron temperature is equal to the mean gas and ion temperature.

These conditions are easily met in atmospheric flames. Soundy and Williams[39] have demonstrated that equation 7.8 is of the right form, but found for a flame burning at one atmosphere, the positive saturation current measured was several orders of magnitude greater than predicted. This requires that the response of a probe used to measure absolute ionisation levels, must be calibrated in a flame containing a known amount of ions. The above workers used the Cs^+ ion as a standard since in these flames caesium will reach its equilibrium level as calculated from the Saha equation.

The final form of the calibration relationship given is

$$N_i = C\left(\frac{1 + {}^{Mg}/_{M_{Cs^+}}}{1 + {}^{Mg}/_{M_{I^+}}}\right)^{2/3} (I_i)^{4/3} \qquad 7.9$$

Where Mg is the mean mass of the neutral gas species, and M_{I^+} and M_{Cs^+} the masses of the particular ion to be measured and of the caesium ion.

The constant C is found from a match of the plot of Log $(I_i)^{4/3}$ against Log $[M]$, M being the molarity of the atomiser solution, with the theoretical plot of $[Cs^+]$ against $[Cs]$ at equilibrium, with some adjustment being made for the formation of CsOH in the flame. This method is similar to the calibration of the atomiser from the measurement of the electron concentration by microwave attenuation, described in Chapter 3.

7.viii. Ion Collection in a Collision Dominated, High Density, Flowing Plasma

A recent advance in the characterisation of the operation of probes in high density plasmas is that of Clements and Smy[105, 106], who have developed the theory of Lam[107] for a probe in a flowing plasma or flame, for both the thick and thin sheath situations. The basic idea is that for plasmas with convective velocities of 1 ms^{-1} or greater flowing relative to a negative probe, convective transport of the ions travelling with the plasma velocity vf is more important than diffusive transport. The probe then sweeps out a section of the flame and leaves a depleted volume of plasma in its wake. The two cases are shown diagrammatically in Figure 19.

Figure 19 sheath conditions

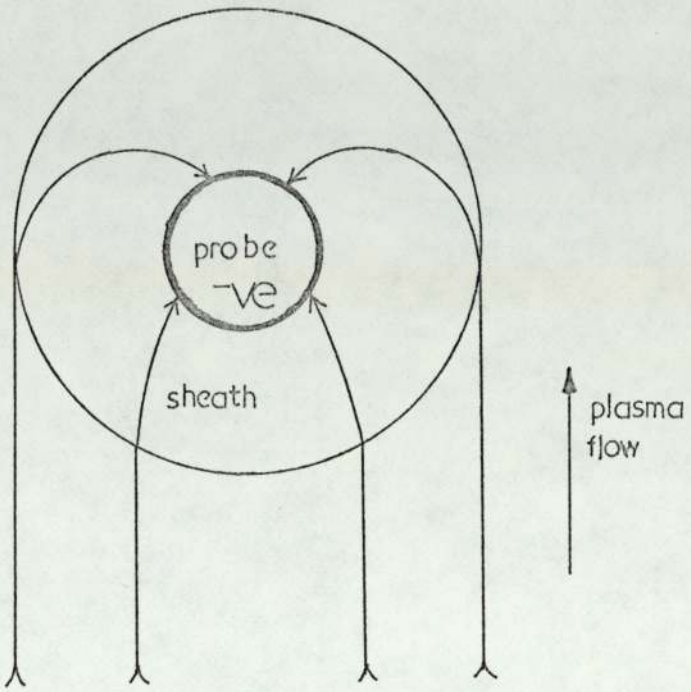

thick sheath

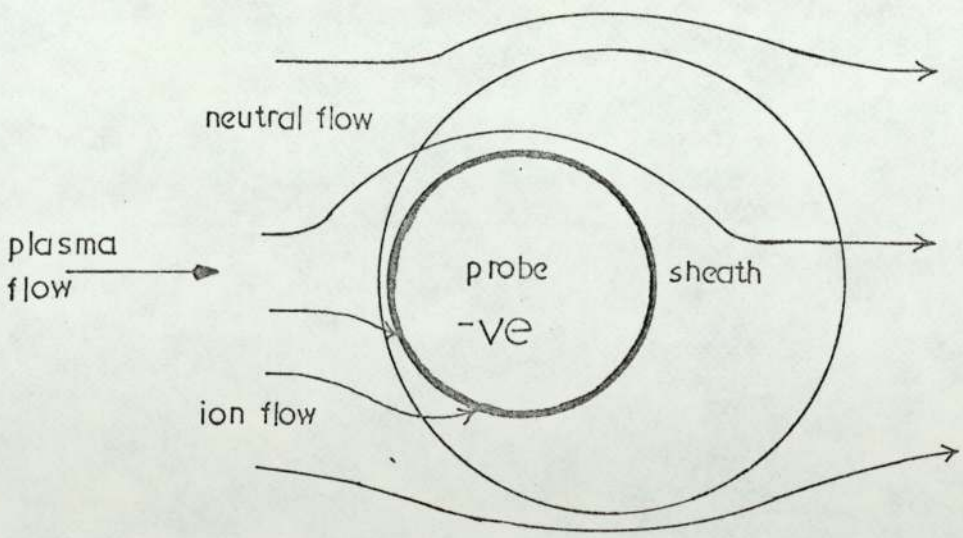

thin sheath

The conditions of Lam's theory are as follows:

(1) $\alpha = \lambda_D/L \ll 1$, where λ_D is the Debye length, and L a length characteristic of probe dimensions, typically 2a, the probe diameter.

(2) $\chi = \frac{e\ V_p}{kT_e} \gg 1$, where T_e is assumed = T_i.

(3) R, the electric Reynolds number, is given by:-

$$R = \frac{v(f)\ L}{U_i(kT_e/e)} > 1$$

Essentially $R \simeq \frac{v(f)}{v(d)}$, where vd is the upward diffusive velocity of ions for the stationary plasma case. For large values of V_p or small electrodes, and with $R \propto \chi^2 > 1$, when $\chi \gg 1$, the current I_i per unit length of probe, is related to the charge number density n_e, for positive ion saturation, by:-

$$I_i = \frac{2\ (\pi\ \mu_i E_o)^{1/3}\ (n_e e v(f)\ V_p)^{2/3}}{\log\ (I_i/2n_e e\ v(f)\ a)^{2/3}} \quad \text{(M.K.S.)} \qquad 7.10$$

for the thick sheath situation, E_o being the permittivity of free space.

The equation derived for the thin sheath condition is

$$I_i = 5.3\ E_o^{\frac{1}{4}}\ e^{\frac{3}{4}}\ \mu_i^{\frac{1}{4}}\ a^{\frac{1}{4}}\ v(f)^{\frac{3}{4}}\ n_e^{\frac{3}{4}}\ V_p^{\frac{1}{2}}\ L \quad \text{(M.K.S.)} \qquad 7.11$$

which is of the same form as equation 7.8 derived from the work of Su and Lam except for its inclusion of a dependence on plasma velocity.

Using these relationships Smy and Clements have been able to predict currents drawn by a negative probe in flame plasmas with velocities of 5 ms^{-1} and above, to within 20% of the experimentally measured values.

7.ix. Apparatus used for Probe Measurements

The burner, gas delivery system, and flame characteristics, have been previously described in Chapter 3. Figure 20a shows the arrangement of the probe and the external circuit; the alternative circuit 20b was used when it was found necessary to reduce the stray capacitance without increasing the amount of A.C noise pick up. The cylindrical probe constructed of platinum wire, 2.5×10^{-4} m in diameter, and 1×10^{-2} m in length, was supported in a born nitride rod and swept through the flame at approximately 1 ms^{-1}. This ensured that the probe never reached such a temperature that thermionic emission became important, but was sufficiently slow to prevent the probe sweeping its own atmosphere into the flame[108]. Cooled probes may be used for this purpose, but have the disadvantages of disturbance of the sheath by the water cooling circuit, and insulation problems from the condensation of water from the flame onto the probe assembly.

Over a period of operation it was noticed that currents received by the probe decayed with time of usage, presumably due to the collection from the flame of relatively non-conducting materials on its surface. To remedy this the platinum surface was cleaned with concentrated hydrochloric acid, and heated to dull redness before each run.

The probe was originally designed to be at 35° to the horizontal so that any distrubance caused by the boron nitride support to the flame gases would be down stream from the point of measurement. For investigations where maximum spacial resolution was required, the platinum wire was made horizontal.

Values of the load resistor of between 0.1 and 1 megohm, were used and the current from the probe was measured as the voltage drop across them using a Cossor C.D.U. 110, or Tecktronix 547b oscilloscope.

Figure 20 probe assembly

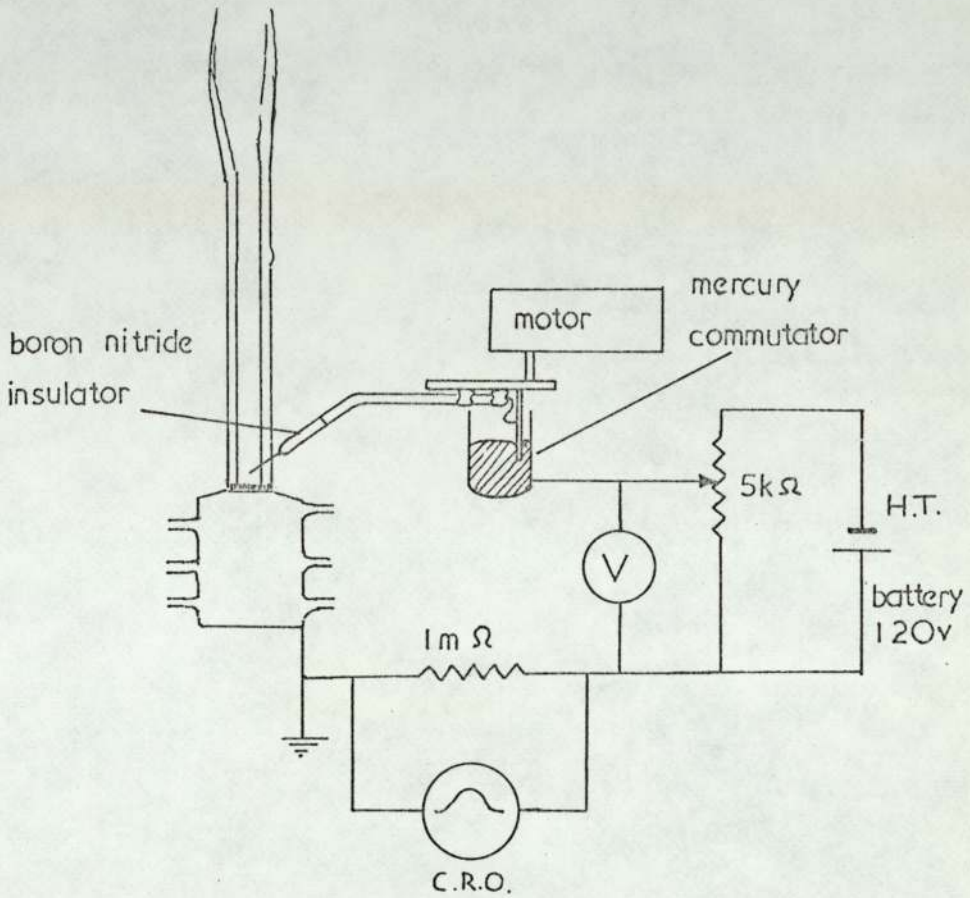

A normal circuit

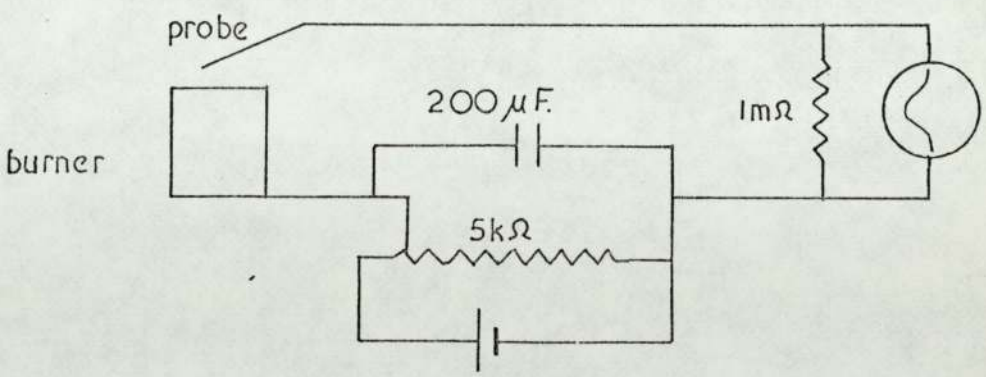

B low R.C. circuit

Figure 21 breaking bubble atomiser

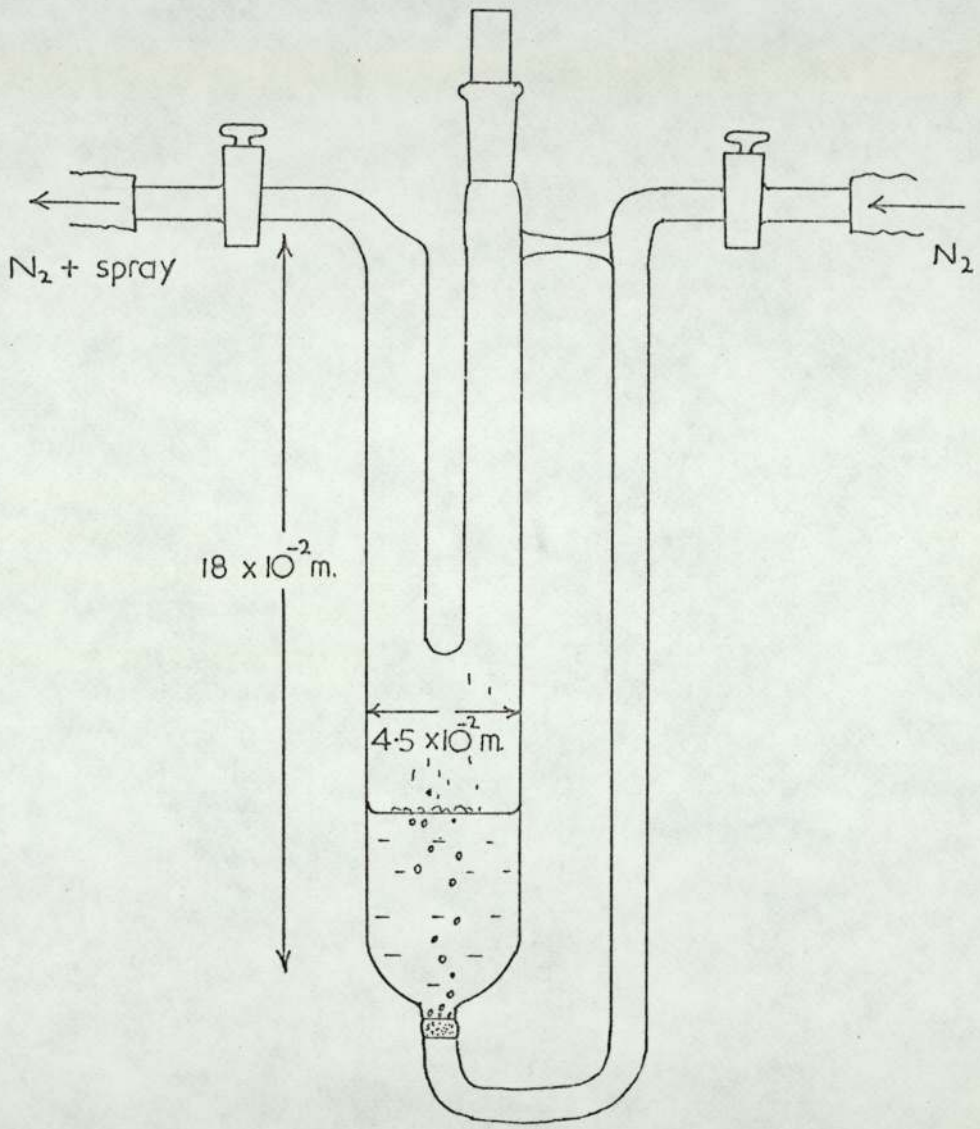

A small magnet mounted on the probe armature operating a reed switch as it rotated was used to trigger the oscilloscope as the probe passed into the flame region. Recordings of the C.R.O. display were made either by eye or by photography using a type AC, 2/25 camera manufactured by D. Shackman & Sons.

For the introduction of lanthanum hexaboride particles, the apparatus of Miller was used. The solid was held over a glass sinter, at the base of a large elutriating vessel leading vertically into the inner flame. Flows of up to 1 litre min^{-1} of nitrogen were passed through the powder as it was mechanically agitated, and the dust-laden stream allowed to mix with the unburnt gases at the base of the burner.

In the delivery of the dilute sprays of the metal salts, a so-called "breaking-bubble atomiser" was used, and is shown in Figure 21. The solution was held above the glass sinter and low flow rates of nitrogen (less than 1 litre min^{-1}) were passed through, causing bubbles to form on the liquid surface. The bursting of the bubbles produced a small number of droplets which were carried up with the nitrogen and mixed with the gases supplying the inner flame. No quantitative estimate of the delivery could be made with certainty, but from the effects seen in the flame it would be reasonable to assume that the number of droplets produced in this way was several orders of magnitude below that from a conventional pneumatic atomiser. One advantage of this delivery system was that no restriction was laid on the strength of solution used.

In the work it was found necessary to handle very small signals from the probe; in the order of 1×10^{-10} A, and mains A.C. pick-up became a serious problem; therefore, meticulous attention was paid to the screening of the circuit.

CHAPTER 8

PROBE EXPERIMENTS IN DUST LADEN FLAMES

8.i. The Work of Miller

Since Miller[3] was the first to study the phenomenon of "spikes", detected in flames containing condensed particles, and many of the techniques employed by him were used in this study, it is useful to restate the principle conclusions reached in his work.

Miller found that when the probe was passed through dust-laden flames, the normally smooth profile of the C.R.O. display was broken up into a series of "spiky" responses as shown in Figure 22. This was found for a number of materials, including aluminium, lanthanum hexaboride, carbon, barium oxide, and tungsten carbide[9]. After examining a number of possible explanations, it was concluded that when the incandescent particles, of radii up to 10 μm, made contact with the negative probe, they were free to emit a saturated electron-current, thus giving rise to the pulses. This allowed an estimate to be made of the work-function of the materials used under flame-conditions.

The distribution of the peak heights of the "spikes" was found to correlate closely to that of the radii of the particles being introduced, the source of this distribution being the parabolic velocity profile across the tubes carrying the particles. In fact only half the distribution was seen for the spikes, most of them being small and therefore hard to measure. The sampling procedure adopted was: at each experimental point some 200 - 500 pulses were recorded, and the top 10 or 15 per cent in terms of peak height selected and measured. The mean peak height for each set of conditions then referred to a constant, if broad, section of the distribution.

Figure 22 probe C.R.O. profiles

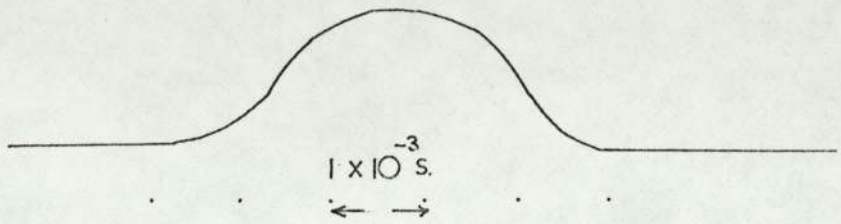

normal probe response

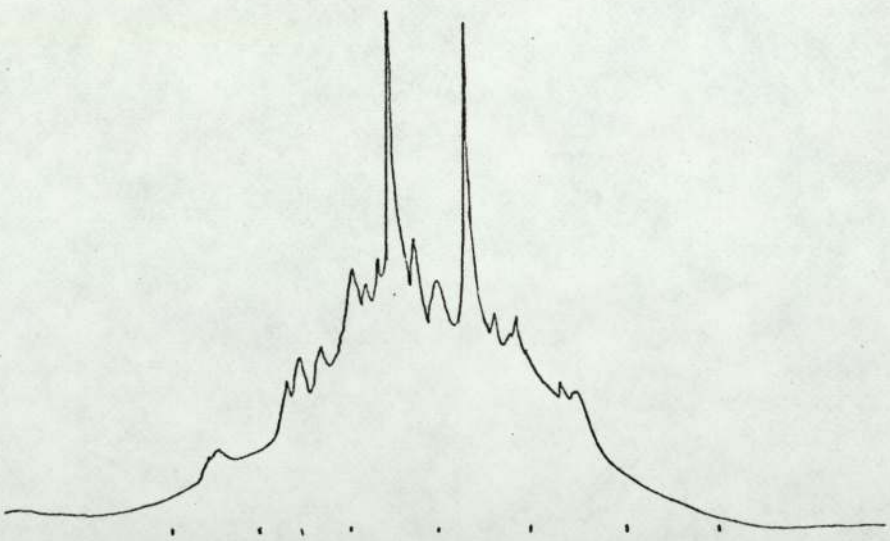

response from breaking bubble atomiser or particulate delivery

Of the shapes of the pulses, the rise time was related to the contact time of the particles with the probe, and the decay was thought to be due to elements of the external circuit. The principle RC contribution from the circuit was thought to be the resistance of the flame coupled with the stray capacitance of the AC noise shielding components. When the resistance of the flame was lowered by more than an order of magnitude by seeding with caesium chloride, however only a marginal reduction on the decay times was observed. The rise time of the pulses in the order of 3×10^{-4} s seems to be too large for the contact time of the particle and the probe. Using the calculated flame speeds, the time taken for a particle to roll around half the circumferences of a spherical probe, 1.75×10^{-3} m in diameter, would be 1×10^{-4} s and for a cylindrical probe of diameter 2×10^{-4} m, 3×10^{-5} s. Probes of these dimensions were used in the work but the rise times showed little or no dependency on probe dimension.

It was concluded that although the above author dealt with the magnitude of the "spikes" in terms of thermionic emission, with reasonable success, the explanations presented for their duration were less satisfactory. Consequently, it was decided to pursue this line of work, beginning with a repeat of the work on lanthanum hexaboride, to ascertain the possible human error involved in making rather tedious and difficult measurements.

8.ii. Further Experiments in Flames seeded with Lanthanum Hexaboride

Using the delivery system already described lanthanum hexaboride particles were introduced to a flame at 2370 K, with the probe bias at -100 V. The top 10% in peak height of the "spikes" recorded at various distances above the burner-top were measured, and the results are shown in Figure 23. For the mean pulse height, the results agree

Figure 23 results from LaB_6 particles

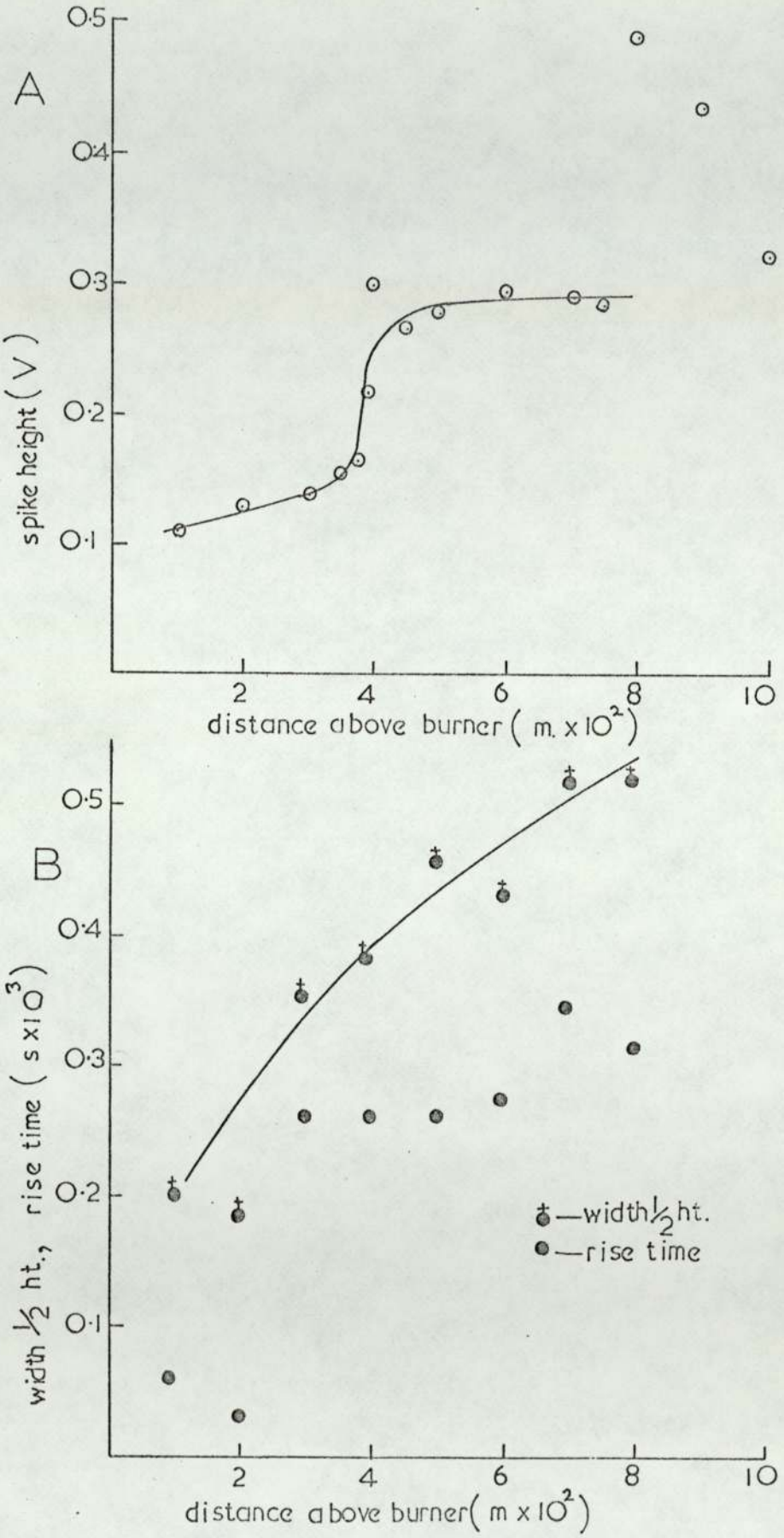

well with those of Miller, showing the emission current increasing up to a point C, where it then remains on a plateau, in accord with the particles heating up and coming to equilibrium with the flame temperature. The sudden rise at 8×10^{-2} m is harder to account for.

It is possible that at this height entrained air has raised the gas temperature enough to melt the material giving rise to either increased emission from the liquid surface or an increased number of charged gaseous species that have evaporated from the particle. The melting point of lanthanum hexaboride is around 2500 K, however, and there was no indication, from other measurements, of a sudden temperature rise of over 100 K at this height.

In Figure 23b, half-widths and rise-times are plotted, and both are seen to increase with height in the flame. Assuming that the original pulse is either triangular or gaussian, then the rise-time will be seen to lie between the apex and the extrapolated termination point according to the relative values of pulse time and RC time constant. Therefore the rise time may show some dependence on the decay time. The increased decay time might well be attributed to an increased R contribution to the time constant, with the increasing length of flame involved. This however envisages the flame to have a specific resistivity.

Taking the background pulse below the spikes to indicate the gaseous ion density, when the probe is operating under positive ion saturation, the real resistance of the flame may be evaluated from the Ivs V characteristic in this region. Since both the slope of the characteristic and the current from the probe will, to a first approximation, be constant with height in the flame, it would seem incorrect to think of a resistance per unit length of flame involved in the probe circuit, under these conditions.

The real situation existing seemed to be that of an RC time constant shaping the pulses to a certain degree, but with the variation of rise- and decay-times being a genuinely physical, as opposed to an electronic, phenomenon. Of special interest also, was the sudden jump in the rise-time above 2×10^{-2} m, indicating a change of physical conditions around the particles.

CHAPTER 9

PROBE EXPERIMENTS IN FLAMES SEEDED WITH NEBULISED SOLUTIONS

9.i. Introduction

Pneumatic, electrostatic and ultrasonic methods are found in common use as a means of generating a fine mist of droplets from a solution of a material, with which it is desired to seed a flame. In many systems, in their passage to the flame, the droplets are surrounded by dry gases, and will have evaporated to leave small crystals entering the reaction zone. By the use of various baffles and adjustment of the length of tubing involved, the large droplets may be removed from a spray, and the delivery to the flame will be approximately uniform, a desired result for many ionisation studies and spectrometric investigations.

If the generally held view is accepted that particles of alkali metal salts, having boiling points considerably less than normal flame temperature, and of size about 1 μm will evaporate within the reaction zone, then the probe response to the gaseous ionisation of the metal will be as in Figure 22 for a spray from a normal atomiser. If the supply is not continuous then fluctuations will appear on the perimeter of the profile. This effect can be observed immediately after the atomiser has been turned off, when the delivery of droplets to the flame decays with time.

Under steady conditions a "spikey" profile is obtained, when salts of some heavy metals, such as chromium and vanadium, are sprayed into the flame, as noticed by Kelly and Padley[8]. This would seem to be connected with the presence of condensed oxide phases since these metals have involatile oxides and the characteristic streaks of grey body radiation are clearly seen emitted from the particles in the burnt gases[109]. It was observed, however, that a flame seeded with

lanthanum nitrate, showed a marked decrease in the intensity of the luminous tracks, when the ambient temperature of the flame exceeded the melting point of lanthaum oxide (La_2O_3 M.P. 2588 K). A corresponding decrease in the "spike" effect was also observed under the same conditions, indicating again the connection of the phenomenon with hot condensed phases.

Using the normal pneumatic atomiser delivery, the probe profile was examined in a flame at 2507 K under the highest possible resolution with the apparatus available, for a series of aqueous solutions. These solutions were 0.2 molar aluminium sulphate, and nitrate, strontium nitrate, uranyl nitrate, ammonium chromate and potassium and caesium chlories. The smallest fluctuations were found for aluminium sulphate and the largest for uranyl nitrate and ammonium chromate, overall the variations being between one and five per cent of the total probe prof le height. Only one salt, thorium nitrate, was investigated, which gave no measurable response to the probe. Also little radiation was observed, a surprising result in view of the high melting point of the dioxide ThO_2 of 3323 K.

Of the materials examined, both uranyl nitrate and ammonium chromate might be expected to form oxide particles in the flame, but their behaviour with regard to "spikes" on the probe profile was almost indistinguishable from the volatile species such as caesium chloride. To make further progress the need was for a method of delivery of droplets that was steady, but dilute enough to allow resolution of the individual spikes on the profile.

Using 0.2 molar potassium chloride as the test material, various methods of diluting the spray produced from the atomiser were tried. Firstly, the length of tubing between the atomiser and burner was increased tenfold, but this had the effect of reducing the size of the

spikes but not their frequency. Likewise the passing of the spray over cellulose filters and through capillary tubes coated with silicone oil, failed to be successful in reducing the flux of droplets reaching the flame. Eventually the breaking bubble atomiser, described previously, was found to be effective and was used to examine the probe response from individual crystallites of various materials. Operating the flow at rates of up to 0.5 litres min^{-1} of nitrogen, through the solution, a probe response of resolved spikes was obtained, residing on a continuous pulse from the background positive ion level of the burnt gases.

9.ii. A Quantitative Study of the Spikes

Four solutions were studied in detail in a flame at 2507 K, with the probe at 100 V negative to the burner and a flow of 0.3 litres min^{-1} through the solution. Measurements were made for a range of distances above the burner up to 8×10^{-2} m. These solutions were potassium chloride 0.2 molar, di-potassium hydrogen phosphate 0.2 molar, strontium chloride 0.2 molar and potassium chromate 2.0 molar. During the recording of the spikes, the level of the background pulse was also measured for varying probe bias. The square of the background current is shown plotted against probe voltage in Figure 24, for a flame seeded with strontium chloride, indicating compliance with the relationships of Su and Lam, and the thin sheath condition of Smy and Clements, from equations 7.8 and 7.11. The spikes observed under the above conditions were about 50% of the probe response to the background ionisation, but for all seeding materials used the plots of $(I_i)^2$ vs Vp were found to be identical with that in Figure 24.

Using the sampling and counting method of Miller, some 400 spikes were recorded photographically at each point, and the top

Figure 24 relationship between probe current and probe voltage

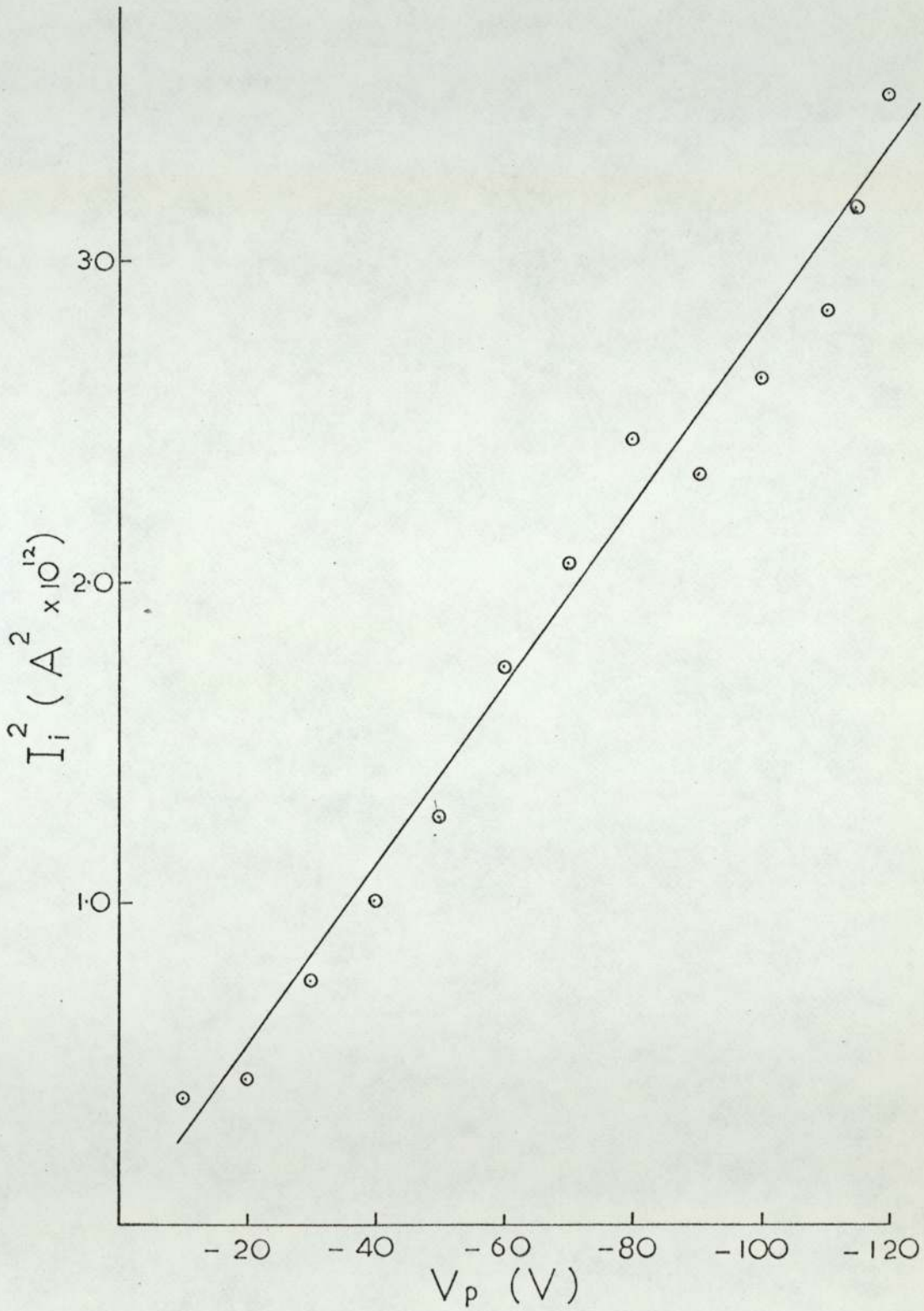

10% in peak height, measured from the developed 35 mm film, in terms of amplitude and half width. The resulting plots are shown in Figures 25 - 28. The peak heights show a different behaviour to those from LaB_6 in Figure 23. Clearly it can be seen that the rise to a steady level is very much more rapid, and for two cases, K_2HPO_4 and $SrCl_2$, there is a decay above 3×10^{-2} m. It must be remembered though that the data for LaB_6 in Fig. 23 was for a flame at 2370 K, and therefore was under slightly different conditions. Miller performed the same series of measurements at a temperature at 2487 K (Figure 29), which show a remarkable similarity to the plots for KCl and $K_2Cr_2O_4$.

Again for the measured half widths, the results from all four salts exhibit the same characteristic, similar to that of LaB_6 in Figure 23, and within experimental error do not vary from salt to salt. The increase in spike width with height in the flame is illustrated in Figure 30. All the salts may be expected to evaporate rapidly into the gas phase except K_2CrO_4 which might form particles of Cr_2O_3, and it would not be unreasonable to assume that the spikes were due to an inhomogeneous distribution of ions in the flame.

The distribution of peak heights is shown in Figure 31 for potassium chloride at 1×10^{-2} m above the burner. If the peak heights were taken to be proportional to the amount of ionisation from each evaporated crystal, which in turn would be related to the crystal volume, then the distribution should be that of the particles entering the flame. The gaussian-type profile most probably originates from the mode of transport of the crystals in the gas streams leading to the flame, where they should obey Stokes Law, and the gas is moving with Poiseuille flow. The maximum droplet size will be controlled by the gas flow immediately above the liquid

Figure 25 results from KCl spray

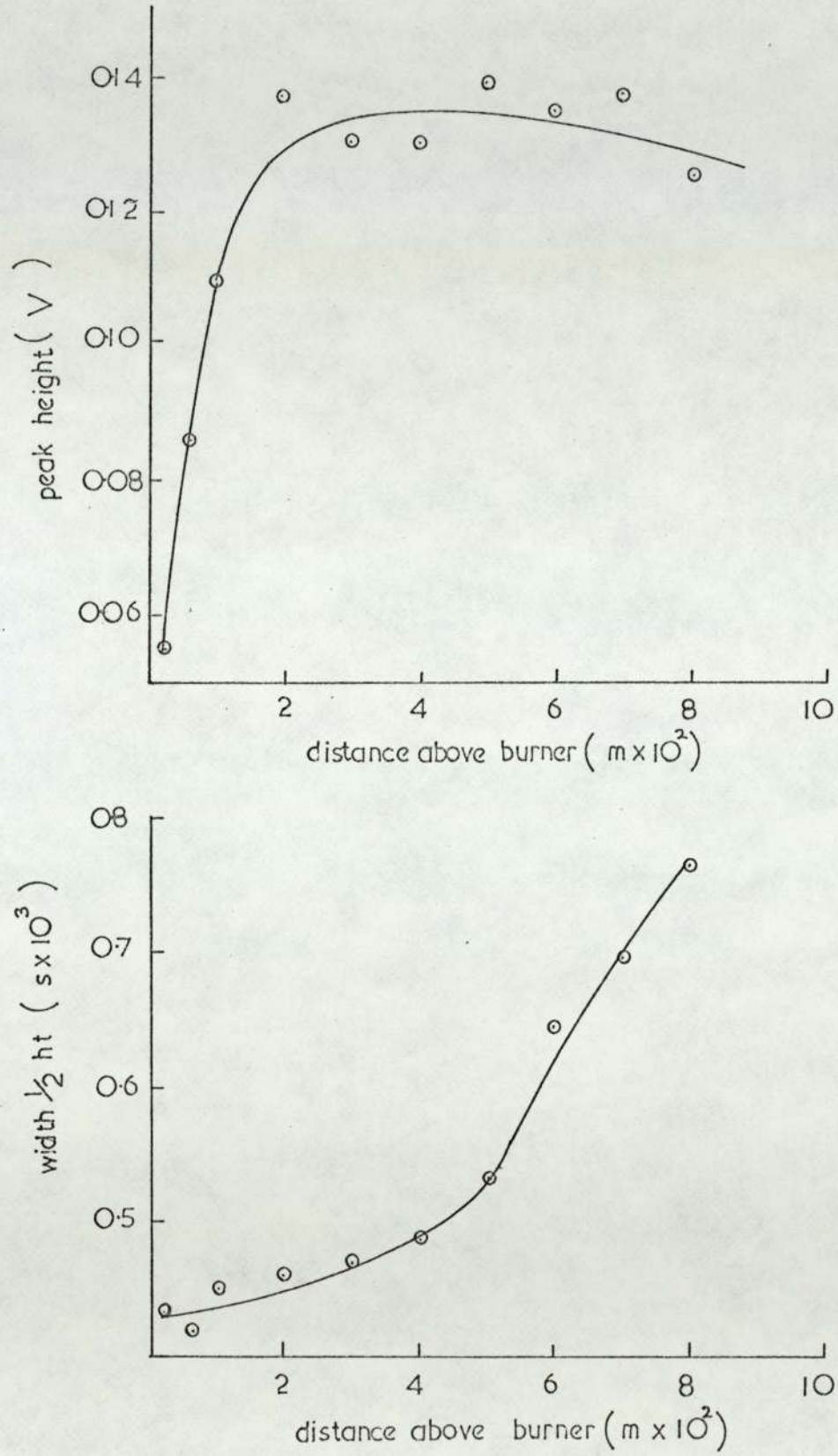

Figure 26 results from K_2HPO_4 spray

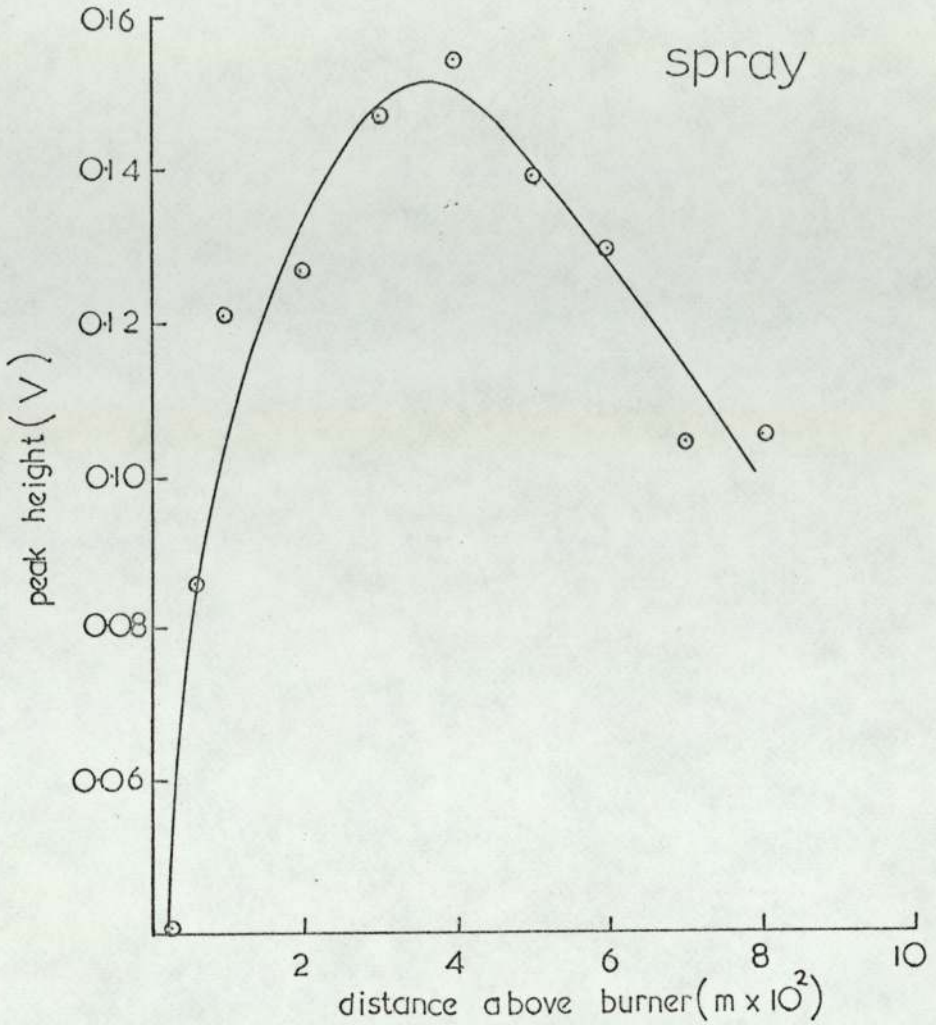

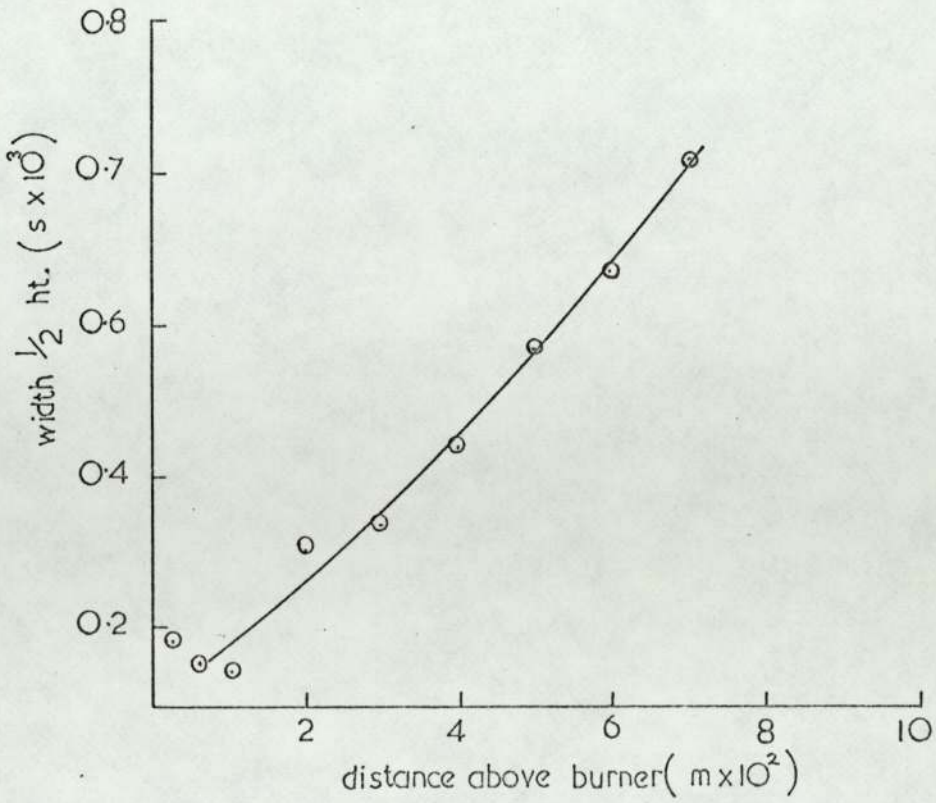

Figure 27 results from $SrCl_2$ spray

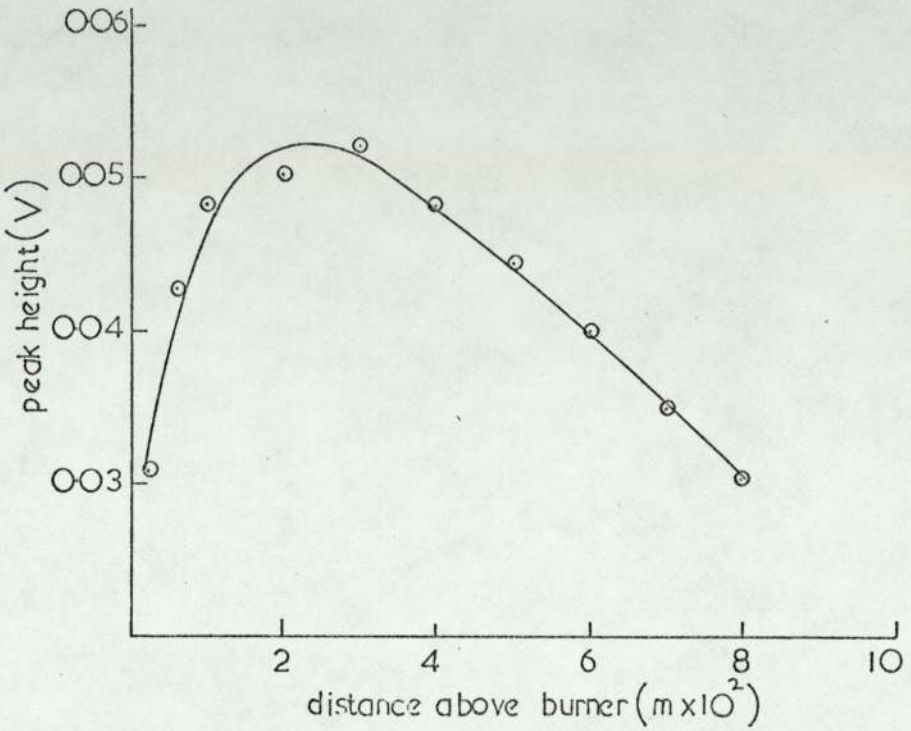

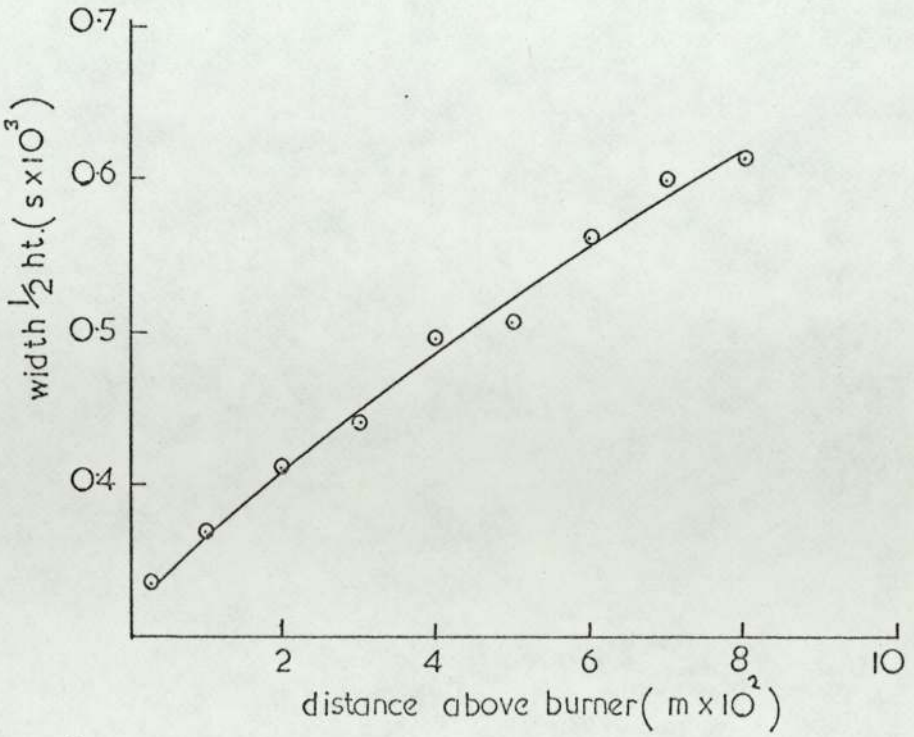

Figure 28 results from K_2CrO_4 spray

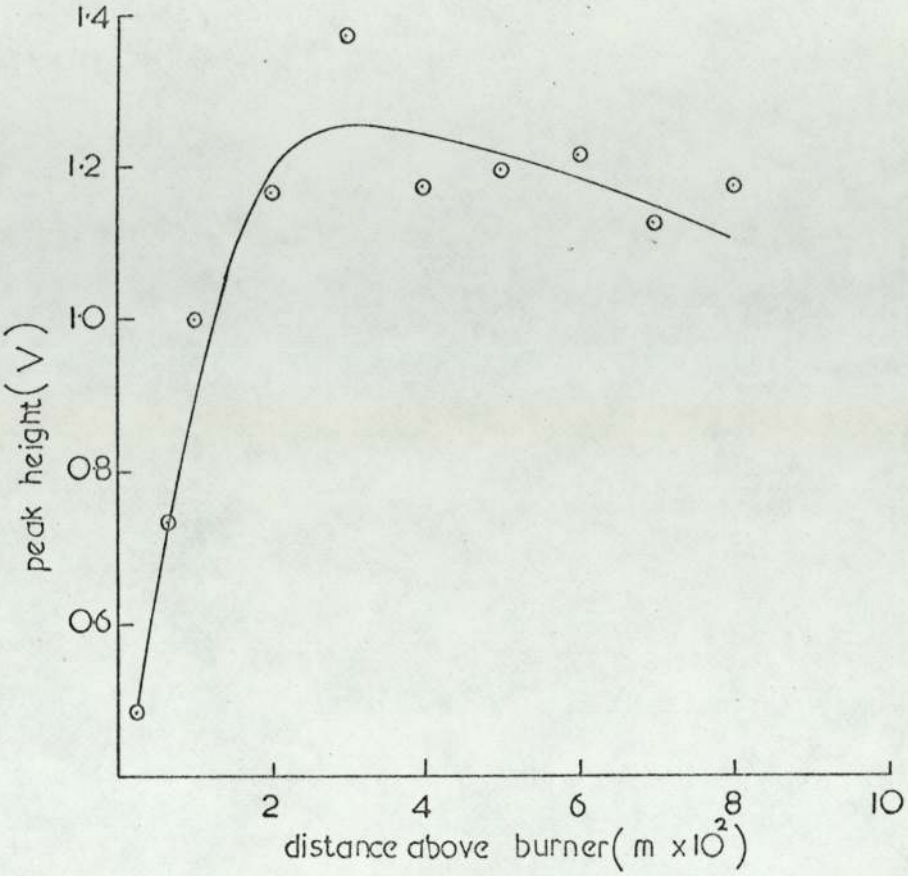

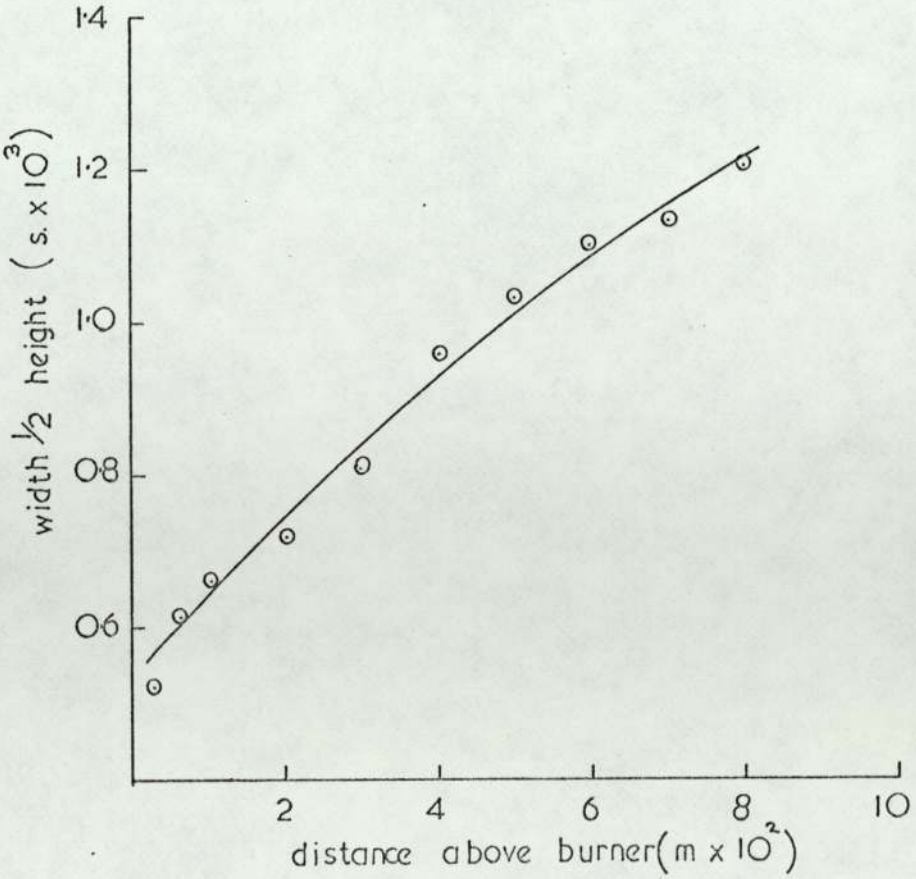

Figure 29 results from LaB_6 a 2487K

(Miller)

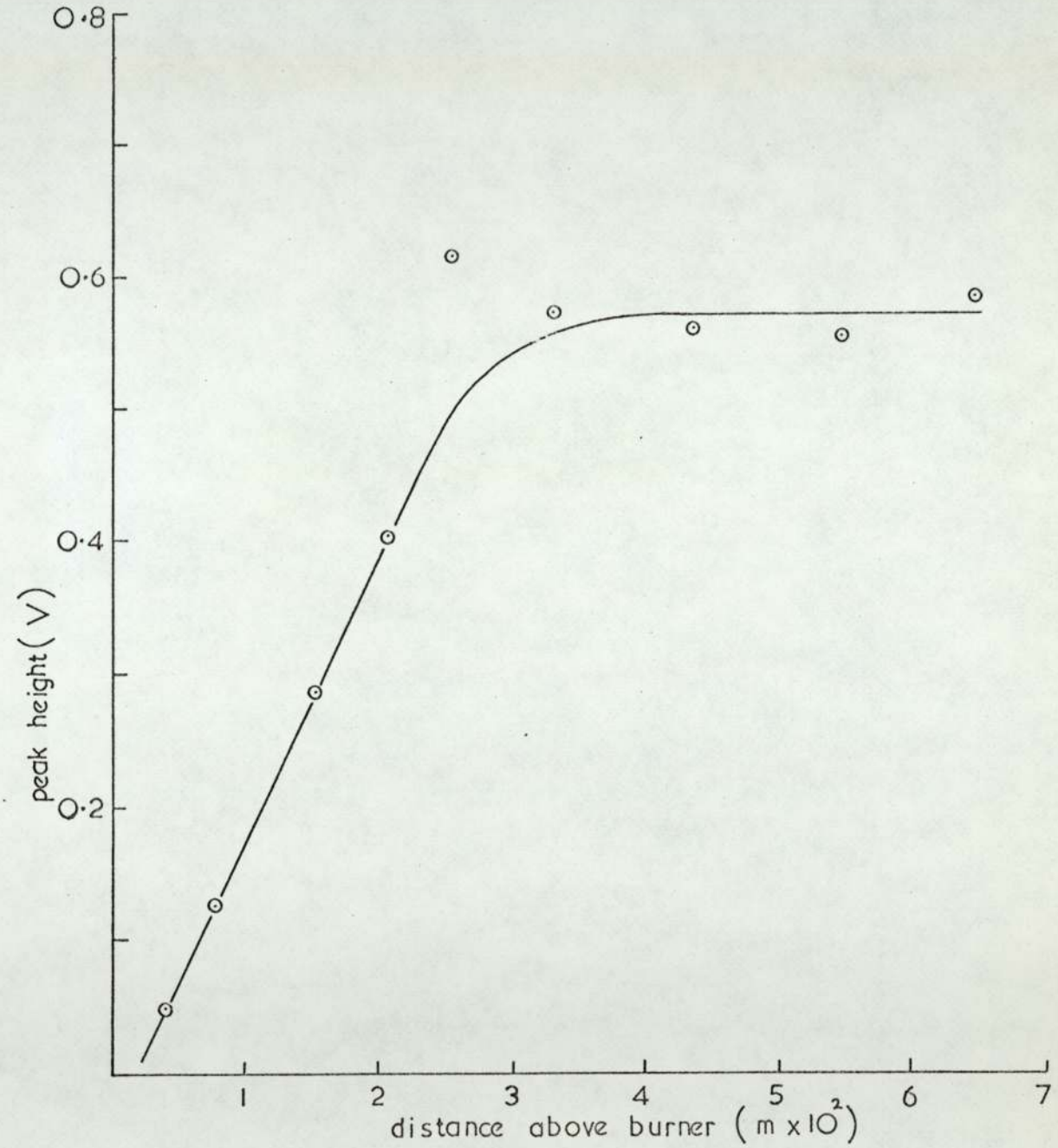

Figure 30 growth of spike width with height in the flame

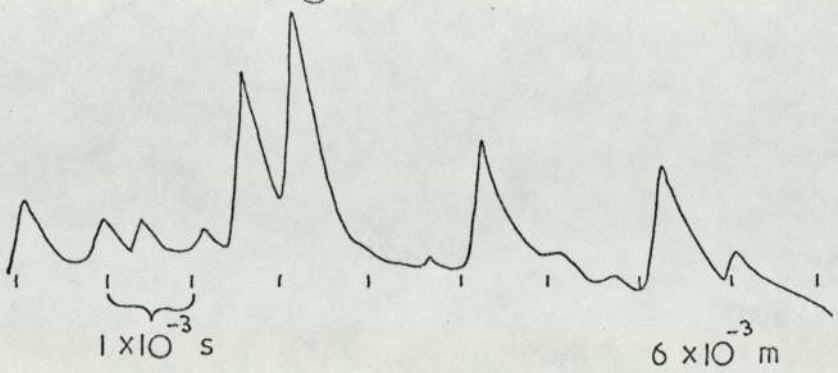

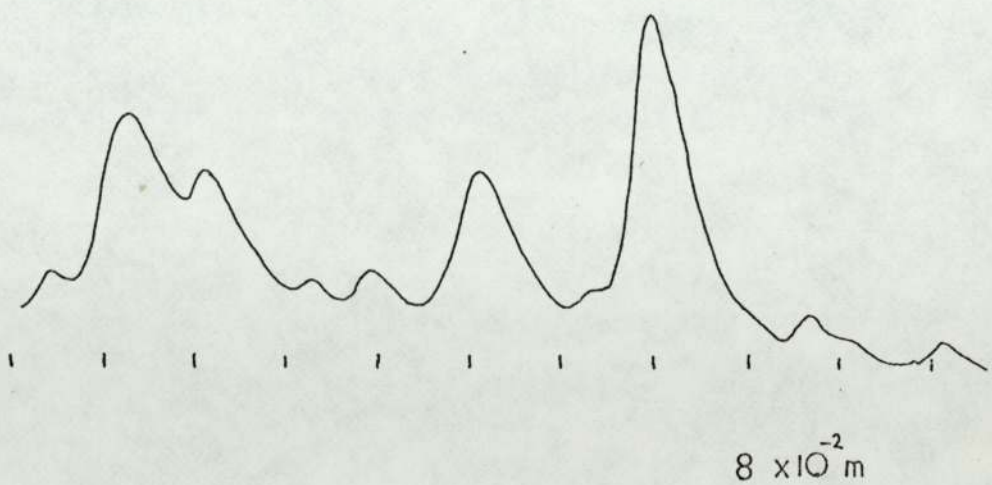

($SrCl_2$, 2507 K)

surface in the breaking bubble atomiser, since this is the slowest moving gas in the system.

From a Stokes Law calculation for a flow of 0.3 litres min^{-1} through the vessel, the largest particles delivered to the burner from a 0.2 molar solution of KCl should be 8.4 μm in diameter. This figure agrees well with that of 6.6 μm, the average diameter of the largest crystals collected on a slide at the burner exist and sized under a microscope. It was found, however, impossible to ascertain the size distribution of the crystals collected since only the largest could be measured at the maximum magnification of the instrument used. The half widths of a large number of peaks of varying height were measured again at 1×10^{-2} m above the burner, and from the results it was concluded that the widths were, to a first approximation, independent of peak height (Figure 32).

From these studies it became clear that the pulses were associated with gaseous ionisation rather than with thermionic emission, and a simple model was constructed to handle their growth with residence time in the flame.

9.iii. The Charge Cloud Model

The model can be summarised conveniently in three statements:-

(i) The probe is regarded as stationary relative to the flame gases, since its sweep velocity was 1.0 ms^{-1} and the convective velocity of the flame at 2507 K, 24.0 ms^{-1}.

(ii) The evaporation of the salts, KCl, $SrCl_2$, $K_2Cr_2O_4$, and K_2HPO_4 takes place in the order of microseconds, whereas the residence time of the material in the

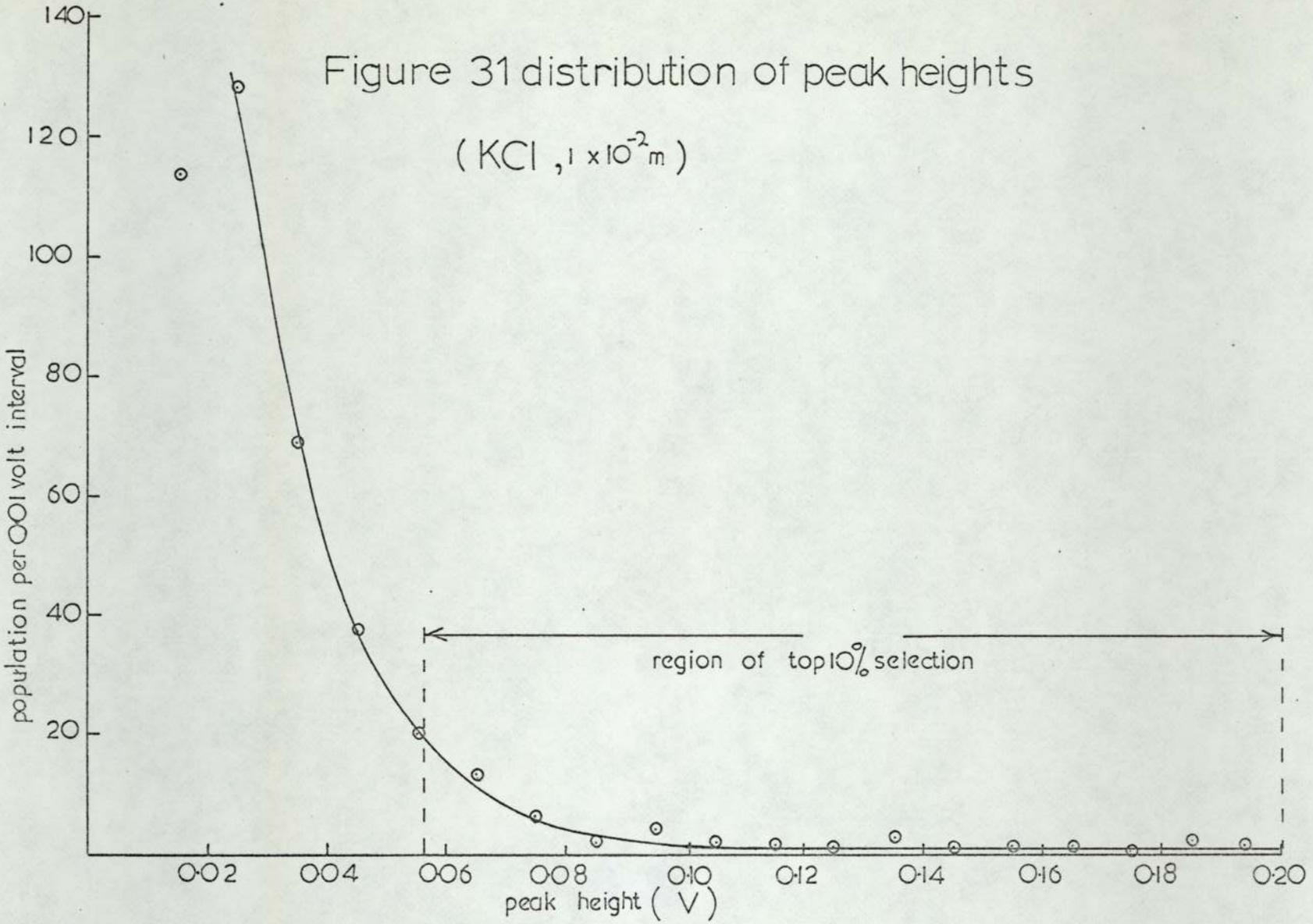
Figure 31 distribution of peak heights
(KCl , 1 x 10⁻² m)
population per 0·01 volt interval
140
120
100
80
60
40
20
region of top 10% selection
0·02
0·04
0·06
0·08
0·10
0·12
0·14
0·16
0·18
0·20
peak height (V)

Figure 32 distribution of peak widths

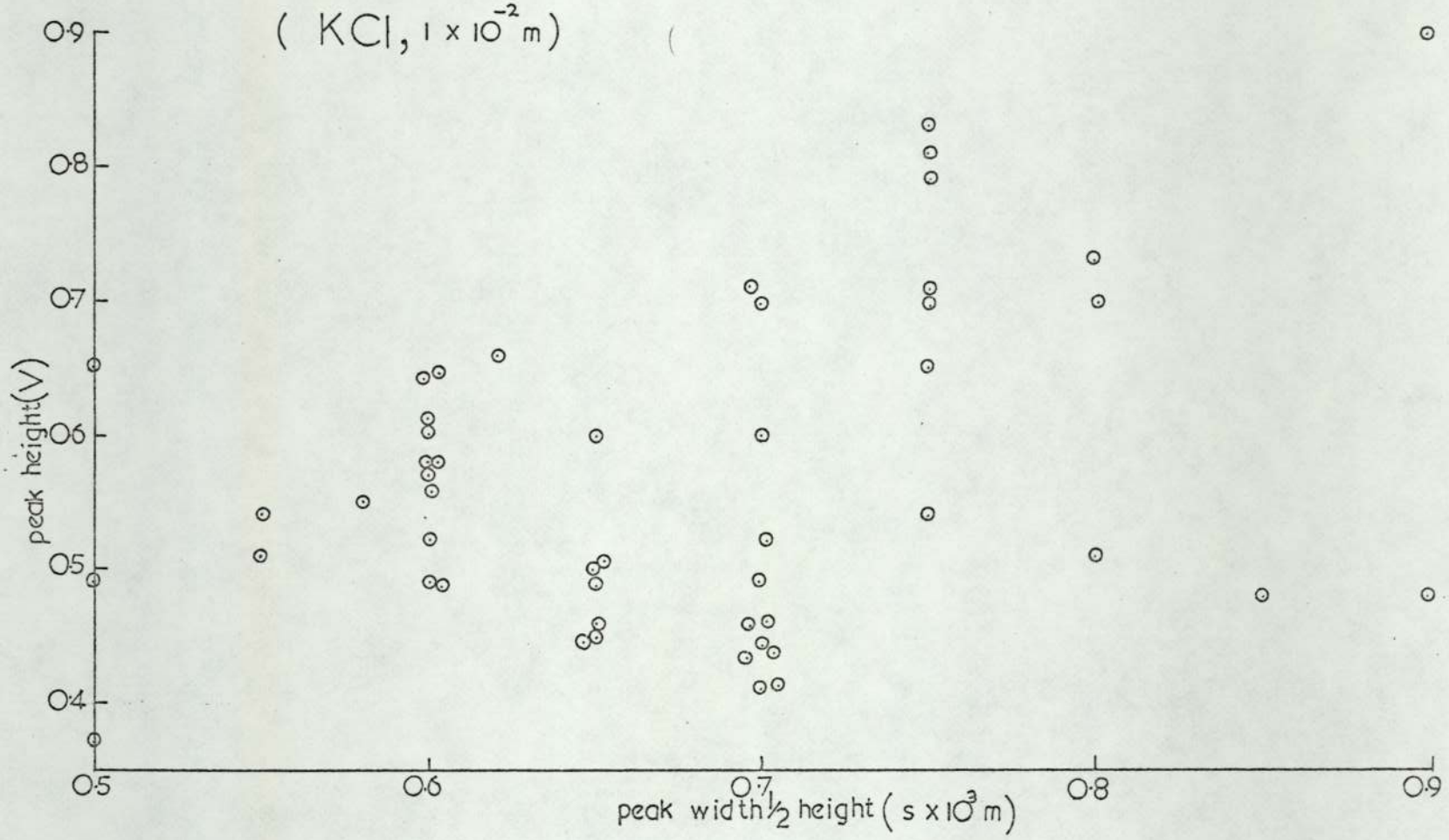

flame is in the order of milliseconds. Therefore the process may be regarded as being instantaneous. The formation of Cr_2O_3 particles from K_2CrO_4 is most probable, but it was thought unlikely that this would inhibit the transport of potassium atoms into the gas phase.

(iii) The flame is perfectly laminar and moving with piston flow, and the ions formed from the volatilised material occupy a sphere of gas, i.e. a charge-cloud of spherical geometry. This cloud travels upwards with the linear velocity of the flame passing over the probe and giving rise to the pulses of ion current seen.

The pulse will start when the edge of the cloud reaches the sheath edge, and finishes as the trailing boundary passes over the sheath edge. If the diameter of the cloud is greater than the cross-section of the sheath, the probe may pass along any section of it. The largest current will be associated with collection from the centre of the sphere, since there will be an exponential decay in density of ions away from this point due to diffusion. Since the largest pulses were selected it is assumed that the path of the probe will be through an axis of the sphere, and the width of the pulse is in fact the time taken to cross any axis of the cloud. When the cloud is smaller than the sheath, the pulse width will also approximate to this time. As the cloud is travelling with the linear velocity of the flame, its diameter may be found from the product of the "spike" width and flame speed.

The increase in widths with residence time in the flame may now be explained by the expansion of the cloud by ambipolar diffusion in three dimensions.

The diffusion coefficient, D, for a gas flowing down a concentration gradient, is given to be (e.g. Loeb[110]):-

$$\frac{dN}{dt} = -D \nabla^2 N \qquad 9.1$$

where N is the number density of the species, t, the time, and ∇^2 the Laplacian operator. The exponential decay of gas density at any radial distance, r, from an original point source of gas, is defined by Einstein's relationship:-

$$N(r) = \frac{No}{(4\pi Dt)^{\frac{3}{2}}} \exp - \left\{ \frac{r^2}{4Dt} \right\} \qquad 9.2$$

in which No is the number density at t=o, r=o, and N(r) is the number density at distance r, and time t. D has the dimensions of $L^2 T^{-1}$.

If at any time t the density at the point r=o, is N(c) then

$$N(c) = \frac{No}{(4\pi Dt)^{\frac{3}{2}}} \qquad 9.3$$

and

$$\frac{N(r)}{N(c)} = \exp - \left\{ \frac{r^2}{4Dt} \right\} \qquad 9.4$$

When $N(r) = \frac{1}{2} N(c)$ then

$$0.5 = \exp - \left\{ \frac{r^2}{4Dt} \right\} \qquad 9.5$$

If the measured half width of the pulses is w seconds and the velocity of the flame vf, then assuming the pulses to be symmetric

$$\frac{vfw}{2} = r \qquad 9.6$$

and, taking the natural logarithums of 9.5 then

$$\frac{(vfw)^2}{16Dt} = 0.694 \qquad 9.7$$

and

$$\frac{d\,(vfw)^2}{dt} \approx 11D \qquad 9.8$$

A plot of $(vfw)^2$ against r, the residence time in the flame, is shown in Figure 33 for potassium chromate at 2507 K, and D from the slope is found to be 4.5×10^{-3} m^2 s^{-1}. Inspection of Figures 25, 26 and 28, shows that the behaviour of the half widths was similar for the potassium salts the mean value of D for the potassium ion being 5.0×10^{-3} m^2 s^{-1}. The results from strontium chloride give D for the positive ion involved to be 4.5×10^{-3} m^2 s^{-1}.

If X is the field set up by the charge separation, $\mu-$, $\mu+$ the mobilities, $\bar{v}+$, $\bar{v}-$ the mean velocities and n+, n- the charge densities then

$$n+v+ = -D+\nabla n+ + \mu+Xn+$$

and $$\qquad 9.9$$

$$n-v- = -D-\nabla n- + \mu-X\bar{n}$$

Rearranging and assuming that $n+ = n- = n$, and that $\bar{v}+ = \bar{v}- = \bar{v}$, the mean velocity $\bar{v}$ is given by:-

$$\bar{v} = \frac{-D + \mu- + D-\mu+ \nabla n}{(\mu+ + \mu-)\, n} \qquad 9.10$$

Using Einstein's relationship for the ionic mobility:-

$$\frac{\mu+}{D+} = \frac{Ne}{P} = \frac{e}{kT} \qquad 9.11$$

Figure 33 estimation of D(K_2CrO_4, 2507K)

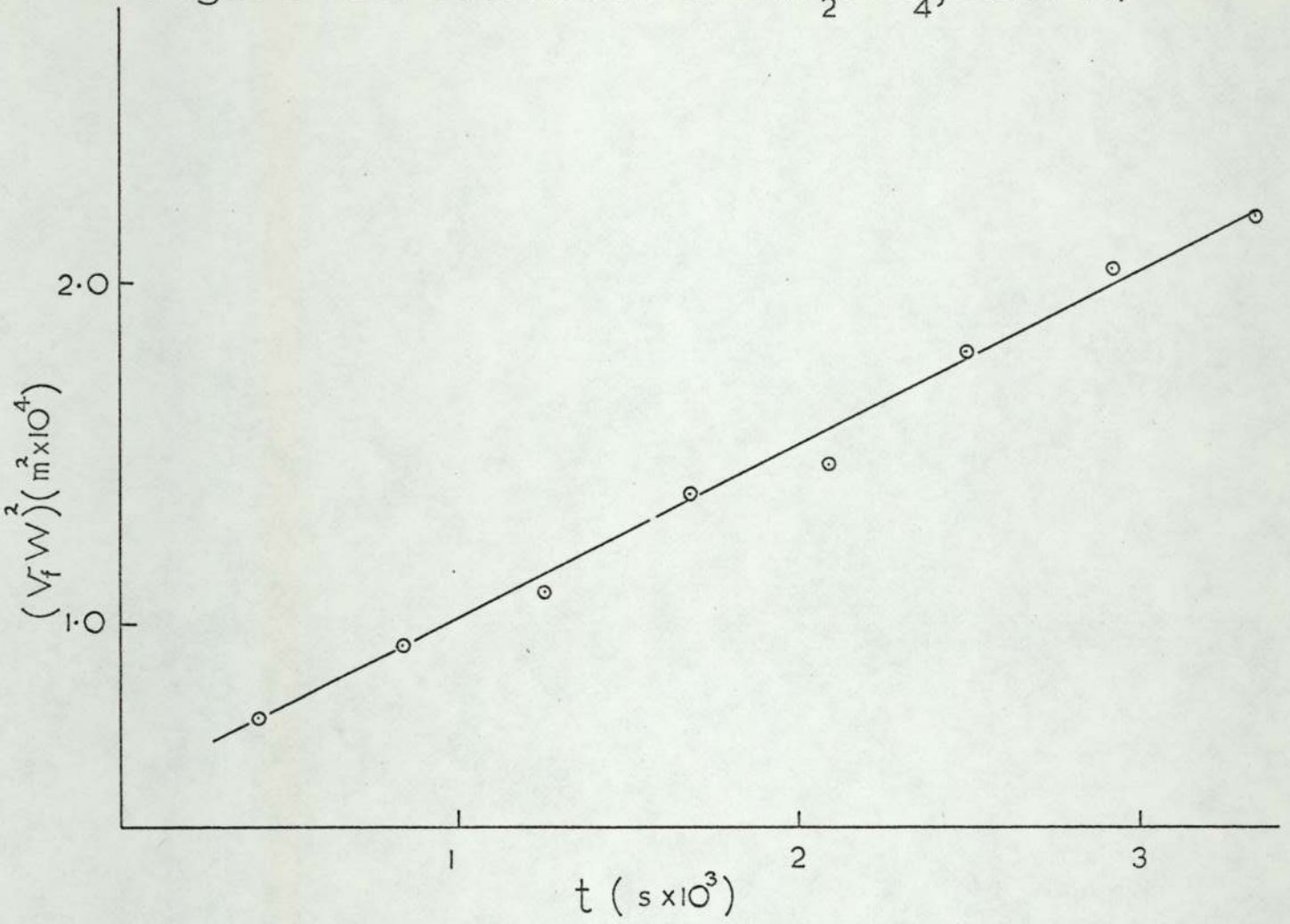

where P is the pressure, then:-

$$D_{\pm} = \frac{D_+\mu_- + D_-\mu_+}{\mu_+ + \mu_-} = \frac{k}{e}(Te + Ti)\mu \qquad 9.12$$

and for the case of Te = Ti, which is assumed to be so in flames at atmospheric pressure, $D_{\pm} = 2D_+$. The true diffusion coefficient of the positive ions will be half the values quoted above.

Using equation 9.8 and values for the ion mobility μ_+, from Kaye and Laby[111], and a temperature dependence of D_+ of $T^{1.5}$, the diffusion coefficient for a typical positive ion should be in the region of 1×10^{-4} m^2 sec^{-1} whereas the values obtained from the spike measurements were much larger at between $2.0 - 2.5 \times 10^{-3}$ m^2 sec^{-1}. This may be interpreted in the fact that the pulses seen were too wide, and by quoting some of the experimental data, in more detail this can be seen to be so.

Taking the pulses to be triangular, the half width will be characteristic of the cloud radius. Using the calculated flame speed at 2507 K, the experimental data predict that from a crystal of potassium chloride of diameter some few microns, a cloud of gaseous K^+ ions, which expands by diffusion to 3.4×10^{-2} m after being in the flame for 3.3×10^{-3} seconds is formed 1.6×10^{-2} m. in diameter almost instantaneously. From a simple calculation a crystal of potassium chloride, 3μ radius, would evaporate and occupy a sphere of radius 1×10^{-4} m, if all other species were excluded from that volume, which is two orders of magnitude greater than the cloud dimension derived above. Furthermore, if the simple model proposed was viable, the extrapolated radius for r=o at the burner surface should be comparable to the original magnitude of the solid crystal, which would approximate to a point source on this scale.

Both the size of the sheath and the shaping of the pulses by external circuit factors might serve to exaggerate the "spike" widths. To examine this point the half widths for the "spikes" at a series of heights above the burner were measured for potassium chloride, with the probe at zero bias and are shown in Figure 34. The probe at zero bias will draw a positive current due to the space potential of the plasma being positive relative to any body immersed in it. A small positive space-charge region will exist in the vicinity of the probe electrons and may now penetrate to the probe to a much greater extent than in the saturation region, and the magnitude of the currents seen will be much smaller. The absolute values of the half widths have been reduced by approximately a factor of two, showing some possible dependence of the "spike" width on the relaxation of conditions around the probe, but they still indicate the presence of charge-clouds about 1×10^{-2} m diameter in the reaction zone of the flame.

9.iv. The Effect of the External Circuit on the Spikes

It has been mentioned earlier that the circuit-elements might markedly effect the decay time of the pulse, and this was investigated for flames again seeded with potassium chloride at zero bias. Although in Figure 20, the flame, which may be assigned a resistance and capacitance, is shown in parallel with the external circuit it was not considered to effect the shaping of the pulses in the normal way for an R.C. network. The chief contributors to the stray capacitance were found to be the mercury commutator, and the coaxial cable. By reducing the length of cable used and increasing the thickness of insulating material between the mercury in the commutator and its earthed shield, the R.C. of the circuit could be considerably reduced. The smallest R.C. was obtained by removing the standard

Figure 34 results from KCl, 0 volts bias

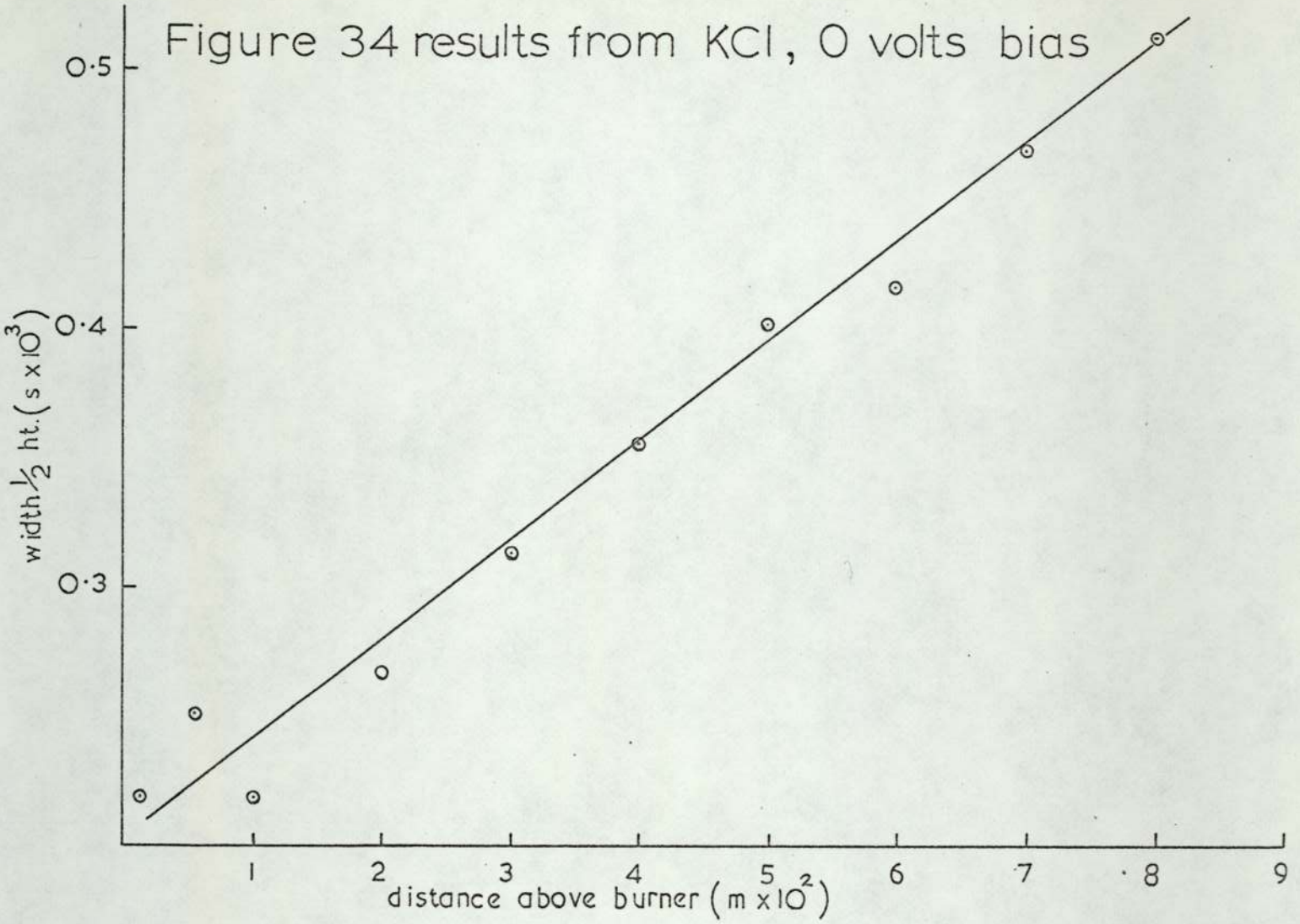

coaxial cable and replacing this by copper wire surrounded by nickel sheet spaced 1×10^{-2} m radially from it.

The capacitance and resistance of the circuit was measured using a capacitance-resistance bridge, and Figure 35 shows the rise time and apparent R.C. of the decay of the "spikes" plotted against the measured R.C. product of the external circuit, for a flame at 2507 K. As can be seen the measured R.C. is greater than the calculated one, although they are of the same magnitude. The rise-time however shows an almost constant value. At the lowest point the shaping of the pulse is in fact small, and the rise-time measured should be due to the original form of the signal. That the measured apparent time constant is slightly less than half the rise-time, would indicate that the shap of the pulse is "skewed" towards the trailing edge.

The measurements for 0.2 molar KCl, at 2507 K were repeated at various heights up to 8×10^{-2} m in the flame, using the low time constant circuit, for 0V and -90 V on the probe. The alternative circuit shown in 20b was used to apply the bias, so eliminating the shielded battery- and potentiometer-housing from the probe side of the circuit. These elements had been found to contain a significant portion of the stray capacitance.

The results from these measurements are shown in Figures 36 and 37. Apart from a slightly increased slope in the high bias run, both plots appear similar, the mean value of the extrapolated half width (r=o) for the two cases being 1.1×10^{-4} s. From the plots of $(vfw)^2$ vs t, and using equation 9.8, diffusion coefficients of 6.96×10^{-4} m^2 s^{-1}, and 9.0×10^{-4} m^2 s^{-1}, were found for the potassium ion from the data at 0V bias and -90 V bias, respectively. These values are still high compared to the figure of 1×10^{-4} m^2 s^{-1} calculated from the mobility, but are more reasonable than those obtained with the original probe circuit.

Figure 35 variation of the circuit time constant

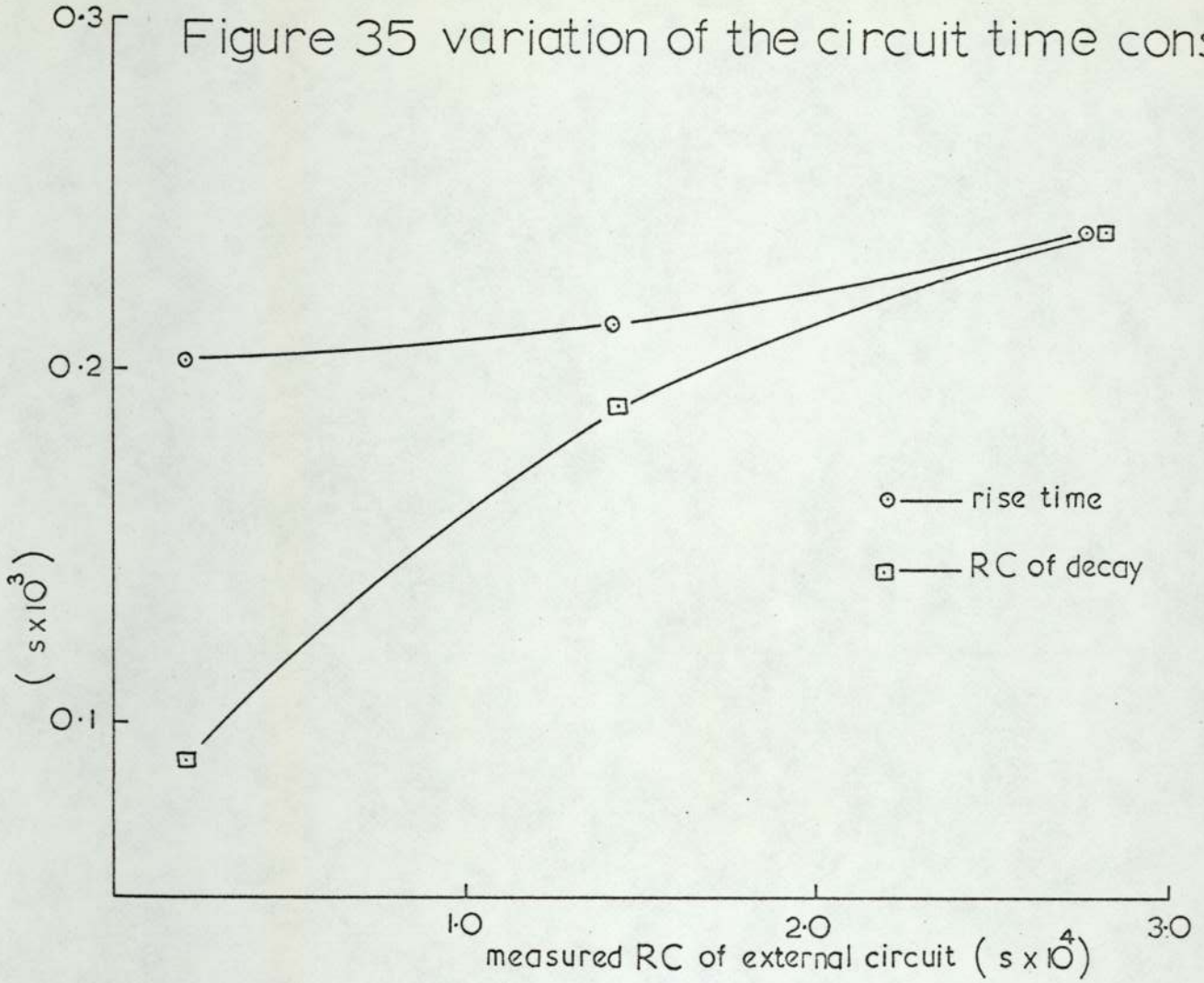

Figure 36 KCl, 0 volts bias, low RC circuit

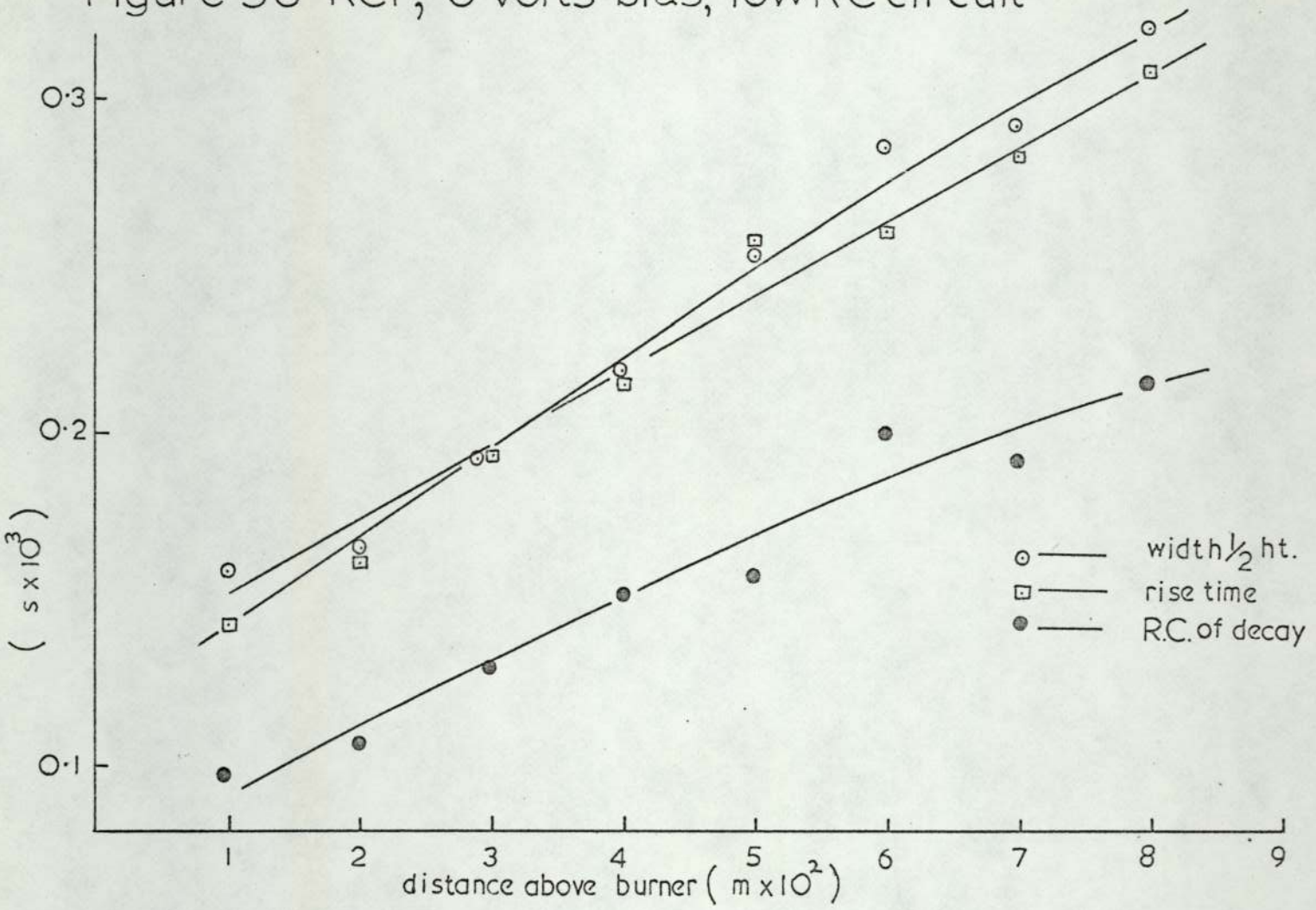

Figure 37 KCl, -90 volts bias, low R.C. circuit

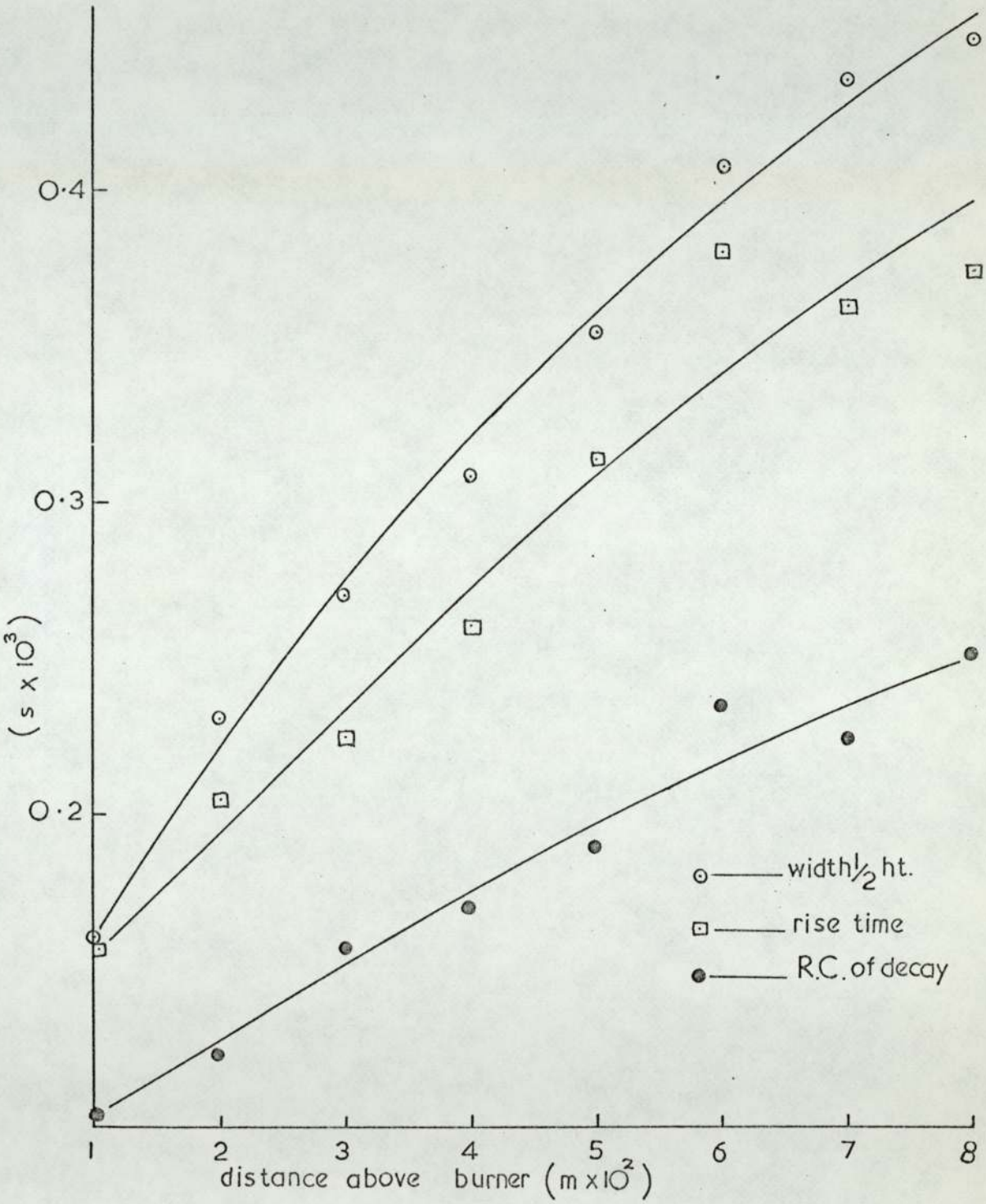

The extrapolated half-width at zero residence time in the flame still indicates a large initial size for the charge cloud of 2.6×10^{-3} m radius. Since it is difficult to envisage a mechanism whereby the crystals could evaporate or explode to produce a spherical distribution of gaseous ions of this magnitude, the conclusion must be drawn that the simple charge cloud model presented is not applicable. An alternative view, would be that the model was essentially correct but that relaxation effects at the probe and sheath region, were broadening the signal, and that the minimum half width represents a lower limit for the probe response. Against this suggestion is that if the time taken for the cloud to pass over the probe was small compared to the relaxation time, the "spike"-widths should not show such a large proportional increase with residence time in the flame.

9.v. The Fluctuating Ion Current to the Probe

As already stated in Chapter 7, no complete theories of time-dependent phenomena associated with probes has yet been evolved, and much of the work in this field has been in connection with variations in the probe bias rather than with discrete variations in the plasma density. The general conclusions reached regarding response times of the probe under such conditions may not be applicable for the present case, where there is a highly negative probe immersed in a high velocity plasma containing small regions of high ion density and yet where the bulk properties such as conductivity and space potential are assumed constant. A further complication stems from the fact that there is an uncertainty as to whether the dimensions of the charge cloud are greater or less than those of the sheath region.

For a steady state sheath condition around a negative probe in a flowing plasma it is assumed that the ions and electrons approach the sheath by convective motion, i.e. at the flame velocity, and that the drift velocities of the ions within the sheath region ~~is~~ are greater than the flame velocity. The second condition implies that within the space charge region the number density of ions decays as the probe is approached. The loss factor of ions, rebounding after collisions, from the sheath has to a first approximation no effect on this picture.

For the condition where Vp and Vs are constant, a small region of high ion density should perturb the sheath in the following way. The cloud approaches to the original sheath boundary, where the positive ions will be accelerated by the field and the electrons will be deflected around the sheath. By virtue of the greater ion density present the shielding of the electrons from the probe field is now more effective, and they may approach to a greater extent than before, i.e. the sheath boundary has been moved closer to the probe. The ions are collected and appear as a pulse of positive current, with no relaxation time involved since they approach the region with the flame speed, and cover the distance across the space charge region at a greater velocity. As the ions are removed by the probe, the closest point of approach of the electrons must move back to the position compatible with the normal flux of ions in the plasma. The situation may now be regarded as being similar to the case of a negative probe biased further negative.

Readjustment of the electrons will take place very quickly but the ion density within the old sheath region is now too high, and reduction by collection will give rise to a small overshoot current. The time taken for this current to be collected will depend on the speed of the ions, and will be typical of the reciprocal of the plasma

ion frequency. For a collisionless plasma, the ion plasma frequency V_i is given by the inverse of the time taken by an ion, with its maximum velocity, to travel across a Debye length, and is given by

$$V_i = \left(\frac{4\pi N i e^2}{m_i} \right)^{\frac{1}{2}} \qquad 9.13$$

Taking a typical value for N_i of 1×10^{14} m^{-3}, V_i will be of the order of 10^6 s^{-1}, and the time taken to cross the sheath region 1×10^{-6} seconds. Obviously such times would not be important in determining the width of the spikes. The same conclusions would be reached for the case where the cloud dimensions are very much less than those of the steady state sheath region. Here the clouds may be viewed as puncturing the sheath and taking the effective boundary closer to the probe.

Since the mean free paths of the ions will be small compared to a Debye length in a flame at one atmosphere and containing 1×10^4 ions m^{-3}, the simple relationship, of equation 9.13 will not be strictly applicable in determining the response time. The Debye length was calculated to be 3×10^{-4} m for this flame, and the probe radius a, was 1.25×10^{-4} m. Although the probe characteristics showed that a thin sheath situation is most likely, an upper limit to the effective sheath radius of 2a will be used in the calculation to give the maximum distance that the ions will have to cross to give rise to a transient ion current. The probe is considered to be collecting at saturation.

The equation derived by Shultz and Brown[97] for the time taken t^+, by a mean ion to cross the sheath around a cylindrical probe is

$$t^+ = \left(\frac{a}{\mu^+} \right) \left\{ \left[\left(\frac{s}{a} \right)^2 - 1 \right] \frac{2\pi \mu^+ \varepsilon_o L}{I_i}^{\frac{1}{2}} \right\} \qquad 9.14$$

where L is the length of the cylindrical probe.

Using the measured clean flame ion current of 2×10^{-7} A for the probe at -90 V, and a value for $\mu+$ of the potassium ion at 2500 K, in an atmosphere of H_2O, N_2 and H_2, of 3.48×10^{-3} m^2 s^{-1} V^{-1}, t+ was calculated to be 8.3×10^{-5} seconds from equation 9.14. The result is the most interesting since this is of similar magnitude to that of the half-widths of the pulses. It must be remembered though that the value of s was taken to give a maximum value of t+. If a probably more realistic ratio were taken of sheath radius to probe radius corresponding to $\frac{s}{a} = 1.10$ appropriate to a thin sheath situation, then the above equation gives t+ to be 2.2×10^{-5} seconds which is almost an order of magnitude less than the total duration of the "spikes".

The magnitude of this transient ion-current is likely to be small as it depends on the background ion density and should not influence the rise time of the spikes. The increase in half-widths would be difficult to account for by this concept, unless there was a direct relationship between the distance travelled by the ions during the transient, and the dimensions of the cloud forcing the sheath to contract. As the cloud diffused with time in the flame the number density of ions within it would decrease, thus diminishing the effective shielding of the electrons from the probe, and lessening the reducing effect on the sheath dimensions. Therefore the most likely results would be to give an apparently smaller growth in the size of the clouds.

A further aspect of the problem arises when the impedance of the sheath is considered to act as a capacitor and resistor in parallel. This description has been used by a number of workers, and the variation of the sheath capacitance and resistance with probe bias frequency, has been discussed in a recent article by Oliver, Clements and Smy[112].

At the floating or wall potential Vf, the resistance of the sheath is given by:-

$$R(Vf) = \left[(2\pi me)^{\frac{1}{2}}/ANe^{2}\right] (Ve)^{\frac{1}{2}} \exp(Vf/Ve) \qquad 9.15$$

where Ve is the electron temperature in electron volts and A the probe surface area. The resistance of the sheath is governed by electrons and so should be independent of frequency provided that this is below the electron plasma frequency. The value of N however will apparently change since the local ion density around the probe will change. So the resistance should show some inverse dependence on the local ion densities, when the sheath is perturbed. Oliver et al have considered the treatment of Crawford and Grard[113] to be most appropriate for deriving the sheath capacitance at frequencies below that of the plasma ion frequency. This is computed from the displacment current caused by the movement of the sheath boundary and is given by:-

$$Cp\ (Vf) = (me/4m_{i})^{\frac{1}{2}} \left[\exp(Vf/Ve)\right]^{\frac{1}{2}} \times (Ve/Vf)^{\frac{1}{4}} A\varepsilon_{o}/\lambda \qquad 9.16$$

for the case of a planar probe. This should give approximately the correct answers for the thin sheath condition of a cylindrical probe.

For frequencies above the plasma ion frequency, the concept of Montgomery and Holmes[114] is preferred, wherein the electrons are seen to move and the positive ions remain frozen. The sheath boundary and probe surface may then be viewed as a parallel plate condenser. Oliver, Clements and Smy[112] have developed this approach for cylindrical geometry, and their expression for the capacitance of the sheath at the floating potential is:-

$$C(Vf) = 2\pi\ \varepsilon_{o}.L./\ln \frac{s}{a} \qquad 9.17$$

Experimental results have shown that the low frequency capacities given by 9.16 will be about a factor of two greater than the high frequency case.

Taking $\frac{s}{a}$ to be equal to 1.10, equation 9.17 would give: C(Vf) as 3.5 pF; and from equation 9.16, as 7pF. If the floating potential is assumed to be close to zero; and the plasma potential to be one or two volts positive to this, then a charge of some 10^{-11} coulombs might be stored at the sheath. As the displacement current should be dependent upon the movement of electrons, its duration should be much less than that of the transient overshoot currents, but for times of about 1×10^{-6} seconds a current of 1×10^{-5} A could be observed during the complete formation or destruction of the space charge region.

It may be concluded that such displacement currents should have little effect on the "spike"-widths, but although because of the real situation existing in flames the amplitude of the current might be very much less than the 1×10^{-5} A quoted above, some contributions by them to the peak heights is possible.

The introduction of a resistance and capacitance in parallel between the probe and the plasma, must be considered for its effect on the total R.C. of the circuit. The resistance in parallel with the 1 MΩ load resistor and oscilloscope impedance, will be of the order of 1×10^{-8} Ω and should have a very small effect. Likewise the capacitance of the sheath of 1-10 pF will be only a minor contribution to the total capacitance of the external circuit.

CHAPTER 10

THE EVAPORATION PROCESS

10.i. Particle Velocities

In the previous chapter it was argued that plasma probe interactions and electronic phenomena could not satifactorily explain the "spike"-widths. Since all reasonable assumptions lead to the fact that gaseous ionisation was the origin of the events seen, it occurred that the idea of a spherical distribution of the ion produced from the evaporated crystal was incorrect.

The horizontal sweep velocity of the probe through the flame, was calculated to be 1 ms^{-1}, and that of the burnt gases in a flame at 2507 K to be in excess of 20 ms^{-1}. Therefore it seems reasonable to regard the probe as stationary to the plasma whilst immersed in the flame. It can be seen that the duration of the pulses will only describe a characteristic distance in the vertical plane and will offer little information on the dimensions of the charge clouds in the horizontal plane without some prior assumption concerning their spatial distribution.

If a meteor trail of ionised atoms or molecules were the result of the evaporation of the volatile material, this would provide a more acceptable description of the "spikes", but would require that during the heating and evaporation process, the particles and the flame would be travelling at different velocities.

Experiments involving the collection of crystals from the unburnt gases at the burner exit and rapid examination under a microscope revealed that during their passage from the atomiser, the droplets had evaporated to leave dry crystals. These crystals will have a settling or drag velocity in the opposite direction to that of the gases.

The terminal falling velocity v of a particle radius r, falling through an infinite fluid of viscosity η, is given by Stoke's Law to be:-

$$v = \frac{2 g r (\sigma - p)}{9\eta}, \qquad 10.1$$

g being the acceleration due to gravity, and σ and p, the densities of the particle and fluid respectively. For a particle of a few microns diameter, v is of the order of 1×10^{-2} ms^{-1}, and is certainly negligible compared to the flame velocities considered here. The drag velocity of the crystals entering the reaction zone, therefore, cannot be used to predict the formation of a meteor trail of gas from the crystal. Following the line of thought, that the particles are travelling at a different velocity to that of the flame gases, then the alternative case in which that the particles are travelling faster than the gas, must be examined.

The mean exit-velocity of the unburnt gases, from the burner tubes was calculated to be 17.3 ms^{-1}, and that of the burnt gases 24.3 ms^{-1}, after allowing for a reduction in volume due to the formation of H_2O, and an increase in volume from the rise in temperature up to 2507 K. This flame-velocity is probably only appropriate to a height of 2×10^{-2} m and above, where temperature equilibration is complete.

Assuming Poiseuille-flow through the tubing, since their length is many times greater than their diameter, the velocity v(r) at any radial distance, r, from the axis of the tube is given by:-

$$v_r = \frac{G (a^2 - r^2)}{4\eta}, \qquad 10.2$$

where a is the radius of the tube, and G the pressure gradient involved.

The volume flow per unit time, V can be found from:-

$$V = \int_0^a \frac{G\,(a^2 - r^2)\,2\pi r\,dr}{4\eta} = \frac{\pi G a^4}{8\eta} \qquad 10.3$$

and

$$G = \frac{8\eta V}{\pi a^4}. \qquad 10.4$$

The mean velocity $\bar{v}$ is therefore $\frac{V}{\pi a^2}$, and the maximum velocity at the centre of the tube, $\frac{2V}{\pi a^2}$, or $2\bar{v}$.

Now the largest crystals delivered will be those carried in the fastest moving part of the gas stream, and large particles appropriate to this velocity will either sink to the walls or possibly move across into the region of high velocity. The supply of crystals or droplets to the mixing chamber at the burner base will also have a distribution due to the parabolic velocity profile in the fuel lines. Since the larger crystals are moving at a greater speed, their delivery rate should also be greater, and most of the "spikes" seen should originate from crystals travelling at the maximum velocity through the centre of the hypodermic tubing. The possibility still remains of a distribution of particle sizes reaching the flame from the central portion of the tubes, since crystals of any size up to a limit may be carried by the fast stream.

Due to the large difference in mass between the gas molecules and the crystals, the latter will be moving at v max. or approximately 34 ms^{-1} which is 10 ms^{-1} in excess of the resultant burnt gas velocity of 24 ms^{-1}. If the time taken, for the particles to adjust to the

gas velocity is greater than the characteristic time for the evaporation process, a trail of gaseous volatilised material will be left behind in the crystal's wake.

Tsuji and Hirano[115] have studied the spatial distribution of positive ions around the reaction zone of a laminar propane-air flame at 2000 K, using a Langmuir probe. The flame was stabilised on a two dimensional nozzle, and it was observed that the results obtained by seeding with potassium salts from a conventional atomiser were very different from those obtained from the background ionisation. In the unseeded flame, the H_3O^+ ions appeared to be evenly distributed around the luminous cone, but the K^+ ions produced from the potassium salts seemed to be concentrated above the apex of the reaction zone of conical section. Other factors such as gas mixtures and temperature were shown to affect the ion distribution, but it is possible that the majority of the spray was delivered through the centre of the nozzle rather than being evenly distributed in the gas stream.

Also of interest are the remarks of ~~Aston~~ Ashton and Hayhurst[116] concerning the assessment of flame velocities produced from a multitube burner. They measured the velocity by illumination and photography of small MgO particles delivered to the central portion of their flame, and found that the results were 20-50% higher than those predicted by calculation. This would fit in well with the idea that the maximum particle velocities from the hypodermic tubes would be greater than that of the burnt gases.

The time taken for the particles to adjust to the gas velocity will be most important, and an estimate of this time may be obtained by considering the drag-forces acting.

Consider a particle moving with a velocity μ_p in a direction x, through a gas of density ρ_g, moving with velocity μ_g. According to Neilson and Gilchrist[117] the drag-force may be expressed by:-

$$m \frac{d^2x}{dt^2} = -Cd\, \rho_g\, (\mu_g - \mu_p)^2\, Ap\,, \qquad 10.5$$

where m is the mass of the particle, Ap its cross sectional area, and Cd the drag coefficient which may be related empirically to the Reynolds-number.

Equation 10.5 may be rewritten in the form:-

$$\frac{d\mu_p}{dt} = -D\mu_p^2\,. \qquad 10.6$$

If μ_g is considered to be zero, and

$$D = \tfrac{1}{2} \frac{Cd\, \rho_g\, Ap}{m}\,, \qquad 10.7$$

therefore integrating with respect to t,

$$\frac{d\mu_p}{\mu_p^2} = -Dt + \text{Const.} \qquad 10.8$$

If $\mu_p = \mu_o$, when t=o, then:-

$$\frac{1}{\mu_p} = Dt + \frac{1}{\mu_o}\,, \qquad 10.9$$

which can be rearranged to yield:-

$$\mu_p = \frac{\mu_o}{1 + \mu_o Dt}\,. \qquad 10.10$$

The variation of the drag-coefficient with Reynolds number is given to be:-

$$Cd = \frac{f\ 24}{Re}, \qquad 10.11$$

where

$$f = \frac{28\ Re^{-0.85} + 48}{24\ Re^{-1.0}}. \qquad 10.12$$

Neilson and Gilchrist have presented the variation of Cd and Re graphically, and, from this, Cd is approximately 10^{2} for a Reynolds-number of 10^{-1}, appropriate to the gas flow over the particles. Using a mean density for the flame-gases at 2507 K of 1×10^{-3} kg m^{-3} and a mean particle radius of 2.5×10^{-6} m, D may be approximated to 10^{1}.

From equation 10.10, it can be seen that an inert particle, under these conditions, would be travelling at 5 ms^{-1} and 1×10^{-2} seconds, taking the maximum possible value of μ_e as being 10 ms^{-1}.

The distance travelled by the particle S, which will give the length of meteor trail produced, can be obtained by the integration of equation 10.10:-

$$S = \int \mu_p dt = \mu_e \int \frac{1}{1 + \mu_e Dt}\, dt, \qquad 10.13$$

and therefore

$$S = \frac{1}{D} \ln(1 + \mu_e Dt), \qquad 10.14$$

for the condition that: S=0 when t=o.

The minimum half width time, at t=o, for potassium chloride, was about 1×10^{-4} seconds, which would, by multiplying the flame-velocity, indicate a trail of 4.8×10^{-3} m in length. Using this value, for S, in 10.4, gives t to be 5×10^{-4} seconds, which although larger than the measured half width, serves to illustrate the feasibility of the meteor trail concept. The velocity differential between the particles and gases is most likely to be an underestimate, since immediately above the reaction zone the flame gases will not have achieved their maximum velocity, and this would serve to increase the length of trail produced. On the other hand evaporation is taking place, with a resultant loss of momentum and increased rate of deceleration, and from this aspect, the calculations would give an over-estimate of the maximum length of trail produced.

The energy, contained as kinetic energy, at t=o, must be lost by frictional heating of the particle, or, in the volatilisation of the material from its surface. The total kinetic energy of the mean particle of potassium chloride moving at 10 ms^{-1} will be about 3.8×10^{-12} and this is to be distributed amongst the 6×10^{11} molecules present. Taking a value for the latent heat of vaporisation of liquid KCl, at 1700 K, of 113 kJ mol^{-1}, and a mean Cp in the liquid range of 72 kJ mol^{-1} from the J.A.N.A.F. tables, then the available energy is sufficient to evaporate approximately 2×10^{7} molecules at the boiling point or raise the liquid droplet temperature by 1×10^{-2} K. Obviously the result of the heating process will be concentrated at the particle surface, but the simple calculations show that this will have a negligible effect on the overall volatilisation rate of the crystals.

10.ii. Heat Transfer

The heat transfer rate to the particle was calculated using the procedure recommended by Conolly[118]. The heat flux between the free stream gases and the cool gases in the boundary layer surrounding the moving particle is calculated by means of the averaged properties of the gas across this temperature gradient. The properties were computed, at various gas temperatures with the known burnt gas compositions, for the unburnt composition of the flame burning at 2507 K. The thermal conductivity thus found includes both normal conduction, and heat transfer from radical recombinations at the surface, or within the cool boundary layer. The heat transfer rates for the heating of the particle through four temperature increments up to its boiling point, were then calculated and extrapolated in order to estimate the total heating time involved.

The Nusselt number, Nu, may be related to the Prandtl and Reynolds numbers by:-[119]

$$Nu = 2 + 0.69\ Pr^{0.33}\ Re^{0.50}, \qquad 10.15$$

and at the low Reynolds number, appropriate to the KCl crystal moving through the gas at a velocity of 10 ms^{-1}, then Nu $\approx$ 2[119]. The following definitions can be written, for the dimensionless parameters used:-

$$Nu = \frac{hd}{\lambda};\quad Pr = \frac{Cp}{\lambda};\quad Re_s = \frac{dG}{\mu_s};$$

$$\bar{Re} = \frac{dG}{\bar{\mu}}, \text{ and } \bar{Re} = Re_s \frac{\mu_s}{\bar{\mu}}, \text{ where d is the diameter of the particle,}$$

h the heat transfer coefficient, λ the thermal conductivity, G the mass flow rate over the particle, and μ the viscosity of the gas. The suffix s indicates free stream conditions, and the bar signifies the mean of the property between the free-stream and the boundary layer.

The Stanton number, St, is defined by:-

$$St = \frac{Nu}{RePr} = \frac{2}{RePr} ; \qquad 10.16$$

and therefore

$$\bar{St} = \frac{2}{\bar{Re}\bar{Pr}} . \qquad 10.17$$

The heat-transfer coefficient may now be given by

$$h = \frac{2\,\bar{\mu}\,\bar{Cp}}{\bar{dPr}} . \qquad 10.18$$

The total heat transfer rate per unit area, q, can be found from

$$q = h\ \Delta T\ \Delta t ; \qquad 10.19$$

where Δt is the time increment, and ΔT the temperature difference between the free stream gas and the particle surface.

From equation 10.19

$$q = \frac{2\,\bar{\mu}\,\Delta H\,\Delta t}{\bar{dPr}} ; \qquad 10.20$$

ΔH being the enthalpy difference between the gases in the free stream, and in the boundary layer. The time taken to heat the particle from T to T + ΔT, can be found from:-

$$\Delta t = \frac{q\,\bar{Pr}\,d}{2\,\bar{\mu}\,\Delta H} . \qquad 10.21$$

Using computed values of $\bar{Pr}$, μ and ΔH, calculated values of q for KCl, with values of Cp KCl taken from the J.A.N.A.F. tables, Δt was calculated for the four temperature increments, 400-800 K, 800-1200 K, 1200-1600 K, and 1600-1800 K. The total time taken to heat the particle to a temperature $\bar{T}$ in the centre of these increments, is

shown against those temperatures in Figure 38. The extrapolated time taken to heat the particle to its boiling or sublimation point (1773 K), is taken from the plot as 2.3×10^{-6} seconds. An allowance for the time taken to transfer the heat of vaporisation of the particle at 1773 K, at the rate found for that temperature, assuming a constant sized particle, reveals that the total heat transfer process should be completed in the order of 1×10^{-5} seconds.

10.iii. Mass Transfer

Having shown that the heat transfer rates are appropriate for the evaporation of the crystal in a fraction of a millisecond, it is important to ascertain whether the mass-transfer rate is also of the same order. The treatment of Bradley and Evans and Whythaw-Gray[120], following the original concept of Fuchs[121], has been used by Woolley[36] to characterise the life time of metal oxide particles in flames of this type. Woolley found from his results that at least for the alkaline earth oxides, the predicted times were too large by about a order of magnitude, but the approach is used here for the volatilisation of a potassium chloride particle.

The diffusion of molecules from the surface is seen as starting from the surface of an enveloping sphere radius $a + \Delta$, where a is the radius of the particle; and Δ is of the order of the mean free path of the surrounding gas molecules.

The number of molecules within the shell is considered to be small, and the rate of evaporation into it is assumed to be that of evaporation into a vacuum. The mass transfer rate into a vacuum will be:-

$$\frac{-dM}{dt} = 4\pi a^2 \nu \propto Co\, m \qquad 10.22$$

Figure 38 heat transfer rate to the particle

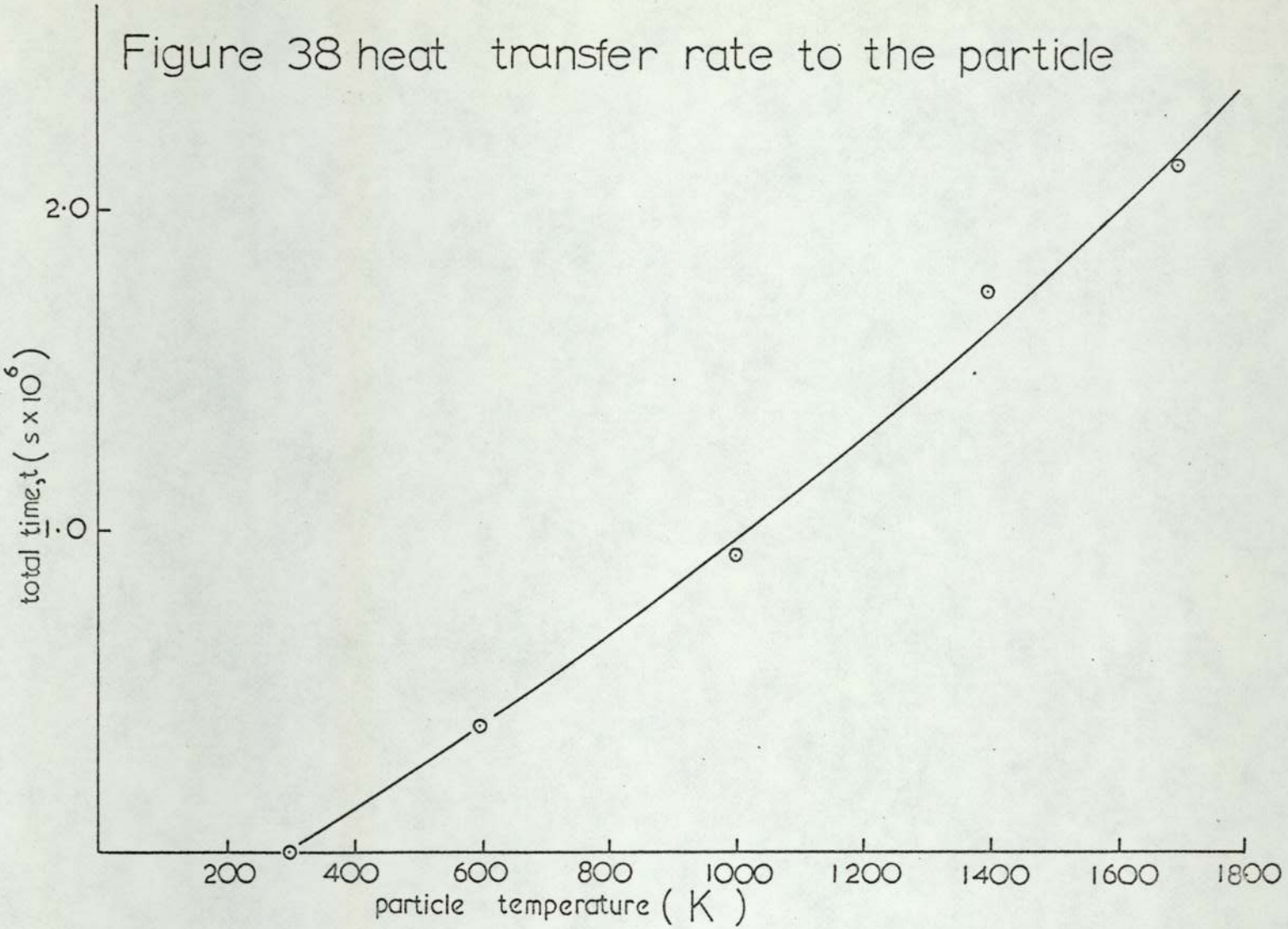

where $\nu = (kT/2\pi m)^{\frac{1}{2}}$, α is the accommodation coefficient of the leaving species mass m, and Co the saturated concentration of the species above the condensed phase. Writing C_1 for the concentration of the vapour at a distance Δ from the surface, then the rate of evaporating molecules leaving the surface of the shell is given by:-

$$\frac{-dM}{dt} = 4\pi a^2 \nu \alpha (Co - C_1) m \qquad 10.23$$

This rate will be equal to the rate of diffusion, I, of the vapour from the concentric shell distance r from the particle, and is assumed constant and may be expressed by:-

$$I = -4\pi a^2 D \frac{dC}{dr} . m \qquad 10.24$$

From equation 10.24 for diffusion into a region where the concentration of the vapour is approximated to zero then

$$\frac{dC}{dr} = \frac{-C}{r}, \qquad 10.25$$

and at the boundary of the shell, the diffusion rate will be given by:-

$$I = -4\pi(a + \Delta) DC_1 m \qquad 10.26$$

Equating 10.23 and 10.26 then

$$\frac{-dM}{dt} = \frac{4\pi a D Co\, m}{D/a\nu\alpha + a/a+\Delta} . \qquad 10.27$$

A further simplification used by Woolley[36] is the approximation that

$$D \simeq \frac{\lambda}{3} (8\, kT/\pi m)^{\frac{1}{2}} \qquad 10.28$$

for case where the particles are smaller than the mean free path of

the gas molecules, λ, and therefore

$$\lambda \frac{D}{\nu} = \Delta . \qquad 10.29$$

In the flame at 2500 K, λ was found to be 1.8×10^{-6} m compared to a particle radius of 3×10^{-6} m, but the approximation was used here, for the case where the evaporation had proceeded to such a point that the condition $a<\lambda$ was satisfied.

Equation 10.27 may be re-expressed in the form:-

$$\frac{-dM}{dt} \approx \frac{4\pi a D Co m}{D/av\alpha} ; \qquad 10.30$$

and the expression for the evaporation into a vacuum is now:-

$$\frac{-dM}{dt} = -4\pi a^2 \rho \frac{da}{dt} = 4\pi a^2 \nu \propto Co\, m. \qquad 10.31$$

where ρ is the density of the particle. The time taken for reduction of the particle size from a_o at t=o, to a at time t, is given by:-

$$(a_o - a) = \frac{\nu \propto Co\, t\, m}{\rho} . \qquad 10.32$$

Values of Co for KCl were calculated from saturated vapour pressure data taken from tables[111], at temperatures corresponding to the melting and boiling points of the material. Using equation 10.32, the times taken for the complete particle to evaporate, while existing firstly at its melting point, 1323 K, and secondly at its sublimation point 2046 K, were 4×10^{-3} s and 3×10^{-7} s respectively, assuming the accommodation coefficient to be unity.

Figure 39 meteor trail model

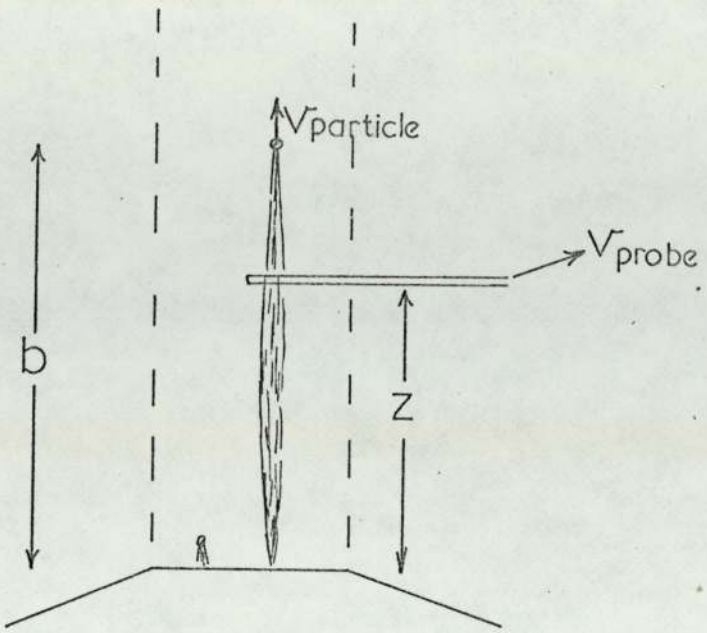

frozen stream

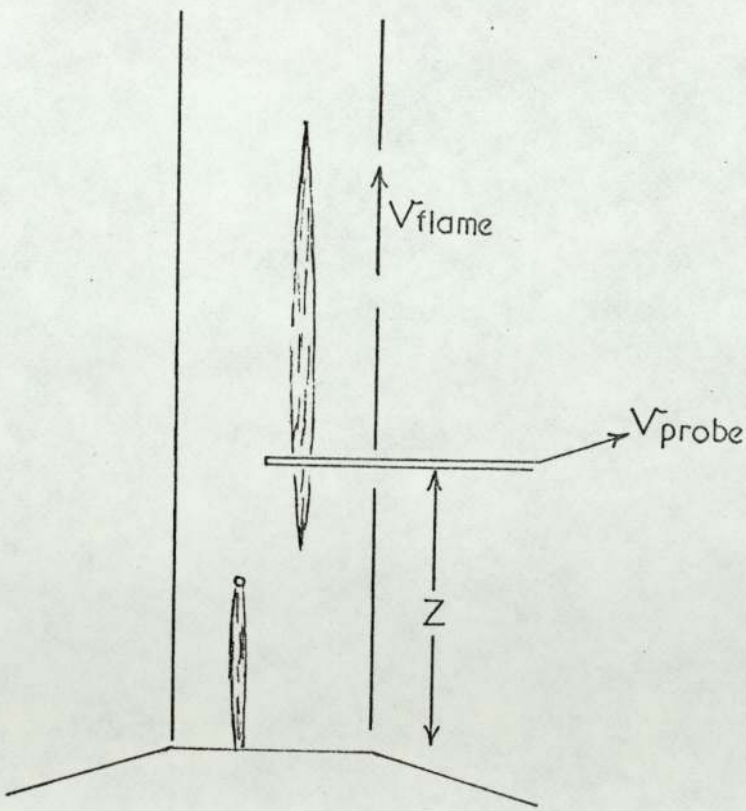

unfrozen stream

These times can be seen to be of the right order for the heat and mass transfer processes to complete the evaporation in 1×10^{-4} s or less. The particle should, therefore, be completely volatilised at a height of some $3\text{-}4 \times 10^{-3}$ m above the burner, and from previous calculations would form a trail of about 1×10^{-3} m in length. The "spike" widths, at this height, indicate a trail some 5×10^{-3} m in length, which, although larger, might be considered to be in reasonable agreement with the theoretical predictions.

It can be shown by examining the proposed model that an upper limit may be assigned to the "spike"-width, and this is illustrated in Figure 39. The probe is positioned at some distance, z, above the burner, and the gas stream is considered to be frozen. The particle moving relative to the gas stream, starts evaporating at a time t=o, and continues to do so, until the process is complete at a distance, b, from the burner, where $b > z$. Assuming, for the sake of simplicity, that the particle velocity, relative to that of the gas, is constant at 10 ms^{-1}, a trail, $t_e \times 10$ m long will be produced, where t_e is the evaporation time. This also assumes that the gaseous products take on the gas velocity, immediately after leaving the particle surface. Since $b \gg z$, when the gas stream is unfrozen, only a length, z, of the trail will pass over the probe in $z\ v_f^{-1}$ seconds. Therefore in the case of measurements made low in the flame, the height of the probe above the burner will decide the pulse width recorded. The converse of this argument leads to the conclusion that at no point in the flame should the product of the "spike"-width and flame velocity exceed the height above the burner. The extrapolated "spike"-width at t=o now indicates a minimum evaporation time for the particle.

The lowest point at which measurements were made with the low RC circuit was at 1×10^{-2} m, and here the trail length calculated from the "spike"-width was 7.2×10^{-3} m, which is within the limits stated above. The calculations also show that to account for the widths exactly, the excess speed of the particles should be some 2.4 times that given by considering Poiseuille-type flow through the hypodermic tubes of the burner.

It is admitted that the meteor trail concept is only partially successful in explaining the "spike"-width. The relative velocities, and the heat and mass transfer rates however, are such as to predict theoretical trails within an order of magnitude of those measured, and considering the overall complexity of the problem this agreement is probably as good as can be expected. Many errors are inherent in the calculations, the chief one possibly being in considering the particles to be spherical, which they almost certainly are not. The irregular shape of the crystallites, would be likely to increase the deceleration rate due to the great drag forces acting, and also to increase the rates of mass and heat transfer, owing to the larger surface area to volume ratio of the particles.

10.iv. The Effect of Acetylene on the Spikes

Whilst attempting to ascertain the effect of various circuit elements on the rise-time of the spikes, the flame conductivity was increased by adding acetylene to the inner flame at a dilution level of 1% (unburnt composition). The effect of adding the acetylene is to produce an initial high concentration of ions, mainly CHO^+ and H_3O^+, which are evenly distributed throughout the flame gases. The most persistent of these ions, H_3O^+, has a relatively short life-time

compared to metallic positive ions; and the ionisation level falls at an easily measurable rate, in the downstream gases.

Using the probe calibration from work performed in conjunction with Mr. W. G. Roberts[37], on the recombination rates of various metal ions, the number density of ions in the flame doped with acetylene at 2500 K, was found to be 5×10^{18} (ions m^{-3}) at 6×10^{-3} m above the burner. When the diluted spray of potassium chloride was introduced, under these conditions, an almost total absence of "spikes" was observed, rather than the expected effect on their widths. The absence of the "spikes" was also found at heights up to 8×10^{-2} m.

The initial explanation for this might be that the ionisation within the trail produced from the crystals, was insignificant compared to that from the H_3O^+ ions, but a simple calculation shows this to be incorrect. The volume of trail produced from a mean crystal, assuming cylindrical geometry, was approximately 1.9×10^{-8} m^3, and at equilibrium would contain 7.2×10^{10} ions. With no interaction between the separate ionisation equilibria, the number of H_3O^+ ions contained in this region would be 9.5×10^{10}, so the spikes should certainly be seen.

An alternative answer lies in the relative rates of the two reactions:-

$$K + M \rightleftarrows K^+ + M + e^- ; \quad (X)$$

and

$$K + H_3O^+ \rightarrow K^+ + \text{Products} . \quad (Y)$$

Reaction X is appropriate to thermal ionisation in a clean flame, and Y to the charge exchange process proposed by Padley[26]. If the potassium atoms within the trail region ionise by reaction Y in the presence of H_3O^+ ions, then the initial distribution of positive ions

in the flame will be the same as that of the H_3O^+ ions, i.e. homogeneous. Diffusion of the K^+ ions will take place outwards from this region, simultaneously with that of H_3O^+ in an incoming direction. To a first approximation, the diffusion rates will be identical and so the homogeneous distribution is maintained.

Depending on the relative rates of X and Y, $[K^+]$ may either be speeded towards it equilibrium level, or taken above it, in which case there will be a decay of ionisation, according to the reverse rate of X. The "natural" ions outside the trail region will undergo recombination downstream from the reaction zone, and should eventually be reduced to such a level that they are below the concentration of the K^+ ions, and the inhomogeneous distribution again produced. It is possible, on this last point, that by diffusion the potassium ions will have distributed themselves sufficiently that the remaining inhomogeneity is not detected by the probe.

Clarification of these observations was not possible, due to a lack of time, and a certain amount of alteration to the apparatus was needed to continue this line of study. To measure the effect of varying amounts of acetylene added to the flame, would necessitate the removal of all rubber surfaces from the system, since these had been found to absorb the gas to a large extent, and to de-gas, on subsequent runs.

In the light of the knowledge gained from many previous ionisation studies in flames of this sort, the above explanation seems to be the most readily acceptable one, however it is interesting to consider the possibility that the charge transfer concept does not suffice.

Discounting the buffering effect of the natural ionisation on the metal ionisation, from previous arguments, in this work, the disappearance of the "spikes" must be attributed to the absence of trails. On this basis, the high level of natural ionisation must, by some mechanism, have speeded up the evaporation process so that spheres, as opposed to trails, of gaseous ions were formed from the crystals. Such developments would be of great interest with regard to the widely established charge transfer reactions of metal atoms with H_3O^+ ions in these flames.

CHAPTER 11

GEOMETRIC CONSIDERATIONS AND DIFFUSION

11.i. Cylindrical Distribution

A closer examination of the meteor trail model, reveals that geometric factors will decide whether the growth of the "spike"-widths is controlled by axial or radial diffusion, of the cloud of ions.

The trail of gaseous material left by the particle is considered to be contained in a cylinder of space, radius r, and length b, where $b >> r$. The gases are travelling at a uniform velocity, v_f, and the horizontal sweep velocity of the probe is v_p. Now the time taken for the cylinder to pass over the probe will be b/v_f, and during this time, the probe will have travelled a horizontal distance of $v_p\, b/v_f$. If the length of trail is such that $v_p\, b/v_f > 2r$, then the pulse width defines the characteristic distance 2r, in the horizontal plane, and conversely if $v_p\, b/v_f > 2r$, the trail length b is defined. In the former case as r goes to zero on the scale used, i.e. at the burner face, then the limiting case of the "spike"-widths at t=o will be the width of the sheath region, which for the thin sheath condition will be the diameter of the probe.

The minimum extrapolated half width, from Figure 36, was found to be 1.2×10^{-4} seconds, giving a horizontal distance 1.2×10^{-4} m, using a probe sweep velocity of 1 ms^{-1}., compared to 1.25×10^{-4} m, the radius of the platinum wire probe. The agreement is good, but is also possibly fortuitous and is not an absolute proof of the condition that $v_p\, b/v_f > 2r$. The shape of the spikes too, appears more appropriate to a density profile across the trail rather than to one along a stream line, though the exact form of the latter is somewhat unknown.

Since the probe may measure the ion density profile in the horizontal plane, the possibility that more than one crystal contributed to one "spike" arises. Aston and Hayhurst[116] have used a similar approach to obtain a thin column of seeded flame in a study of the diffusion of sodium atoms, by introducing a continuous aqueous spray from a conventional atomiser, to a single tube of a multitube burner.

The establishment of the delivery-rate proves to be a very difficult problem due to its very low numerical value. Examination of the crystals collected on a glass slide held above the burner, was possible, and used in a qualitative manner, but it was not thought possible to accurately relate the number collected to the number density in the gas stream. Also, methods based on the rate of loss of material from the breaking bubble atomiser would involve serious errors, further complicated by the distribution of particle size and the unknown settling rate on the walls of the system. It was concluded therefore that no direct proof could be obtained as to whether one crystal caused a single "spike".

A useful exercise, however, is to calculate the number of ions per unit volume produced from a single mean crystal and compare this to the number of charges collected by the probe, per unit volume swept out by it. This should show whether appreciable overlap of the trails from different crystals occurred.

The ions are considered to be evenly distributed within the cylindrical "trail" of length b, decided by the pulse width, and r the breadth, calculated from the relationship:-

$$\bar{r}^2 = 4Dt \qquad 11.1$$

for diffusion in two dimensions. The term $\bar{r}^2$ is approximated to r^2,

the actual distance covered by the particles in time $t^{\frac{1}{2}}$. Taking D as $1 \times 10^{-4} m^2 s^{-1}$, and the pulse width at 3×10^{-2} m above the burner for KCl, the volume of the cylinder is found to be 1.9×10^{-8} m^3. This volume of the flame gases contains 5.7×10^{16} atoms and molecules, so that the partial pressures of 6×10^{11} potassium atoms released from the mean particle is 1.05×10^{-5} atm.

Assuming that the process

$$K \rightleftarrows K^+ + e^-$$

is equilibrated, then

$$Kp = \frac{P_K x^2}{(1 - x)}, \qquad 11.2$$

where Kp is the equilibrium constant for the reaction, P_K the partial pressure of potassium in all forms, and x the degree of dissociation. Kp was calculated to be 1.928×10^{-7}, from the Saha equation, taking the ionisation potential of potassium to be 4.318 e.v. Using these values in equation 11.2, x was calculated to be 0.12, and consequently the number of K^+ ions contained in the cylinder, 7.2×10^{10}. If for the largest events seen, the axis of the probe passed down the axis of the trail, then the volume of the ionised cylinder swept out by the probe is 1.5×10^{-9} m^3, and assuming that all the ions are collected the "spike" should contain 5.9×10^9 charges, whereas the mean "spike" at -90 V bias, was equivalent to 8.1×10^8 charges. The number of charges calculated to be within the cylinder will be an overestimate, owing to the distribution of ions; in fact the majority will exist at a higher partial pressure than considered above. Also, the ionisation process may not be fully equilibrated and no account has been taken of the lateral motion of the probe, during collection from the trail.

That the number of ions collected was less than the predicted figure does not in itself preclude the possibility that more than one particle contributed to one "spike", but merely illustrates the feasibility of relating one event to the evaporation and ionisation of potassium atoms from one crystal introduced to the flame.

11.ii. Radial Diffusion

For the case where the trail is of sufficient length that its radial distribution is described by the probe, the diffusion will be that of an infinite cylinder, and axial diffusion may be ignored. The distribution of particles from a point source on a surface after a time t is given by Crank[122] to be

$$Nr = \frac{No\ e^{\frac{-r^2}{4Dt}}}{4\pi Dt} \qquad 11.3$$

Following the same arguments as in 9.iii., then

$$\frac{d(vpw)^2}{dt} = 11D, \qquad 11.4$$

where w is again the measured half width of the "spikes", and vp the probe sweep velocity, taken as 1 ms^{-1}. The use of equation 11.4 takes no account of the time taken for a cylinder of radius r to be traversed by a cylindrical probe of radius a, where a >> r. A further complication inherent in the treatment is the shaping of the pulses due to the changes in surface area of contact beteeen the trail and the probe. In spite of these reservations, the relationship should provide a rough measure of the radial diffusion of the trail.

Figure 40 shows a plot of $(wvp)^2$ vs t, for the potassium chloride delivery at 2507 K and 0 volts bias; and the slope produces a value for D of 1.07×10^{-6} m^2 s^{-1}. This low figure would seem to indicate that the approach was incorrect, since D should be of the order of 1×10^{-4} m^2 s^{-1}. The point remains, however, that the shape of the pulses seems appropriate to the density profile, along a radial section of the trail.

11.iii. Axial Diffusion

If the "spike"-width is assumed to describe the length of the meteor trail, then the observed profile is a function of many factors, including the heat and mass transfer rate of the evaporation process axial diffusion and the path of the probe through the trail. An exact solution for the situation would undoubtably be complex, but a simple mathematical model was required to enable the diffusion coefficient to be calculated to an order of magnitude.

In the model the ionised trail is envisaged as being contained in a cylinder of length b, and within this region, the ions are evenly distributed. The "spikes" are considered to be symmetrical; and so the rise time, W_R, is approximated to half the length of the trail. The rise time at t=o, therefore gives the length b/2 of the cylinder, which is essentially unaffected by diffusion. The axial growth is seen to be due to the diffusion of two hemispheres of radius Y, at each end of the cylinder.

The radius Y of the hemispheres is given at any time t in the flame by

$$Y_{(t)} = \left(W_{R(t)} - W_{R(t=o)} \right) vf. \qquad 11.5$$

Now the rise time W_R was measured from an extrapolation of the leading

Figure 40 estimation of D, radial diffusion

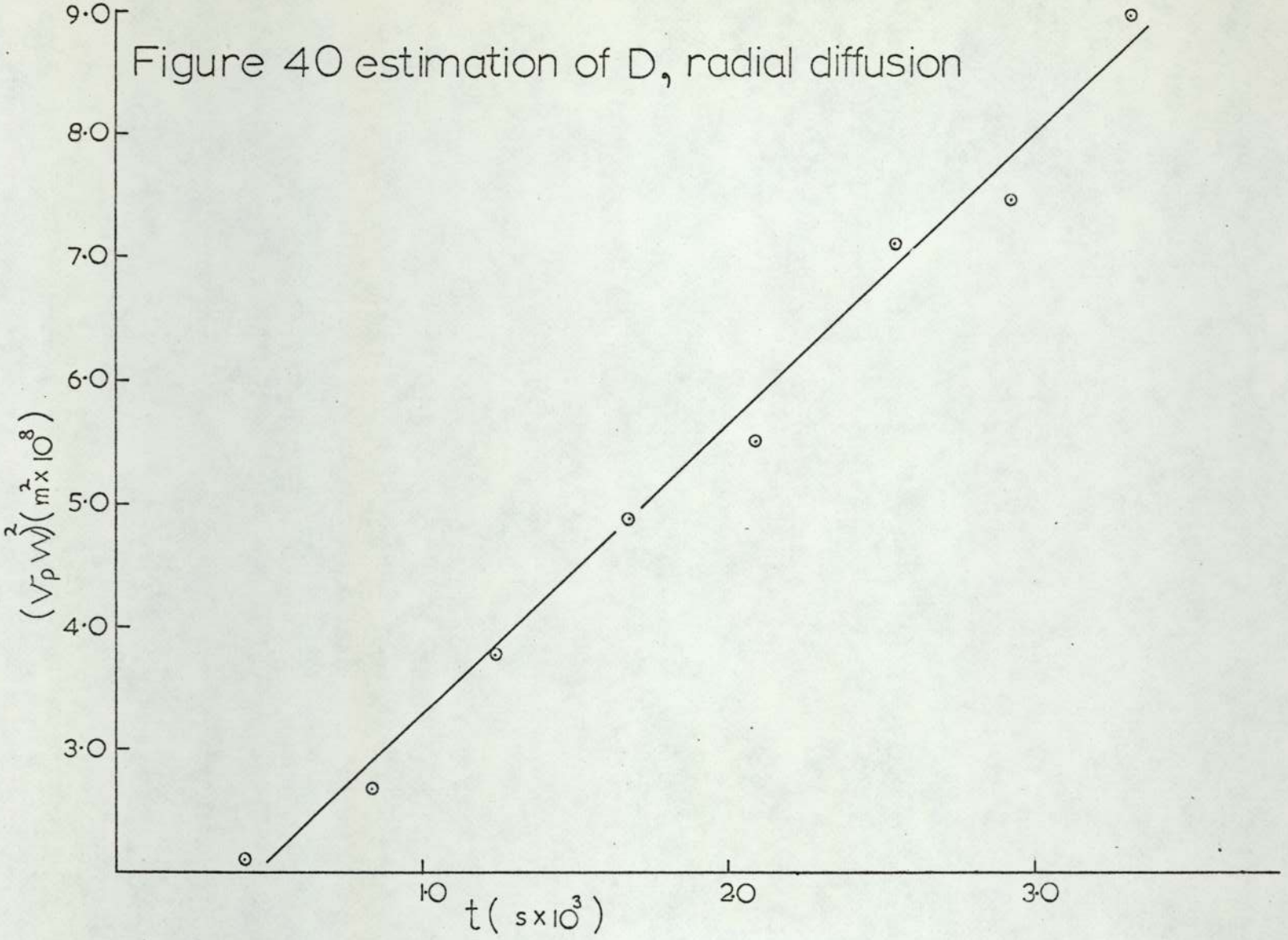

Figure 41 estimation of D,
axial diffusion

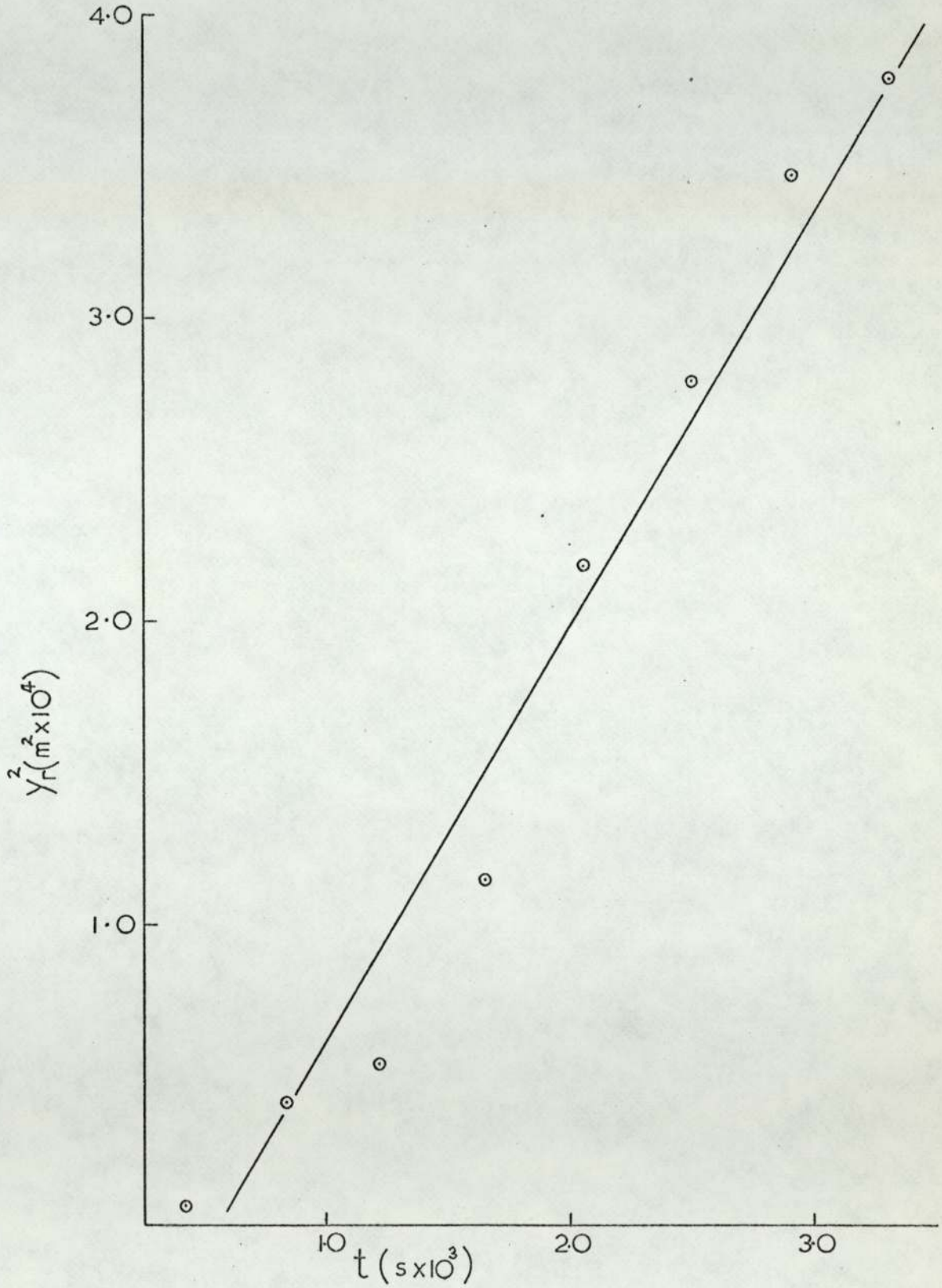

slope and ignores the asymptotic tail of the pulse. To account for this, W_R is taken arbitrarily to be the point where $N_Y/N_C = 5/100$. Following the same procedure as before, then

$$\frac{N_{C(t)}}{N_{Y(t)}} = 20 = e^{Y^2_{(t)}/4Dt}, \qquad 11.6$$

and

$$\frac{dY^2_{(t)}}{dt} = 5.21D \ . \qquad 11.7$$

Figure 41 shows $Y^2_{(t)}$ plotted against t for the conditions V_p = -90 V, T= 2507 K, using potassium chloride, and from the slope, D was found to be 5.3×10^{-4} m^2 s^{-1}. A similar treatment of the data for the probe, at 0 v bias, yielded a value, of D, of 3.0×10^{-4} s^{-1}.

Moseley, Gatland, Martin and McDaniel[123] have studied the diffusional behaviour of K^+ ions, in a drift tube experiment using nitrogen carrier gas. They were able to simultaneously measure the longitudinal and transverse coefficients, D_L and D_T, and the ion mobility. At low values of E/N where E is the applied field in the axial direction, D_L and D_T were found to be equal, over a range of ambient pressures of 01 - 1 torr. Taking the quoted value of 1.31×10^{-2} m^2 s^{-1} for D under the conditions P = 0.418 torr and T = 300 K, the extrapolated value, at flame conditions is 1.73×10^{-4} m^2 s^{-1}, by using the well known relationship:-

$$D = \text{const.}\ T^{1.5}/P \ . \qquad 11.8$$

In practice, the dependence on temperature is found to lie between $T^{1.75}$ and T^2, and using the latter, the extrapolated value of D becomes 5.0×10^{-4} m^2 s^{-1}.

The excellent agreement between these figures and those from the "spike"-measurements reinforces the view that the "spikes" describe the axial dimensions of the trails. No allowance has been made for the different atmospheres used, one of nitrogen, and the other, a mixture of N_2, H_2O and H_2, etc., and this, coupled with the basic incorrectness of the double hemisphere approach, requires that some reservations must be attached to the above conclusions. This concept would, in the limit, lead to a dumb-bell appearance to the trail, and the values of D produced will be overestimates, since the diffusion becomes that of two spheres rather than two hemispheres.

CHAPTER 12

THE RESPONSE OF THE PROBE IN THE PRESENCE OF SOLID PARTICLES

12.i. The Temperature Dependence of the Probe Current

The spikes produced from dilute deliveries of KCl and other salts to the flame have been shown to be due to the probe passing through regions of high ion concentration contained therein. The observations of peak height and width however, show a remarkable similarity to the results obtained by Miller from his work on solid particles, in particular lanthanium hexaboride, and some attempt must be made to reconcile this apparent paradox.

If the ionisation detected in the presence of solid particles, was of gaseous origin from material ablated from the surface in the form of meteor trail, the ion precursors could be of two distinct forms. Firstly, the particles may have been contaminated with impurities such as alkali metal salts, and secondly, the possible combustion, or evaporation of the materials, must be taken into account.

Considering the process

$$A \rightleftharpoons A^{+} + e^{-}$$

to be fully equilibrated under flame conditions, the equilibrium constant Kp for the reaction may be found from the Saha equation, expressed as

$$Kp = \frac{Q_{A^+} Q_{e^-}}{Q_A} kT \exp - X/kT. \qquad 12.1$$

Kp may also be expressed in terms of the partial pressures or

concentrations of the reacting species:-

$$Kp = \frac{[A^+][e^-]}{[A]} . \qquad 12.2$$

Following again the derivation used in section 3.iv., assuming a charge balance and with $[Ao]$ as the total A in all forms, then for $K >> [Ao]$, $[A^+] = [Ao]$, and for $[Ao] >> K$, $[A^+] = (K[Ao])^{\frac{1}{2}}$. Working in terms of number densities $[A^+]$ may be related to the probe current via the relationship of Clements and Smy[106] for the thin sheath condition:-

$$I_i = 5.3\, \varepsilon o^{\frac{1}{4}}\, e^{\frac{3}{4}}\, \mu^{\frac{1}{4}}\, a^{\frac{1}{4}}\, \nu f^{\frac{3}{4}}\, N_{A^+}^{\frac{3}{4}}\, V^{\frac{1}{2}}\, L \; . \qquad 12.3$$

where N_{A^+} is the number of N_{A^+} ions per unit volume

For constant values of a, V, and L, equation 12.3 may be rewritten as

$$N_{A^+} = \frac{\text{Const } I^{4/3}}{\mu^{1/3}\, \nu f^{1}} . \qquad 12.4$$

Now both μ and νf are functions of temperature; $\mu \propto T^{\frac{1}{2}}$, and to a first approximation, $\nu f \propto T^{1}$, and these proportionalities may be usefully included in 12.4 to yield

$$N_{A^+} = B\, I^{4/3}\, T^{-7/6} , \qquad 12.5$$

where B is a constant dependent on the nature of A^+ and conditions at the probe.

Re-expressing equation 12.5 in terms of partial pressures, then

$$P_{A^+} = B\, I^{4/3}\, T^{-7/6}\, P/N_{TOTAL} , \qquad 12.6$$

where P is the total pressure, and N_{TOTAL} is the total number of

particles per unit volume. By eliminating contributions to Q_{A^+} and Q_A from excited states, and taking $Q_{e^-} = 2\,(2\pi me\,kT)^{3/2}/h^3$, then equation 12.1 becomes:-

$$K = \frac{g_o A^+ \, 2\,(2\pi me)^{3/2} \, k^{5/2} \, T^{5/2}}{g_o A \, h^3} \exp -X/kT \,. \qquad 12.7$$

Using the condition $[Ao] >> K$, and combining 12.6 and 12.7, then

$$I^{8/3} = \frac{g_o A^+ \, 2\,(2\pi me)^{3/2} \, k^{5/2} \, T^{5/2} \, T^{14/6} \, N_{TOTAL}^2 \, P_{Ao}}{B^2 \, g_o A \, h^3 \, P^2} \exp -X/kT. \qquad 12.8$$

At constant pressure, $N_{TOTAL} \propto 1/T$; and equation 12.8 can be expressed as

$$I^{8/3} = C \, P_{Ao} \, T^{17/6} \exp -X/kT \,, \qquad 12.9$$

where C is a constant, containing all the non temperature dependent terms. For the condition that $K >> [Ao]$ and $[A^+] = [Ao]$ then:-

$$I^{4/3} = C \, T^{1/6} \, P_{Ao} \,. \qquad 12.10$$

12.ii. Application to Miller's Results from Lanthanum Hexaboride

If the "spikes", seen by Miller, were due to the contamination of the solid particles, then it is likely that evaporation of the impurities goes to completion after a short time in the flame, and P_{Ao} is not a function of temperature. On the other hand, if the species A is derived from the particle material itself, P_{Ao} will

depend upon temperature. To take account of this, P_{Ao} may be written for the general case, as

$$P_{Ao} = M \exp -E/kT \ , \qquad 12.11$$

where M is a constant, though possibly a function of temperature; and E is an energy term, which may include heats of evaporation, dissociation, and desorption.

The condition for $[Ao] >> K$ would seem most likely to apply in the trail of the particle, and for the ionisation of surface impurities, equation 12.9 gives:-

$$\frac{d \ln I}{d\ 1/T} = \frac{3}{8}\left[\frac{17T}{6} - \frac{X}{K}\right] . \qquad 12.12$$

The equivalent relationship for the case in which the particle materials are involved, is:-

$$\frac{d \ln I}{d\ 1/T} = \frac{3}{8}\left[\frac{17T}{6} - \frac{X}{K} - \frac{E}{k}\right] , \qquad 12.13$$

assuming d ln M/d 1/T to be zero. Miller's data for the varation of spike height with temperature, for lanthanum hexaboride at 5×10^{-2} m, and at a mean temperature of 2240 K, gives d ln I/d 1/T as 18.7×10^{3} (deg. K); and from equation 12.12 with potassium as a surface impurity, d ln I/d 1/T is 7.98×10^{3} (deg. K). The agreement is obviously poor though it might be possible to add energies of desorption, and allow for non-equilibrium ionisation, which would raise the second figure.

An alternative is to consider the evaporation and ionisation of compounds of lanthanum, from a surface layer of La_2O_3 formed on the

particle, by such schemes as

$$\begin{aligned} &A \quad La_2O_{3(S)} \rightleftarrows 2LaO + O ; \\ &B \quad\quad LaO \rightleftarrows LaO^+ + e^- ; \\ &C \quad\quad LaO \rightleftarrows La + O ; \\ &D \quad\quad La \rightleftarrows La^+ + e^- \end{aligned}$$

The above reactions are regarded as equilibrated under the conditons of the experiment. For this situation the ion concentration is more conveniently discussed in terms of P_A, the ion precursor, than in terms of the total A in all forms.

From equation 12.1, assuming $P_{A^+} = P_{e^-}$ then

$$P_{A^+}^2 = \frac{P_A Q_{A^+} Q_{e^-}}{Q_A} kT \exp -X/kT; \qquad 12.14$$

and using 12.6:-

$$I^{8/3} = \frac{P_A T^{4/3} B'^2 k Q_{A^+} Q_{e^-}}{Q_A} \exp -X/kT . \qquad 12.15$$

The equilibrium constant, K_A, for reaction A above, will be given by

$$K_A = P^2_{LaO} P_O , \qquad 12.16$$

assuming $La_2O_{3(S)}$ to have unit activity. Therefore with LaO^+ being the principle ionic species, then

$$I^{8/3} = \sqrt{\frac{K_A}{P_O}} \frac{T^{4/3} B'^2 k Q_{A^+} Q_{e^-}}{Q_A} \exp -X/kT . \qquad 12.17$$

Therefore

$$\frac{d \ln I}{d\, 1/T} = -\frac{3}{8}\left\{ -\frac{1}{2}\frac{d \ln P_O}{d\, 1/T} - \frac{1}{2}\frac{\Delta H^{\circ}_{A_T}}{K} + \frac{4T}{3}\frac{-X}{K} \right\} . \qquad 12.18$$

ΔH°_{2240}, for reaction A, was estimated as +1675 kJ mol^{-1}, using the following data:- ΔHf°_{o} $La_2O_{3(S)}$ = -1940 kJ mol^{-1}; Cp $La_2O_{3(S)}$ = 94.6 + 22.6 × 10^{-3} J mol^{-1} deg^{-1}, from Kubaschewski[124], and D°_{o} LaO = 779 kJ mol^{-1}, after Chupka, Inghram and Porter[125]. Cp, for LaO, was taken to be similar to that for AlO, and d ln P_o/d 1/T was found from the measured values of P_O for the flames used. Using Miller's figure for d log I/d 1/T of - 8.1 × 10^{3} (deg. K), equation 12.18 predicts the ionisation potential of LaO to be approximately -498 kJ mol^{-1}, which is clearly not a sensible result..

The formation of La^{+} might seem to be more likely than the ionisation of LaO, and using an estimated value for ΔH_C of +2510 kJ mol^{-1}, this produces a value for the ionisation potential of La of -1110 kJ mol^{-1}, expressed in molar terms. Chupka, Inghram and Porter, from their study of the gaseous equilibria above $La_2O_{3(S)}$, by mass spectrometry, have concluded that the appearance potentials 5.5 e.v., and 4.4 e.v., found for La^{+} and LaO^{+} represented their respective ionisation potentials. These figures may be re-expressed as 513 kJ mol^{-1} and 448 kJ mol^{-1}.

The agreement with these figures is non-existent, and the principle reason for this would seem to be the assumption that the gaseous species are in equilibrium with the particle surface constituents. As it is likely that at least initially the particles are travelling faster than the gas molecules, then any reactions

involving the condensed phase may tend to become irreversible, or rather, under kinetic control. The reasonably low ionisation energies for La and LaO however, would permit the existence of appreciable quantities of the ionic species, providing that sufficient vapour pressures of the ion precursors, above the particle, could be produced at the flame temperature.

The formation of a surface coating of B_2O_3 was considered, with the production of LaO or La in the gas phase, using the energetics for the reaction

$$LaB_{6(S)} = La_{(g)} + 6B_{(S)} \quad \Delta H^{o}_{2113} = 563 \text{ kJ mol}^{-1},$$

quoted by Gordienko, Guseva and Fesenko[126]. It can be seen that reactions such as

$$10\,O + LaB_{6(S)} \rightleftharpoons LaO + 3B_2O_{3(S)} \quad \Delta H^{o}_{2200} = -5060 \text{ kJ mol}^{-1}$$

or similar processes involving large energy changes, will produce ionisation potentials of the correct sign, but of too great a magnitude.

The best agreement therefore was obtained by considering the "spikes" to be due to evaporated alkali metal impurity, in this case potassium, which was possibly residing on the surface of the particle. Further it was observed that the Richardson plots constructed by Miller for LaB_6, WC, and C, had, understandably, a significant degree of scatter and very similar slopes, and it is possible that surface impurities were important in all three cases.

12.iii. Application to Miller's Results from Barium Oxide

The Richardson plots obtained from the "spikes", with barium oxide particles delivered to the flame exhibited rather unique behaviour. A distinct change of slope was observed in the region of the melting point of the oxide, with an increased negative slope of higher temperatures. The interpretation given was that the different work functions of the liquid and solid surfaces were being measured above and below this point. The values obtained were:- 0.6 ev for the solid and 1.94 ev for the liquid, as opposed to the literature value of 1.66 ev for solid barium oxide. No study of the "spike"-widths was carried out, but as barium oxide was the most volatile of the few compounds studied, and it is known that alkaline earth metals can produce high levels of gaseous ions in flames, the possibility of explaining these results, in terms of gaseous ionisation was examined.

Firstly, the existence of a stable liquid phase of BaO above 2300 K, under flame conditions, is in doubt. To the author's knowledge, no experimentally determined boiling point exists, but the Handbook of Chemistry and Physics[127] quotes the melting point as 2196 K and gives a calculated boiling point of 2273 K. Assuming that at, 5×10^{-2} m. in the flame, the particle will evaporate or sublime completely into the vapour phase, the behaviour in the higher temperature range may be described in terms of the gaseous ionisation of barium compounds, where the total amount of barium, in all forms, will no longer be a function of temperature. In the lower range, the level of the ion precursors will be controlled by the rate of evaporation from the solid, or by the equilibrium vapour pressures above it.

It has been shown that the majority of the barium present in these flames will be in the forms BaOH and $Ba(OH)_2$. Considering the processes:-

$$^{128}\text{(E)}\quad Ba(OH)_2 \rightleftarrows Ba + 2(OH),\quad \Delta H_o^o = 891\ kJ\ mol^{-1};$$

$$^{129}\text{(F)}\quad Ba + O \rightleftarrows BaO,\quad \Delta H_o^o = -466\ kJ\ mol^{-1};$$

$$\text{(G)}\quad OH + OH \rightleftarrows H_2O + O,\quad \Delta H_o^o = -78\ kJ\ mol^{-1};$$

to be fully equilibrated, then

$$\text{(H)}\quad Ba(OH)_2 \rightleftarrows BaO + H_2O,\quad \Delta H_o^o = 347\ kJ\ mol^{-1}..$$

The metal hydroxide ion will be the most dominant one in flame conditions[29], and the energetics for the production of the ion $SrOH^+$ have been measured:-

$$SrO + H \rightleftarrows SrOH^+ + e^-,\quad \Delta H_o^o = 150\ kJ\ mol^{-1}.$$

Taking the same energy change for the corresponding process for barium, then the ionisation of barium in the flame will be controlled by

$$\text{(I)}\quad Ba(OH)_2 + H \rightleftarrows BaOH^+ + H_2O + e;\quad \Delta H_o^o\ \ 497\ kJ\ mol^{-1},$$

With KpI representing the equilibrium constant for reaction I, and $[BaOH^+] = [e^-]$, then

$$P^2_{BaOH^+} = \frac{KpI\ P\ Ba(OH)_2\ P\ H}{P\ H_2O}. \qquad 12.19$$

Substituting for $P\ BaOH^+$ using equation 12.6

$$I^{8/3} = \frac{K_I\ P\ Ba(OH)_2\ P\ H\ T^{1/3}}{B^2\ P\ H_2O}; \qquad 12.20$$

and therefore

$$\frac{d \ln.I.}{d\ 1/T} = \frac{3}{8}\left\{\frac{T}{3} - \frac{\Delta H^{\circ}_{I\ 2400}}{K} + \frac{d \ln P\,H}{d\ 1/T} - \frac{d \ln P\,H_2O}{d\ 1/T}\right\} \qquad 12.21$$

if P $Ba(OH)_2$ is effectively constant over the temperature range used.

The slope from the Richardson plot in the "liquid range" gives d ln.I./d 1/T as -16×10^3 (deg. K), and using the measured values of P H and P H_2O, the application of equation 12.21 gives a value of -23×10^3 deg. K, at the mean temperature of 2400 K.

The low numerical value of the slope in the lower temperature or "solid range" is harder to account for. Inclusion of a heat of sublimation for $BaO_{(S)}$, given by Inghram, Chupka and Porter[130] as 436 kJ mol^{-1}, will give a greater, rather than lesser, temperature dependence, by considering the reaction

$$BaO_{(S)} + H \rightleftarrows BaOH^+ + e^-, \quad \Delta H^{\circ}_{2050} = 586 \text{ kJ mol}^{-1},$$

to be describing the overall equilibrium.

Since thermodynamic arguments predict the wrong trend, the correct explanation may be in the kinetics of the processes:-

$$\text{I} \quad BaO_{(s)} \underset{k_{-1}}{\overset{k_1}{\rightleftharpoons}} BaOg$$

$$\text{II} \quad BaO_{(g)} + H \underset{k_{-2}}{\overset{k_2}{\rightleftharpoons}} BaOH^+ + e^-.$$

The rate of change of $[BaO_{(g)}]$ with time will be given by

$$\frac{d[BaO_{(g)}]}{dt} = k_1[BaO_{(s)}] + k_{-2}[BaOH^+][e^-]$$

$$k_{-1}[BaO_{(g)}] - k_2[BaO_{(g)}][H] . \qquad 12.22$$

Using the steady state approximation that:- $\frac{d[BaO_{(g)}]}{dt} = 0$:- and with $[BaOH^+][e^-] = [BaOH^+]^2$ then

$$[BaOH^+]^2 = k_2 \frac{[BaO_{(g)}][H] + k_{-1}[BaO_{(g)}] - k_1[BaO_{(s)}]}{k_{-2}} .$$

12.23

If reaction II is in equilibrium, then the solution to 12.23 requires that, $k_{-1}[BaO_{(g)}] = k_1[BaO_{(s)}]$, i.e. that reaction I is equilibrated. Therefore the steady condition implies that both reactions are in equilibrium, and a large temperature dependence of $[BaOH^+]^2$ will appear as before.

Assuming that a stable condition is not reached but that reaction II is equilibriated at all times, then

$$\frac{d[BaO]}{dt} = k_1[BaO_{(s)}] - k_{-1}[BaO_{(g)}] , \qquad 12.24$$

With the conditions that $[BaO_{(s)}] = 1$, and $[BaO_{(g)}] = 0$, at t=o, then equation 12.24 may be solved to give:-

$$[BaO_{(g)}] = \frac{k_1}{k_{-1}}(1 - e^{-k_{-1}t}). \qquad 12.25$$

Substituting for $\left[BaO_{(g)}\right]$ to give 12.26 again predicts a large temperature dependence:-

$$\left[BaOH^{+}\right]^{2} = \frac{k_1}{k_{-1}} \frac{k_2}{k_{-2}} \left[H\right] (1 - e^{-k_{-1}t}) \qquad 12.26$$

when $(1 - e^{-k_{-1}t}) \approx 1$; or by taking $e^{-k_{-1}t}$ to be independent of temperature, by virtue of the low activation energy of the reverse rate of reaction I. The simple thermodynamic and kinetic treatments of the production of gaseous ions from the solid barium oxide particles therefore do not provide a satisfactory explanation of the low temperature dependence of the ion current observed by Miller in the lower temperature range.

CHAPTER 13

CONCLUDING REMARKS ON THE PROBE EXPERIMENTS

The aims of the work were to reinvestigate and develope the use of the electrostatic probe as a diagnostic tool in flames where there existed an inhomogeneous distribution of ions, and also condensed phases. The similarity between the previous observations using largely involatile materials and those of the authors with volatile compcunds, has thrown some doubt upon the conclusions reached concerning the former, but has in no sense disproved them in an absolute manner. The appearance of the time-dependent components of the probe response in the presence of solid or liquid particles would, from the evidence gleaned so far, indicate that their origin was in gaseous material associated with the particles rather than thermionic emission from them. No reason exists though why Miller's method could not be employed to measure the work functions of clean inert particles in flames.

In his discussion Miller has criticised to some extent the work of Kelly and Padley[8], in which an electrostatic probe was used to investigate the ionisation from various metals including Sn, Cr, Fe Mo, U and La. It was inferred that a greater part of the probe response was due to thermionic emission during collisions with oxide particles, formed from these metals in the flame. The above authors had concluded that they were detecting gaseous ionisation, and of the two mechanisms proposed:-

$$\text{A}\quad (\text{M} \times \text{Oy})n_{(s)} + \text{X} \rightarrow (\text{M} \times \text{Oy})n_{(s)} + e^- + \text{X};$$

$$\text{B}\quad (\text{M} \times \text{Oy})n_{(s)} + \text{X} \rightarrow (\text{M} \times \text{Oy})(n-1)(s) + \text{MO};$$

$$\text{MO} + \text{H} + \text{X} \rightarrow \text{MOH}^+ + e^- + \text{X};$$

$$\text{M} + \text{O} + \text{X} \rightarrow \text{MO}^+ + e^- + \text{X}.$$

B was preferrred. The work here would seem to support this general idea. It must be stated though, that the exact description of the situation is complex, due to an incomplete knowledge of the nature of the ionic species, and an uncertainty as to whether the ion level is ocntrolled by the kinetics or thermodynamics of the overall process.

The chief criticism of the study must be that the original method devised to measure and count the "spikes" was not improved upon. In defence of this, it was found that the method used gave meaningful results, and that the more exotic electronic procedures envisaged, though feasible, and effective, in most cases proved prohibitively expensive. In any future work on this topic one of the major tasks should be to implement better measuring techniques in order to reduce the tedium and length of time involved in the recording of results.

Development of this general approach should be of use in investigations of the evaporation of droplets, or the formation of particles in flames; and might also be developed to provide data on the diffusion rates of ionic species contained therein. Some thought was in fact given to the exact solution of the diffusion equation for various co-ordinate systems appropriate to the "meteor trail" model, but following advice concerning the complexity of the mathematics involved[131], this was not pursued.

Further work in flames containing condensed phases formed from initially gas phase material was prevented through a lack of available time. The delivery of aluminium to the flame via the vapour of its isopropoxide seemed a suitable system to employ, but in the form in which constructed it was not ideal, due to the passage through th flame of occasional particulate material, which had condensed on the walls of the fuel lines. In such an experiment, the problem of the condensed phase moving relative to the burnt gases, should not arise.

ACKNOWLEDGEMENTS

I would like to express my gratitude to Professor F. M. Page for his guidance and encouragement during the work and to Mr. H. Williams for his cheerful and expert advice.

Also I must thank the following: Dr. D. E. Woolley and Dr. E. R. Miller for acquainting me with the "art" of flame studies, Dr. M. H. Everdell for many consultations on thermodynamic aspects; Mr. C. Chapman for his comments on the probe circuitry, Mr. T. E. Jennings for providing a critical ear to my wild hypotheses, Mr. W. G. Roberts for his long sufferance of my sense of humour, and Miss Barbara Gardiner and Miss Marion Carter for their most welcome distractions during the writing of this dissertation.

Finally I am grateful to the Ministry of Defence for the award of a Research Assistantship for the duration of the work.

REFERENCES

1. Gaydon, A. G., Wolfhard, H. G., Flames, Chapman & Hall Ltd., London, (1960).
2. Edse, R., Rao, N., Strausse, W. A. and Mickelson, M. E., J. Opt. Soc. A., 53, 436 (1963).
3. Vanpee, M., Seamans, T. F., Symp. Combust., 11, 931 (1967).
4. Parker, W. G. Wolfhard, H. G., Nature 162, 259 (1948).
5. J.A.N.A.F., Thermochemical Tables, (1965).
6. Gurvich, L. V., Veits, I. V., Dockl. Akad. Nauk. S.S.S.R. 108, 659 (1956).
7. Miller, E. R., Ph.D. Thesis, University of Aston in Birmingham, (1969).
8. Kelly, R., Padley, P. J., Trans. Faraday Soc., 65, 367 (1969).
9. Pauling, L., Wilson, E. B., Introduction to Quantum Mechanics, Magraw-Hill, New York, (1935).
10. Mavrodineanu, R., Boiteux, H., Flame Spectroscopy, John Wiley & Sons Inc., (1965).
11. Walker, S., Straw, H., Spectroscopy Vol. II, Chapman & Hall, London, (1962).
12. Fraser, P. A., Can. J. Phys., 32, 515 (1954).
13. Wallace, L. V., Nicholls, R. W., J. Atmos. Terr. Phys., 7, 101 (1955).
14. Michell, A. C. G., Zemansky, M. W., Resonance Radiation and Excited Atoms, 2nd Ed., University Press, Cambridge, (1961).
15. van der Held, E. F. M., Z. Phys. 70, 508 (1931).
16. James, C. G., Sugden, T. M., Proc. Roy. Soc., A227, 312 (1955).
17. Sugden, T. M., Trans. Faraday Soc., 52, 1465 (1956).
18. Bulewicz, E. M., James, C. G., Sugden, T. M., Proc. Roy. Soc., A235, 89 (1956).

19. Bulewicz, E. M., Sugden, T. M., Trans. Faraday Soc., 54, 830 (1958).

20. Calcote, H. F., Kurzius, S. C., Miller, W. J., Symp. Combust., 10, 605 (1965).

21. Feugier, A., van Tiggelen, A., Symp. Combust., 10, 621 (1965).

22. Fontijn, A., Miller, W. J., Symp. Combust., 10, 623, (1965).

23. Sugden, T. M., Progress in Astronautics and Aeronautics, 12, Edit., Shuler, K. E., 145, Academic Press, New York, (1963).

24. Sugden, T. M., Symp. Combust., 10, 539 (1965).

25. Calcote, H. F., Ions in Flames, Aerochem. Research Laboratories Inc., Princetown, NJ., Rep. AFBMD-TR-61-54, Dec., (1960).

26. Padley, P. J., Sugden., T. M., Symp. Combust., 8, 164 (1960).

27. Jensen, D. E., Padley, P. J., Symp. Combust., 11, 351 (1966).

28. Kelly, R., Padley, P. J., Trans. Faraday Soc., 65, 355 (1969).

29. Schofield, K., Sugden, T. M., Symp. Combust., 10, 589 (1965).

30. Sugden, T. M., Thrush, B. A., Nature 168, 703 (1951).

31. Einbinder, H., J. Chem. Phys., 26, 948 (1957).

32. Smith, F. T., Proceedings of the Third Conference on Carbon, p. 419, Pergamon, (1959).

33. Weinberg, F. J., Proc. Roy. Soc., A307, 195 (1968)

34. Mayo, P. J., Weinberg, F. J., Proc. Roy. Soc., A319, 351 (1970).

35. International Critical Tables, Vol. 5, Magraw-Hill Inc., (1933).

36. Woolley, D. E., Ph.D. Thesis, University of Aston in Birmingham, (1969).

37. Roberts, W. G., University of Aston in Birmingham, unpublished work.

38. Woodford, M., B.Sc. Thesis, University of Aston in Birmingham, (1971).

39. Soundy, R. C., Williams, H., 26th Meeting of Propulsion and Energetics Panel, Agard. Pisa, Italy, September, 6-9, (1965).

40. Gaydon, A. G., Wolfhard, H. G., Flames, p. 301, Chapman & Hall Ltd., London, (1960).

41. Corliss, C. H., Bozman, W. R., "Experimental Transition Probabilities of Spectral Lines of Seventy Elements", Natl. Bur. Std., (U.S.) Monograph 53, (1962).

42. Drew, C. M., Gordon, A. S., Knipe, R. H., Progress in Astronautics and Aeronautics, 15, Edit., Wolfhard, H. G., Glassman, I., Green, L. G., p. 17, Academic Press, New York, (1964).

43. Bruzowstowski, T. A., Glassman, I., Progress in Astronautics and Aeronautics, 15, Edit., Wolfhard, H. G., Glassman, I., Green, L. G., p. 451, Academic Press, New York, (1964).

44. Bruzowstowski, T. A., Glassman, I., Progress in Astoonautics and Aeronautics, 15, Edt., Wolfhard, H. G., Glassman, I., Green, L. G., p. 75, Academic Press, New York, (1964).

45. Bruzowstowski, T. A., Glassman, I., Progress in Astronautics and Aeronautics, 15, Edit., Wolfhard, H. G., Glassman, I., Green, L. G., p. 117, Academic Press, New York, (1964).

46. Mellor, A. M., Glassman, I., Progress in Astronautics and Aeronautics, 15, Edit., Wolfhard, H. G., Glassman, I., Green, L. G., p. 159, Academic Press, New York, (1964).

47. Macek, A., Friedman, R., Semple, J. M., Progress in Astronautics and Aeronautics, 15, Edit., Wolfhard, H. G., Glassman, I., Green, L. G., p. 3, Academic Press, New York, (1964).

48. White, W. C., Reinhart, J. S., Allen, W. A., J. Appl. Phys. 23, 198 (1952).

49. Allen, W. A., Mayfield, E. B., J. Appl. Phys., 24, 131 (1953).

50. Vanpee, M., Hinck, E. C., Seamans, T. F., Combustion and Flame, 9, 393 (1965).

51. Vanpee, M., Kineyko, M. R., Caruso, R., Combustion and Flame, 14, 381 (1970).

52. Brewer, L., Searcy, A. W., J. Am. Chem. Soc., 73, 5308 (1951).

53. Drowart, J., de Maria, G., Burns, R. B., Inghram, M. G., J. Chem. Phys. 32, 1366 (1961).

54. Gatz, R. C., Rosser, W. A., Smith, F. T., U.S. Dept. Com.. Office, Tech. Serv. A. D., 258, 777, pp. 105, (1961).

55. Walter, R. E., Efimenko, J., Lofgren, N. L., Planetary Space Sci., 3, 24 (1961).

56. Gurvich, L. V., Veits, I. V., Opt. i Spektroskopyiya, 1, 22 (1956).

57 Schofield, K., Sugden, T. M., Trans. Faraday Soc., 62, 566 (1966).

58. Cotton, D. H., Jenkins, D. R., Trans. Faraday Soc., 65, 376 (1969).

59. Gurvich, L. V., Veits, I. V., Izvest. Akad. Nauk. S.S.S.R., Ser. Fiz. 22, 673 (1958).

60. James, C. G., Sugden, T. M., Nature 175, 333 (1955).

61. Morrison, M. E., Scheller, K., Combustion and Flame, 13, 93 (1969).

62. Jensen, D. E., Trans. Faraday Soc., 65, 2123, (1969).

63. Pearse, R. W. B., Gaydon, A. G., Identification of Molecular Spectra, 2nd Ed., Chapman & Hall Ltd., London, (1950).

64. Goodlett, V. W., Innes, K. K., Nature 183, 243, (1959).

65. Krishnamachari, S. L. N. G., Narasinham, N. A., Mahair Singh, Can. J. Phys., 44, 2513 (1966).

66. Tyte, D. C., Nature 202, 383 (1964).

67. Macdonald, J. K., Innes, K. K., J. Mol. Spectros. 32, 501 (1959).

68. Coheur, F. P., Rosen, B., Bull. Soc. R. Sci. Liege, 10, 405 (1941).

69. Inghram, M. G., Porter, R. F., Chupka, W. A., J. Chem. Phys., 25, 498 (1956).

70. Rosenburg, N. W., Golamb, D., Allen, E. F., J. Geophysics Research 69, 1451 (1964).

71. Bulewicz, E. M., Sugden, T. M., Trans. Faraday Soc., 52, 1475 (1956).

72. Bulewicz, E. M., Sugden, T. M., Trans. Faraday Soc., 52, 1481 (1956).

73. Becart, M., Declerck, F., Comptes Rendus, 251, 2153 (1960).

74. Tyte, D. C., Proc. Phys. Soc., 92, 1134 (1967).

75. Newman, R. N., Page, F. M., Combustion and Flame, 15, 317 (1970).

76. Newman, R. N., Page, F. M., In Press.

77. Wilhoit, R. C., J. Phys. Chem., 61, 114 (1957).

78. Padley, P. J., Sugden, T. M., Proc. Roy. Soc., A248, 248 (1958).

79. Harteck, P., Reeves, R. R., Bull. Soc. Chim. Belges, 7, 682 (1962).

80. Rautenburg, T. H., Johnson, P. D., J. Opt. Soc. Am., 50, 602 (1960).

81. Zhadanova, L. V., Sokolov, V. A., Zh. Prikl, Spectroskopii, 1, 272 (1964).

82. Brinkley, S. R., Kirkwood, J. G., Richardson, J. M., "Tables of the Properties of Air along the Hugoniot and Adiabetic Terminating in the Hugoniot". O.S.R.D. Report, 3550, (1944).

83. Herbert, G. R., Tyte, D. C., Proc. Phys. Soc., 83, 629 (1964).

84. Gaydon, A. G., Page, F. M. Private communication.

85. Powell, D. E., University of Aston in Birmingham, private communication.

86. Coppens, P., Smoes, S., Drowart, J., Trans. Faraday Soc., 64, 630 (1968).

87. Berkowitz, J., J. Chem. Phys., 36, 2583 (1962).

88. Cotton, A. F., Wilkinson, G., Advanced Inorganic Chemistry, 2nd Ed., John Wiley & Sons, (1967).

89. Jensen, D. E., Jones, G. A. Private communication.

90. Newman, R. N., Roberts, W. G., University of Aston in Birmingham, unpublished work.

91. Chen. F. F., Plasma Diagnostic Techniques, Edit., Huddlestone, R. H., Leonard, S. L., p. 113, Academic Press, (1965).

92. Mott-Smith, H. M., Langmuir, L., Phys. Rev., 28, 727 (1926).

93. Johnson, E. O., Malter, L., Phys. Rev., 80, 58,(1950).

94. Travers, B.E. L., Williams, H., Symp. Combust., 11, 657 (1965).

95. Bills, D. G., Holt, R. B., McClure, B. T., J. Appl. Phys., 33, 29 (1962).

96. Oskam, H. J., Carlson, R. W., Okuda, T., Aeronaut. Res. Labs. Rept. No. A.R.L., 62-417, (1962).

97. Shultz, G. J., Brown, S. C., Phys. Rev., 98, 1642 (1955).

98. Calcote, H. F., King., I. R., Symp. Combust., 5, 423 (1955).

99. Calcote, H. F., Symp. Combust., 8, 484 (1962).

100. Calcote, H. F., Symp. Combust., 9, 622 (1963).

101. Bohm., D., Burhope, E. H. S., Massey, H. S. W., The Characteristics of Electrical Discharges in Magnetic Fields, Edit., Guthrie, A., Wakerling, R. K., Chapter 2, Magraw-Hill, (1949).

102. Jensen, D. E., Kurzius, S. C., Combustion and Flame, 13, 219 (1969).

103. Su, C. H., Lam, S. H., Phys. Fluids, 6, 1479 (1963).

104. Bernstein, I. B., Rabinowitz, I., Phys. Fluids, 2, 112 (1959).

105. Clements, R. M., Smy, P. R., J. Appl. Phys., 40, 4553 (1969).

106. Clements, R. M., Smy, P. R., J. Appl. Phys., 41, 3745 (1970).

107. Lam, S. H., A.I.A.A.J., 2, 256 (1964).

108. Williams, H. Private communication.

109. Bulewicz, E. M., Jones, G., Padley, P. J., Combustion and Flame, 13, 409 (1969).

110. Loeb, L. B., Basic Processes of Gaseous Electronics, University of California Press, Berkeley, (1961).

111. Kaye, G. W. C., Laky, T. H., Tables on Physical and Chemical Constants, 13th Ed., Longmans, London, (1966).

112. Oliver, B. M., Clements, R. M., Smy, P. R., J. Appl. Phys., 41, 2117 (1970).

113. Crawford, F. W., Grard, R., J. Appl. Phys., 37, 180 (1966).

114. Montgomery, R. M., Holmes, R. A., "Physico-Chemical Diagnostics of Plasmas", in Proceedings of the Fith Biennial Symposium on Gas Dynamics, Ed., Anderson, T. P., Springer, R. W., Warder, R. C., 131, Northwest University Press, Evanston, Ill., (1963).

115. Tsuji, H., Hirano, T., Combustion and Flame, 15, 47 (1970).

116. Aston, A. F., Hayhurst, A. N., Trans. Faraday Soc., 66, 824 and 833 (1970).

117. Neilson, H. N., Gilchrist, A., J. Fluid Mech., 33, 131 (1968).

118. Connolly, R., Ph.D. Thesis, University of Aston in Birmingham, (1971).

119. Langmuir, I., Phys. Rev., 12, 368 (1918).

120. Bradley, R. S., Evans, M. G., Whytlaw-Gray, R. W., Proc. Roy. Soc., A186, 368 (1946).

121. Fuchs, N., Phys. Z. Sourject, 6, 225 (1934).

122. Crank, J., The Mathematics of Diffusion, Clarendon Press, Oxford, (1956).

123. Moseley, J. T., Gatland, I. R., Martin, D. W., McDanial, E. W., Phys. Rev., 234, 178 (1969).

124. Kubaschewski, O., Evans, E. L., Alcock, , "Metallurgical Thermochemistry", 4th Ed., Pergamon, (1961).

125. Chupka, W. A., Inghram, M. G., Porter, R. F., J. Chem. Phys., 24, 792 (1956).

126. Gordienko, S. P., Guseva, E. A., Fesenko, W., Teplofiz. Vys. Temp., 6, 821 (1968).

127. Handbook of Chemistry and Physics., 49, Chemical Rubber Co., (1968).

128. Cotton, D. H., Jenkins, D. R., Trans. Faraday Soc., 64, 2988, (1968).